PRODUCT QUALITY MODELING & CONTROL BASED ON VISION INSPECTION WITH AN APPLICATION TO BAKING PROCESSES

A Dissertation

Presented to

The Academic Faculty

By

Yingchuan Zhang

In Partial Fulfillment

Of the Requirements for the Degree

Doctor of Philosophy in the

School of Electrical and Computer Engineering

Georgia Institute of Technology

March, 2005

PRODUCT QUALITY MODELING & CONTROL BASED ON VISION INSPECTION WITH AN APPLICATION TO BAKING PROCESSES

Approved by:

Dr. Jennifer E. Michaels, Committee Chair
School of Electrial & Computer Engineering
Georgia Institute of Technology

Dr. Bonnie Heck Ferri
School of Electrial & Computer Engineering
Georgia Institute of Technology

Dr. George J. Vachtsevanos
School of Electrial & Computer Engineering
Georgia Institute of Technology

Dr. Magnus Egerstedt
School of Electrial & Computer Engineering
Georgia Institute of Technology

Dr. Farrokh, Ayazi
School of Electrial & Computer Engineering
Georgia Institute of Technology

Dr. Sheldon M. Jeter
School of Mechanical Engineering
Georgia Institute of Technology

Date Approved: March 30, 2005

TO MY PARENTS, ZHENWU ZHANG AND SHUQIN SUN,

MY HUSBAND, GUANGFAN ZHANG,

AND MY DAUGHTER, CHERYL ZHANG,

WHO MADE THE JOURNEY ENJOYABLE

ACKNOWLEDGMENTS

First of all, I would like to give my special thanks to my advisors, Dr. Bonnie Heck Ferri and Dr. George Vachtsevanos. They inspired me with their unique personalities, their ample knowledge and their faith in me. I thank them for all their encouragements and patience, and understanding and respect for their students. I believe that I have benefited greatly from this opportunity to work with them and will continue to see that benefit throughout my entire career. I would also like to thank Doug Britton, my project supervisor, for his support and technical discussions.

Secondly, I wish to thank Drs. Jennifer E. Michaels, Magnus Egerstedt, Farrokh Ayazi and Sheldon Jeter for serving my committee. I thank them for their time, support, and suggestions. I must thank Dr. Sheldon Jeter for spending so much time teaching me and having discussions with me. His suggestions expedited my research progress considerably.

I want to extend my gratitude to all present and past members of the Intelligent Control Systems Laboratory, who have given me all kinds of assistance, encouragement, and friendship. Special thanks must be given to Dr. Yuhua Ding, Dr. Lichu Zhao, Dr. Liang Tang, and Dr. Biqing Wu, for their sincere friendship, warm-hearted and on-demand help to me and to my family, and technical and moral support throughout the research.

Many thanks to Mingxuan Jiang, Sai Zeng, Jie Yang, Ke Wang, and Wanru Wu. They are my closest friends who have been in my life everyday, listening to my struggles

and successes. They have made my life full of joy. I want to thank all of them for being my friends.

I feel grateful to my family: my parents, my two sisters and brother-in-law. I am lucky to have parents who are very open-minded. They provided the best educational environment for their three daughters. I thank my two sisters, Ying and Yingqi, for being my soul models, my teachers, my friends, and my caregivers throughout the years.

Finally, deep in my heart, I want to thank my husband Guangfan Zhang, who shared with me the good times and supported me through the bad times with his love, encouragement, incredible understanding, great tolerance, and sacrifices. Special thanks to my daughter Cheryl, who brought me joy everyday and made even the hardships enjoyable.

TABLE OF CONTENTS

LIST OF TABLES

Table

LIST OF FIGURES

Figure

SUMMARY

Manufacturing industries are facing major challenges in terms of improving product quality and increasing throughput while sustaining production costs to acceptable levels. Product-oriented processes, both legacy and new, are poorly monitored and controlled on the basis of distributed loop controllers that are aiming to maintain critical process variables within acceptable bounds. Thus, poor quality product results when such processes are subjected to large disturbances – operational failures, environmental changes, and changes in loading conditions. In this research, product quality modeling and control based on a vision inspection methodology is proposed to improve product quality and increase productivity.

The main contributions of this research are twofold. First, this research introduces a product quality modeling methodology that combines both physical-based modeling and data-driven modeling. The quality model is the link between information coming from the inspection of product features and the specification of process control strategies. It is essential to control and optimize the process. Physical-based modeling is used to model the product temperature profile, and data-driven modeling is used to train the mapping from the product temperature profile to each quality metric. The break down of the sub models increase the flexibility of model development and reduce the effort to change the model when the quality metrics change.

The second contribution is the development of a novel approach to control product quality based on vision inspection, which is developed as part of a hybrid,

hierarchical architecture. The high-level control module involves scheduling of multiple plant processes, diagnostics of the failure condition in the process, and the supervision of the whole process. The mid-level control module, which is the focus of the work presented here, takes advantage of baking product quality indicators and oven parameter measurements to optimize zone temperature and conveyor speed set points so that the "best" product quality is achieved even in the presence of disturbances. The low-level control module consists of basic control loops. Each of them controls parameters of each operation in the process separately. They are generally simple and easy to implement.

CHAPTER 1

INTRODUCTION AND BACKGROUND

In recent years, interest has been growing in the application of advanced process monitoring and control strategies to improve manufacturing operations. Such interest is motivated primarily by the desire to maintain a high degree of product quality while operating at the highest possible production rate. For example, the U.S. baking industry now employs modern automated high-volume baking systems (1000 buns per minute). The usual inspection process is for workers to remove a few samples of the product each hour and to inspect them manually against customer specifications. Customers are pushing for a more accurate and uniform assessment process as well as more advanced process control strategies to improve the product quality.

With advances in sensor techniques and computing power, intelligent hierarchical monitoring and control can be implemented more efficiently for industrial processes to improve product quality and increase the throughput of the process. For example, there has been a lot of work on the methodology and application of vision-based grading and quality assessment systems [3, 4, 5]. A problem with these quality control strategies is that even if there is accurate and uniform inspection of the product, there is no coordinated control for the process based on the feedback of quality information. The waste is extremely high under these circumstances because the process cannot be adjusted in real-time according to the quality of the product. The use of product images

for automated control of the industry process is a novel concept that is highly desired by the customers, but is not yet available.

Generally an industrial process involves several operations. Each operation has its own control loop to control the operating parameters to desired values. Quite often there is coupling effect between operations. Adjusting the set point of one operation may also have an effect on other operations. Therefore, a systematic approach is needed for efficient coordinated control of the process to improve product quality and productivity.

This research develops a hierarchical control strategy for industrial processes in order to improve quality using real-time feedback of a quality metric. The quality metric is used in a high-level control algorithm in order to determine set points of low-level process controllers. The application in this thesis is the quality control of baked goods using color as the feedback variable and oven temperature set points as the low-level control parameters. The color is measured using a vision inspection system that is able to inspect 100% of the product. The high-level quality control algorithm utilizes both a feed-forward component as well as a feedback component, so modeling of the relationship between the low-level control parameters and the quality metric is a key part of this thesis.

In the following context, the state-of-the-art of the quality control and quality improvement will first be reviewed. Then the topic will be restricted on the process modeling and control based on vision inspection for quality improvement purpose, which is the primary interest of this research.

1.1 Quality control and quality improvement

Quality concepts have been widely accepted for quite a long time. Historically, the notions of quality have been reactive and inspection-oriented. More recently, notions of quality assurance and management for quality have emerged. There are numerous papers concerning Quality Assurance (QA) and Quality Control (QC) programs [12]. Most of them discuss QA and QC programs from the view-point of management. Juran [29] identifies three major efforts as a quality control trilogy: quality planning, quality control, and quality improvement. In the quality planning effort, internal and external customers and their needs are identified. Generic product features that are indicative of customer needs are identified, as well as associated quality goals. A quality control process is then designed to meet or exceed product specifications, including product quality specifications. The capability of the process to produce the intended result is then established, and this leads to the desired quality improvement.

A number of technologies are available to support the above mentioned quality control and quality improvement strategies. Sage [14] provided an excellent overview and perspective on a large number of contemporary works on quality improvement and productivity, especially productivity through systems engineering. The Robust Design method pioneered by Dr. Genichi Taguchi, also called the Taguchi Method, has been used widely in the process design stage for quality control and quality improvement purposes. It is the goal of robust design to search for and obtain the state of robustness in product/process designs. Robust design enables the engineer to efficiently gather the technological information required to produce high quality, low cost products [28]. Statistical Process Control (SPC) is another systematic approach for understanding,

monitoring, controlling and improving the quality of an industrial process by means of statistical methods. Successful applications of SPC for quality control and quality improvement purposes are presented in [7, 8, 9, 10].

Though robust design and SPC are very powerful tools for quality control and process improvement, they still have shortcomings for real-time quality maintenance and process control. Robust design is mainly used in the process design stage, and SPC is a reactive control technique that passively monitors the critical process variables, prompting necessary corrective actions only after it accumulates sufficient evidence that process abnormalities have occurred.

Alternatively there are some applications that apply feedback control to improve quality. Feldmann and Sturm [15] developed a closed loop quality control system for printed circuit board assembly which used real time inspection and feedback control. Montague [33] developed advanced control technologies to improve french fry quality. There are numerous technologies that support real time inspection and quality control. In this research, we restrict our interest to the topics of machine vision, process modeling and process control.

1.2 Food quality inspection

A food quality sensor is a device which can respond to some property or properties of food and transform the response(s) into a signal, often an electric signal. This signal may provide direct information about the quality factor(s) to be measured or may have a known relation to the quality factor.

Sensors are usually classified according to their mode of use: on-line, at-line or off-line. On-line sensors operate directly in the process stream, giving a real-time signal which relates to the quality factor. At-line sensors are devices to be used for instance in split-flow measurements, requiring reagent additions or equilibrations/reaction times. They often have short response times (minutes or seconds) and also allow process corrections. Off-line sensors are laboratory devices, responding within hours or days. The great challenge is focused on real-time and on-line sensors, which can provide final product quality to data management systems to control the automated process. We will review the on-line and at-line quality sensors for process quality control.

1.2.1 Food quality sensor review

The on-line or at-line food quality sensors may be classified in different ways, but most often this is done according to the physical nature of the sensor: optical, chemical or electrical. A European Concerted Action called ASTEQ [43] considers the following classifications:

- Biosensors, incorporating a biological material, such as enzymes or antibodies
- Sensors based on an electric signal; for example Potentiometric Chemical Sensors, Metal Oxide Semiconductors (MOS), Field Effect Transistors (FET) or Conducting Polymer Sensors (CPS)
- Sensors based on interactions of electromagnetic waves, in particular sensors using visible, ultraviolet and infrared (NIR, NIT, FTIR, Thermography) waves, microwaves, radiowaves, X-rays and high frequency waves (Nuclear or Electronic Magnetic Resonance)

- Sensors based on interaction with ultrasound waves (100kHz-1MHz)
- Sensors based on variations in frequency, for instance Quartz Crystal Microbalance (QCM) and Surface Acoustic Wave (SAW)
- Sensors involving selective agents, such as molecular films or complexing films

Among all these sensors, sensors based on the interaction of foods with electromagnetic waves are most often used. Such sensors have been on the market for many years, in particular for laboratory purposes. On-line examples are also numerous: x-rays, visible light sensors or machine-vision based inspections, near-infrared sensors, or microwave sensors. Table 1 [44] lists the electromagnetic sensors classified on the basis of the wavelength of the electromagnetic waves applied.

This research utilizes a machine vision-based quality inspection system to provide on-line real time quality information of the baking product to the control system.

Table 1. Electromagnetic waves (EMW) and their interactions [44]

Wavelength Metre (m)	Region	Interaction	Examples
	Radio frequency (1-10 m)		Water, salt, density, Particle size
* 10 exp -1	Magnetic resonance (0.01-10 m)	Electron/nuclear spin	Water, oil quality
* 10 exp -3	Microwaves (0.01-0.15 m)	Dipole (4-15 cm)	Water, density, sucrose, Fat, density
	Far-IR MIR (2.5-30 mm), Raman, thermography (1-15 mm)	Vibration and rotation	Qualitative, quality, temperature
* 10 exp -6	NIR (700-2500 nm)	Vibration overtones	Water, oil, protein, qualitative measures
* 10 exp -7	Visible (400-700 nm) Ultraviolet	Electrons	Many organic compounds, colour
* 10 exp -9	X-rays	Ionisation	Foreign bodies
* 10 exp -11	y-rays	Ionisation	

1.2.2 Machine Vision-based Quality Inspection System

Recently, machine vision has been used in many applications. For example, Rabie [19] discussed machine vision technologies used for traffic control. Zeng [22] introduced vision-based motion tracking technologies used for analysis of breast self-examination (BSE) technique. Dickmanns [17] and Kosecka [23] presented machine vision based technologies used for task planning in unmanned vehicles. Piepmeier [20] and Kwolek [21] explained how machine vision technology is being used for robot motion control. All of these applications utilize machine vision for the purposes of recognizing objects, tracking and locating.

In recent years, with the rapid development of the computer vision systems, it is much easier to build an automated vision-based inspection system for quality control purposes. There has been a lot of work on the methodology and application of vision-based grading and quality assessment systems [3, 4, 5, 6]. With these advanced methodologies, accurate and uniform inspection of various products is possible.

Machine vision is also widely used for manufacturing processes. The primary goal of machine vision systems in manufacturing is to improve productivity and quality of the product through quality inspection. For example, Graves [26] showed how a vision system determines whether parts or sub-assemblies are acceptable or defective, and then directs motion control equipment to reject or accept them. Blackwell [18] presented an example of machine vision in the tire industry. It is used in three categories: non-contact measurement, process verification, and product identification. The real benefit of machine vision is realized when the inspection data can be tied back in to the machine control architecture for true automatic closed loop process modification. Feldmann [15]

also presented a vision-based inspection system for closed loop quality control in printed circuit board assembly. In this research, a machine vision-based feedback system is incorporated into a hierarchical monitoring and control system for the baking process.

In her Ph.D. thesis, Ding [27] pointed out the general scheme for real-time inspection as shown in Figure 1. It consists of three modules: image acquisition module, image processing module, and decision making module. Her work is now discussed in the context of the proposed work and we specifically consider how this scheme fits into quality inspection for feedback control.

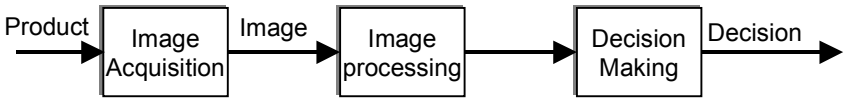

Figure 1: General scheme for machine vision-based inspection [27].

- Image acquisition

Imagery for inspection purposes can be generated from a variety of techniques, for example, visible, infrared (IR), ultraviolet (UV), laser, and x-ray sensors. An imaging system usually consists of the following components:

  - Camera: the camera generates an image of the scene.

- Data acquisition board (frame grabber): the board collects the data generated by the camera, forms the image, and transmits the image to the data storage unit of the processor.
- Illuminator: it is designed to maximize contrast both between the product and background (such as a conveyor belt) and between abnormal and normal objects, while minimizing artifacts.

Current process control in manufacturing processes mainly relies on process monitoring data acquired from temperature, pressure, or speed sensors. Due to rapid progress in the computer industry, the cost of an imaging system is decreasing rapidly while the speed and reliability are increasing. This makes the real-time imaging for quality inspection feasible.

- Image processing

To implement a machine vision application successfully, it is essential to understand the characteristics of the parts and sub-assemblies which the vision system will examine, as well as the specifications of the production line itself. Key characteristics include specific part dimensions, part tolerances, the level of measurement precision required, the minimum size of defects to be detected, and the speed of production line.

The purpose of image processing for quality inspection is to extract useful information from the images acquired, and thus obtain the quality features of the product. Segmentation is a critical step in this image understanding process to extract the useful information. There exist a lot of techniques for segmentation, such as thresholding

technique, adaptive thresholding method, morphological methods, snake-based algorithms, or neural-net based segmentation algorithms. Unfortunately, many of these segmentation algorithms are time-consuming and thus not suitable for real-time applications. A common solution is to incorporate techniques that take full advantage of the *a priori* knowledge of the object and background characteristics.

- Decision making

The quality of the product is represented by quality features extracted from the images after segmentation. The decision making module often contains a feature extraction module and a classification module. Various numerical features are first computed by the feature extraction module based on the region map obtained from the image processing module, and then a classifier is deployed to determine the quality level. This quality information is then fed back to the process control module to improve the product quality. Candidate quality features for baking products include color and color distribution, shape, size, seed coverage and seed distribution, and other features that include a priori information about the object and its background, such as moisture and thickness.

The quality features are usually obtained on the basis of the consumer's requirements, and are predefined in the quality planning stage by the quality control staff. The quality control staff evaluates the quality in classes of these features. For example, five classes characterizing biscuit color, ranging from over-cooked to under-cooked, are defined in [34].

Classification algorithms are usually applied in order to assign a class to each considered region on feature distribution map. There are two particularly important

aspects that are related to object classification. The first is the problem of, given an input feature vector, deciding whether it belongs to some specific predefined class, which is usually known as supervised classification. The second equally important aspect of object classification is how to define or identify the involved classes in a population of previously unclassified objects. This represents a difficult task, and expert knowledge acquisition problems are usually involved. The latter situation is known as unsupervised classification or clustering.

1.3 Process modeling

High fidelity process models and product quality models are essential to control and optimize the process. Numerous modeling techniques support both steady-state models and dynamic models. Assuming that the low-level controllers are responding fast enough to control to the desired operating parameters, then the mid-level control can be treated as a static optimization. However, this should contain some constraints based on the ability of the low-level control to follow the command. Under this assumption, this research focuses on the steady-state modeling of two aspects: the coupling effect between the process operations, and the product quality.

1.3.1 Product quality model

There are two basic ways of modeling product quality: analytical models and empirical models. Analytical models of simple processes can be obtained by developing differential equations that describe the conservation of mass, energy and momentum that occur in these processes. However, it is important to consider the relative complexity of the physical and chemical transformations that occur in baking processes. This complexity makes it time-consuming and difficult, if not impossible, to develop accurate process

models from first principles alone. Sablani [30] did a good review of several papers that modeled heat transfer during the baking process using a finite difference method based on the differential equations that describe the conservation of mass, energy and momentum. These finite difference models are primarily used for the design purposes to analyze heat transfer in the baking process so that the optimum quality of the baking products can be obtained, but are not suitable for control purposes. Empirical models, on the other hand, rely too much on the data. In some cases, it is not feasible to implement all the experiments to obtain enough data to train the models. Therdthai [31] conducted experiments designed by a multi-level partial factorial. Based on 96 experiment results, using linear regression, he established mathematical models to describe the effects of tin temperature and baking time on bread quality attributes. There are also papers discussing intelligent quality models generated from neural networks, expert knowledge systems and fuzzy logic [32] [33] [34] [35] [15]. All are established to link operation set points directly to quality metrics. Thus, when there is any change in the quality metric index, the model has to be re-established, and the experiment and training effort will be very high.

1.3.2 Decoupling model

Large industrial ovens usually include several heating zones in order to improve the temperature profile control. However, due to the heat flow, there is an interaction among these zones. As in other cases of multiple-input multiple-output (MIMO) systems this interaction may become relevant and cause serious coupling effect.

Though the heating process in an oven is a nonlinear process, it can be shown that for some temperature profiles the system behaves linearly allowing a linear analysis and design. Galvez [37] presented a linear simplified tri-diagonal matrix transfer function

model for a nonlinear, six-heating –zones electrical oven system. Lu [38] also presented a diagonalized plant model derived for decoupling purpose in his paper. Jia [39] proposed to describe each channel of the multiple-input–multiple-output system by a first-order transfer function with variable coefficients and a fixed time delay. A model reference adaptive control scheme, which can simultaneously achieve adaptive decoupling and model matching, is also proposed by Jia.

In this research, since only the steady-state coupling model is considered, it would be easier to establish the coupling model. Assuming the baking oven exhibits only mildly nonlinear behavior within a certain operating temperature range, the local linearization modeling techniques will work well in this situation. Thus we can conduct experiments of step responses to test the steady-state output responses for each input. By summing them together, a coupling model would be generated. Also by testing the responses under different burner failure conditions, the weights of the sum operation under each condition can be acquired and the model can be made adaptive.

1.4 Process control

At the turn of the 20th century, control was exercised primarily by process operators making manual adjustments. In the decades since, control theory and practice have evolved to the extent that, today, highly sophisticated control schemes make possible the efficient manufacture of a whole range of products [1]. But not all processes have a ‘state of the art’ control system. In the food processing industry, for instance, process control has meant for many years off-line sampling and manual correction. This approach to process control comes about primarily due to the difficulties involved in measurement.

Measurements such as taste, texture and cooked product color are difficult to make and even in some cases problematic to quantify [2].

With intelligent sensing technology that makes quality assessment consistent, people start to concentrate on a higher level of quality control --- to improve the process for increased productivity and assured quality based on feedback information from inspection of the product. A good example is presented by Feldmann in printed circuit assembly [15]. In this paper, a systematic approach for on-line measurements of process conditions and process results is discussed. This approach is possible with in-line integration of automated optical inspection systems and integration of on-line sensing devices into the manufacturing equipment. Correlation of process conditions and quality data enables the analysis and implementation of effective process and quality control mechanisms. Blackwell [18] also examined the use of machine vision as an intelligent sensor for the acquisition of process data and the ways in which that data can be assimilated into closed loop control of the tire manufacturing process to improve the process.

Haley [11] reviewed advanced process control techniques for the food industry as shown in Figure 2.

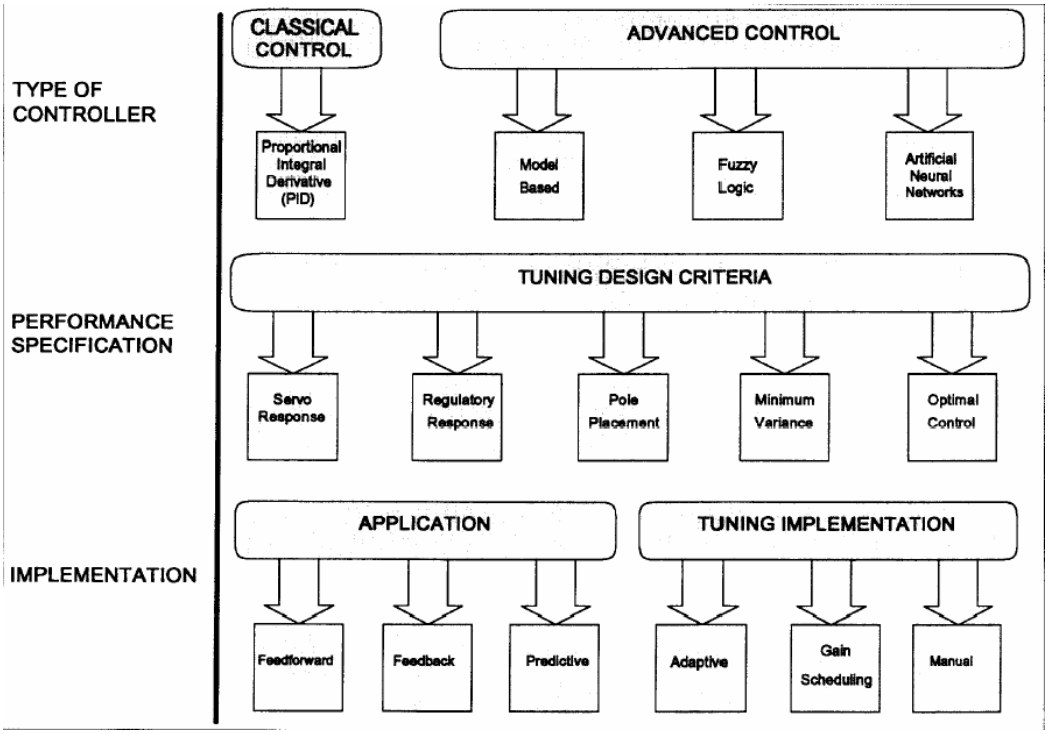

Figure 2: Advanced process control techniques for the food industry [11].

Closed-loop control examples for quality improvement of food processes can also be found. Perrot [34] illustrated fuzzy controller design for baking of biscuits. The color, moisture and thickness of the biscuits were selected as the quality features to be measured. A Colorex sensor (Infrared Engineering) was used on line to measure color, a near infra-red analyzer was used on line (Infrared Engineering, MM55G) to measure moisture, and a caliper was used off line manually to measure the thickness. A fuzzy k-nearest neighbor classification algorithm was developed. The fuzzy controller rules are established based on human experience. The result showed some improvement of biscuit quality, but there was no discussion of stability analysis for the feedback controller.

Neither did this work consider the effect of the long time delay of the feedback information.

Kim [35] illustrated a simulation system in which neural networks were used for modeling the three quality factors of the baking product, and a fuzzy controller was used to control the baking oven based on the prediction from the models. The oven in this application is a stationary oven so that continuous measurements of the quality factors, such as volume and browning, are possible during the baking process via a camera. The neural nets take the measurements of quality factors in time t as inputs to predict the quality factors at time t+1. Based on this prediction, the oven was controlled via a relay operation (that is, ON/OFF) to keep within the pre-set temperature range. Knowledge from the experiments and an experienced operator were used to construct 11 rules for the fuzzy controller. The simulation results showed that the developed neural networks and fuzzy controller can be used to reduce the cost for heating the oven without any loss of bread quality. This work provided some guidelines on controlling the baking process to save energy, but it cannot be used in real time industrial baking processes because for most of the large scale industrial ovens, continuous measurements of the quality factors are impossible since most of the sensors for quality measurement cannot survive the high temperature inside the oven.

Finally, in another food processing application, Montague [33] presented a feed-forward incorporated with feedback control strategy for improving french fry quality, and compared it with the feedback control only strategy. The fry quality parameters measured include the moisture content, fat content, color of fry, texture and chip size distribution,

which were done in the quality control lab once per hour. The inspection was not done real time, on-line, and there was no analysis of stability with the feedback controller.

In this research, not only are advanced process control techniques utilized for quality improvement, but also a hierarchical intelligent control architecture is proposed to provide a systematic way to incorporate each module related to quality improvement. This control architecture is novel for the baking process, and will significantly improve the product quality and productivity.

1.5 Problem statement

The objective of this research is to create a vision-based systems approach to product monitoring and process control for the complex industrial processes. In the application example of this research, color of the baking product is selected as the feedback information for control regulation. The hierarchical monitoring and control architecture consists of a low-level control module, a mid-level control module, a high-level control module and also a sensor module as shown in Figure 3.

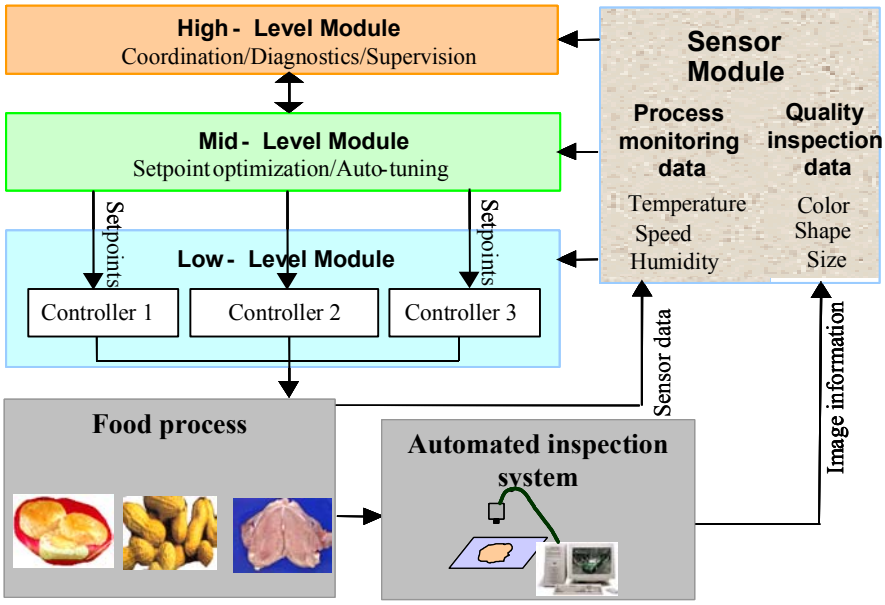

Figure 3. Hierarchical/intelligent control architecture for a baking process

- The low-level control module consists of basic control loops. Each of them controls parameters of each operation in the process separately. They are generally simple and easy to implement.
- The mid-level control module is responsible for generating optimal set points for the low-level control module to coordinate the operations based on the process model, process operation parameters, and feedback information of the product quality. This module is responsible for the real time control for quality improvement based on quality inspection.
- The high-level control module involves scheduling of multiple plant processes, diagnostics of the failure condition in the process, and the supervision of the whole process.

- The sensor module consists of a vision-based inspection system and a process monitoring system. The vision-based inspection system is responsible for monitoring the product quality in real time. The process monitoring system is responsible for monitoring the process operation parameters.

This research is mainly focused on the mid-level control module. The quality information from the quality inspection module is fed back to the mid-level control module. Based on this information, the set points of the low-level control module would be calculated systematically real time, online, to improve the product quality. At the same time, since the feedback control based on the quality inspection may not produce satisfactory performance due to the long time delay of the inspection result introduced by the production time, for example, baking time in baking process, model-based feed-forward control strategy is introduced in combination with feedback control in the proposed work to compensate for the long time delay of the feedback information. More often than not, failure conditions of some components are known a priori to the processing of product. Measurements for some disturbances of the product process are available as well. For example, a burning failure in the baking oven can be detected real time from the process monitoring data. In these cases, feed-forward controllers can generate the corresponding optimal operation set points in advance to assure product quality.

Process models are needed for model-based control strategy. Even though low-level controllers are available in most of the current industries, due to the coupling effect between the process operations, an adaptive coupling model is needed for the mid-level control module to calculate the set points. Also, a static process quality model is

generated for the purpose of establishing the link between information coming from the measurement of product features and the specification of process control strategies. There are two basic types of modeling techniques: physical models and data-driven models. The development of the physical model of the process requires knowledge of relatively complex physical and chemical transformations that occur in the processes. This complexity makes it time-consuming and difficult, if not impossible, to develop accurate process models from first principles alone. Data-driven models have been proposed in recent years based on soft computing techniques such as neural networks and fuzzy logic. The development of a data-driven model requires a lot of training data, which may not be available or acquirable. Recognizing the shortcomings of both the physics-based and the data-driven modeling approaches, we propose a novel architecture that combines both approaches whose primary objective is to predict as accurately as possible the quality of the product so that optimum control set points can be estimated.

The contributions of the research:

- We generate a novel quality modeling method, which combines both physics-based and data-driven models. Since the quality model is broken down into several sub-models, its flexibility is greatly increased. The effort required to change the model when quality metrics change is greatly reduced.
- We apply a hierarchical control architecture to baking processes, which provides a systematic way to incorporate advanced process control techniques based on feedback provided by machine vision-based quality inspection systems.

- We verify the proposed modeling method and control architecture using advanced Design of Experiment (DOE) methods.
- We implement hybrid system analysis methods to validate the performance of the vision-based feedback controller.

The dissertation is organized as follows. In Chapter 2, the product quality modeling methodology is presented thoroughly. The application example for the product quality modeling is then presented in Chapter 3. In Chapter 4, the mid-level control strategy for the architecture is described. Following that is the application example for control strategy in Chapter 5. Finally, the significant contributions of this thesis are summarized and future work is discussed.

CHAPTER 2

PRODUCT QUALITY MODELING

High fidelity models of the baking process are essential to control and optimize the process. Model development is a crucial step to predict the system output for model-based feed-forward control strategy. Typical models are low-level process models, but not the relationship between low-level process and the product quality metric. A product quality model is generated in this research to incorporate with the feed-forward control strategy in mid-level control module.

A data driven model can be developed for each quality metric of the product as in [31]. But this takes a lot of effort to acquire the data and generate each model. Also, if we want to optimize all the quality metrics with the feed-forward control strategy, all the models will be used for multiple-objective optimization. The computation effort is too high in this way. It is also difficult to build a single quality model to cover the variety of the food process product quality metrics that are monitored. A novel generalized quality-modeling framework is developed in this research that breaks the quality model into two sub models: a temperature profile model and a profile quality mapping model. The modeling framework is shown in Figure 4:

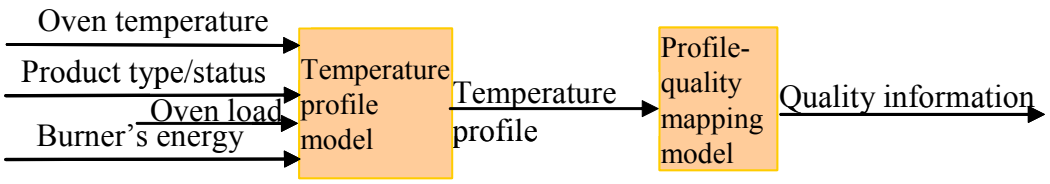

Figure 4. Quality modeling framework for baking product

The temperature profile model predicts the baking product temperature profiles given the inputs. The temperature profile is a plot of temperature versus baking time. The profile is closely related to oven type, oven topology, and product type. A physical-based model is developed to model the heat transfer from the heat sources to the baking product inside the oven, depending on knowledge of the oven type and topology. A data-driven model is also generated to calculate the model parameters for each product type. The second component in the model is the profile-quality mapping model, which is only related to the product type. For each product, this model takes the temperature profile as input, and predicts the quality information. A data-driven model is developed for each product type.

The advantage of this modeling framework lies in following aspects:

- Generalized to all baking products;
- Open and modular. Modularity gives flexibility since it is easy to change or add any quality parameter since only the profile-quality mapping model needs to be changed.
- Flexible for optimization of feed-forward controller. Product temperature profile can be selected as optimization objective using temperature profile

model if all the quality metrics need to be addressed, each single quality metric can also be selected as optimization objective using the whole quality model.

2.1 Temperature profile model

An expanded view of the temperature profile model is shown in Figure 5 for a multi-zoned oven. Its primary objective is to predict as accurately as possible the temperature profile of the baking product so that optimum control set points can be estimated.

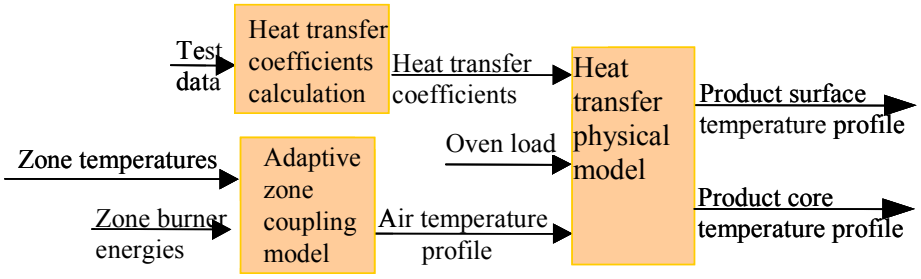

Figure 5. Scheme for modeling baking product temperature profiles

An example of the baking product surface and core temperature profiles is shown in Figure 6.

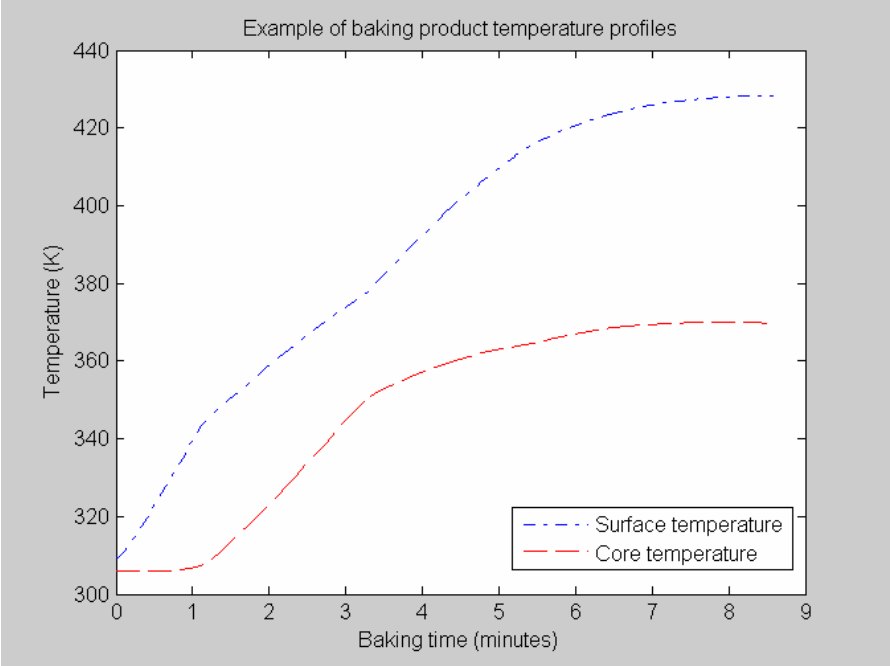

Figure 6. Example of baking product temperature profiles

There are three steps in establishing the profile model:

- Identify the physical model;
- Design experiments according to the identified physical model and calculate heat transfer coefficients using data from the experiments;
- Establish an adaptive zone coupling model using the experimental data.

2.1.1 Heat transfer physical model

There are three types of heat transfer: conduction, convection, and radiation. Generally all of these three types of heat transfer exist in a baking oven. For example, heat can be transferred:

- By conduction to the bottom of the baking product, which is in contact with the baking pan, and by conduction from the baking product surface to the product core.
- By either free or forced convection between the air and the baking product's exposed surface.
- By radiation from the oven wall, and/or radiation from flame.

It is important to identify the mode(s) of heat transfer when we want to establish the physical model to predict the temperature profile. The transfer of heat in the oven by each individual mode can be expressed in terms of temperature driving force, transfer area and heat transfer coefficient, assuming steady state heat transfer.

By conduction: $q_c = KA_c(T_h - T_i)/X$ (2-1)

By convection: $q_f = h_f A_r(T_a - T_s)$ (2-2)

By radiation: $q_r = F_s A_r \sigma(T_w^4 - T_i^4)$ (2-3)

Table 2. Parameters for heat transfer modes

q_c	Heat transferred by conduction
q_f	Heat transferred by convection
q_r	Heat transferred by radiation
K	Average thermal conductivity of the baking product
h_f	Heat transfer coefficient for convection
F_s	Overall coefficient for radiation heat transfer
A_c	Area of baking product exposed to conduction
A_r	Area of baking product in contact with heating medium exposed to convection
σ	Stefan-Boltzman constant
T_h	Hot side surface temperature of baking product
T_i	Initial temperature of baking product
T_a	Temperature of hot air
T_s	Surface temperature of baking product exposed to air
T_w	Wall temperature (or flame temperature)
X	The thickness of the product

For a given product, the above mentioned coefficients can be calculated through experimental data after the heat transfer modes are identified. For example, there is convection between the hot air and the baking product surface, conduction between the hot baking pan and the baking product bottom, and radiation between the hot burner and baking product surface. Experiments can be done to analyze how much each heat transfer mode counts in the total heat transfer. Even though most of the coefficients are functions

of temperature and product status (for example, the moisture, gas, etc. content inside the product), these coefficients can be treated as constants within certain range of temperature. Thus when the types of products are limited in an application, experiments can be designed to calculate a group of coefficients for these products so that the proper model can be used for each product in each stage.

2.1.2 Calculation of heat transfer coefficients

The measurements needed for the calculation of heat transfer coefficients are different depending on the heat transfer modes inside the oven. The following issues need to be considered when designing the experiments:

- Identify variables to be calculated and to be measured
- Select sensors
- Determine sensor locations

A robust design method such as Taguchi's method [42] is often used in the designing stage of a process to optimize the process. It can also be used to design the experiments for calculating heat transfer coefficients so that the data can be acquired to cover the full dynamic range of the model. Taguchi's approach to parameter design [42] is utilized in this research to design the experiments. A key component of Taguchi's philosophy is the reduction of variability. It uses orthogonal array designs to significantly reduce the number of experimental configurations to be studied. This simplifies the analysis and interpretation of results. Furthermore, the conclusions drawn from small scale experiments are valid over the entire experimental region spanned by the control factors and their settings.

Orthogonal arrays were originally discovered as a numerical curiosity [52]. The arrays went largely unnoticed until the 1950s. It was then that these "numerical curiosities" were picked up by the statistics community and put to use in statistical test design. Dr. Genichi Taguchi was one of the first proponents of orthogonal arrays in test design.

Orthogonal arrays are two-dimensional arrays of numbers that possess the interesting quality that by choosing any two columns in the array you receive an even distribution of all the pair-wise combinations of values in the array. Here is some terminology for working with orthogonal arrays:

- Runs: the number of rows in the array. This directly translates to the number of test cases that will be generated by the Orthogonal Array Testing Strategy (OATS) technique. Each row corresponds to one test case.
- Factors: the number of columns in an array. This directly translates to the maximum number of variables that can be handled by this array. For example, we consider the *N* oven zone temperatures to be *N* variables in the test, and the baking product temperature profiles and quality factors are the test results.
- Levels: the maximum number of values that any single factor can have. An orthogonal array will contain entries from 1 to Levels. For example, we consider 3 levels for temperature in each zone. The specific temperature value corresponding to each level might be different in different zones.

- Strength: the number of columns it takes to see each of the Levels^{Stength} possibilities equally often.
- Orthogonal arrays are most often named following the pattern $L_{Runs}(Levels^{Factors})$.

An example of $L_9(3^4)$ orthogonal design with 9 runs, 4 factors, 3 levels, and strength of 2 is shown in Table 3.

Table 3. An $L_9(3^4)$ orthogonal array with 9 runs

		Factors			
		A	B	C	D
Runs	1	1	1	1	1
	2	1	2	2	2
	3	1	3	3	3
	4	2	1	2	3
	5	2	2	3	1
	6	2	3	1	2
	7	3	1	3	2
	8	3	2	1	3
	9	3	3	2	1

In this array, the columns are mutually orthogonal. That is, for any pair of columns, all combinations of factor levels occur; and they occur an equal number of times. Also, if we use –1 to replace level 1, 0 to replace level 2, and 1 to replace level 3,

then all the dot product of any two columns are 0, which is the mathematical meaning of orthogonal for array columns. Note that this design reduces 81 (3^4) configurations to 9 experimental evaluations.

On the other hand, the Taguchi method provides limited information about interactions. Since this research also established an oven zone coupling model to model the interactions between the zone temperatures, this limitation is not important to us.

Given the measurements from the experiments, there are several methods to calculate the coefficients of the heat transfer model. Among them, the regression technique is often used to make estimations about the coefficients. The regression model is fit to a set of sample data. In some instances, the experimenter knows the exact form of the true functional relationship between y and $x_1, x_2, \cdots, x_k$, say $y = \phi(x_1, x_2, \cdots, x_k)$. However, in most cases, the true functional relationship is unknown, and the experimenter chooses an appropriate function to approximate ϕ. Low-order polynomial models are widely used as approximating functions.

This research focuses on multiple linear regression techniques because there are typically more than one design parameter. Each linear regression has this form:

$$y = b_0 + b_1 x_1 + b_2 x_2 + \cdots + b_K x_k + \varepsilon \qquad (2\text{-}4)$$

where y is the variable that we want to model and can acquire some experimental data, x_i's are variables that have effect on y. For example, if we consider the baking product surface temperature profile as a linear function of air temperature profile and baking product core temperature profile, when we use regression to model this function, y is the surface temperature profile acquired from the experiments, x_1 is the corresponding air

temperature profile, and x_2 is the corresponding baking product core temperature profile. Regression result will give the values of coefficients b_1 and b_2.

Models that are more complex in appearance than equation (2-4) may often still be analyzed by multiple linear regression techniques. For example, consider adding an interaction term to the first-order mode in two variables, say

$$y = b_0 + b_1 x_1 + b_2 x_2 + b_{12} x_1 x_2 + \varepsilon \tag{2-5}$$

If we let $x_3 = x_1 x_2$ and $b_3 = b_{12}$, then equation 2-5 can be written as

$$y = b_0 + b_1 x_1 + b_2 x_2 + b_3 x_3 + \varepsilon \tag{2-6}$$

which is a standard multiple linear regression model with three regressors.

2.1.3 Adaptive zone coupling model

The typical industrial baking oven generally has several zones, either linear or spiral, with a conveyor belt moving inside the oven. In most of the ovens, separate control loops exist for burners in each oven zone. There is heat transfer between the zones, which is termed the zone coupling effect. When one of the burners fails, the heat is transferred from adjoining zones, an effect that compensates for the failure. In order to calculate the temperature set points of each zone during one or two burners' failure condition, it is very important to understand the zone coupling effect. The adaptive zone coupling model is established for this purpose.

A model of the zone coupling effect is shown in Figure 7. Let Q_i be the energy absorbed by the *i*th zone after the coupling effect, define the zone coupling as:

$$Q_i = f_i(Q_{b1}, Q_{b2}, \cdots, Q_{bn}, T_1, T_2, \cdots, T_n, L) \qquad i = 1,2,\cdots,n \tag{2-7}$$

where Q_{bi} is the energy generated by the burner in the ith zone, T_i is the temperature in the ith zone, and L is the product load.

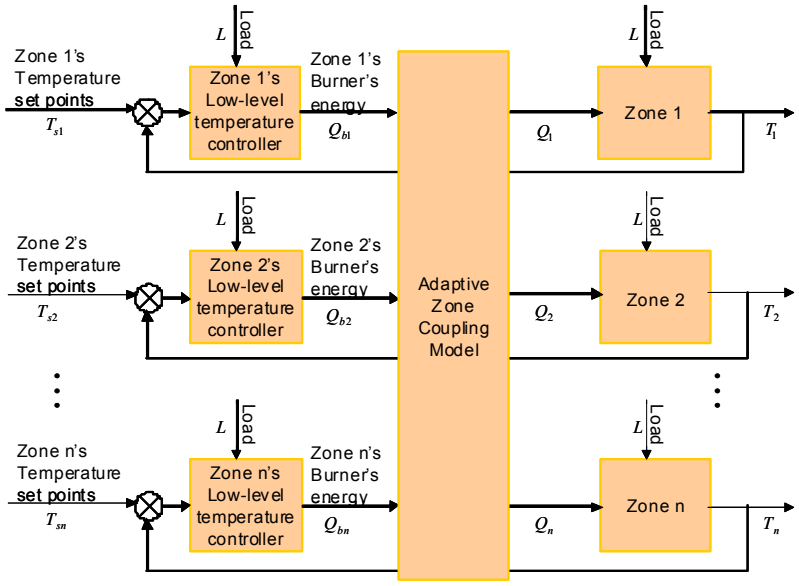

Figure 7. Oven zone coupling schematic

We assume linearity to establish the model for the coupling effect. Within each temperature range that the system can be treated linearly, step responses will be obtained through experiments. Thus when there is a change in the temperature set points, the steady state response of air temperature would be:

$$\Delta T_i = \sum_{j=1}^{n} c_j R_{ij}(\Delta T_{sj}) \qquad i = 1,\ldots,n \qquad \text{(2-8)}$$

where ΔT_i is the step response of zone i with a step input from T_{sj}, $c_j (0 \le c_j \le 1)$ is the coefficient that depends on the online monitoring of zone burner's working condition. Assuming a linear relation, then

$$c_j = \frac{Q_{bj}}{Q_M} \qquad j = 1, \ldots, n \qquad (2\text{-}9)$$

where Q_{bj} is the energy produced by burner j obtained through online monitoring, and Q_M is the maximum heat that a burner can produce.

2.2 Profile-quality mapping model

The second part of the quality model shown in Figure 4 is the profile-quality mapping model, which maps the temperature profiles to the quality metrics. The profile-quality mapping model contains a feature extractor and several quality metric predictor as shown in Figure 8.

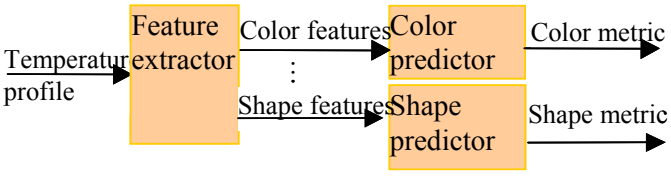

Figure 8. Profile-quality mapping model

- Feature selection

The features used to predict different quality metrics may be different, but several points on the temperature profile are of common interest. For example, the temperature profile shown in Figure 6 is shown again in Figure 9 with the inflection points in the core temperature profile identified. These points divide the baking process into three stages. In the first stage (before Point1), the heat begins to penetrate the surface and migrates to the interior, bringing about a steady rise in baking product surface temperature. In the second stage (between Point1 and Point2), both surface temperature and core temperature are rising. This rise in temperature greatly accelerates yeast activity, producing a rapid evolution of carbon dioxide gas and expansion of dough gases [59]. Enzyme action also reaches a maximum rate, resulting in the rapid dextrinization of starch, sugar formation, and gluten modification. The combination of these reactions produces a marked volume expansion and is known as oven spring. In the third stage (after Point 2), crust formation starts and color is developed. The crust plays an important role in retaining the volume attained during oven spring and preventing further volume expansion. The sugars of the crust are then caramelized under the influence of intensive heat and high moisture, resulting in the browning of the crust. The high temperature results in considerable evaporation of moisture from the baking products, bringing about a slight shrinkage in its volume and a loss of weight.

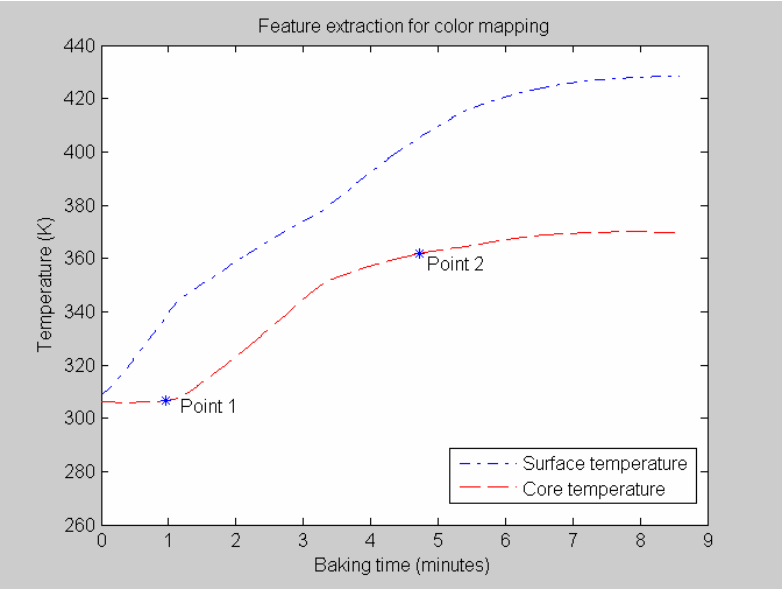

Figure 9. Example of feature extraction for quality mapping

As described above, the second stage and third stage have the most impact on the quality metrics like the color and the size. So the features used to estimate these quality metrics can be calculated by first calculating Point 1 and Point 2. In this research, the proposed features for color mapping are:

- The time period after Point 2
- The mean surface temperature after Point 2

- Modeling

A sugeno type NN fuzzy model is selected to model the quality predictors. As shown in Figure 10, the model inputs are the features extracted from the temperature profiles, and the model outputs are the quality metrics. Training data is obtained through the designed experiments.

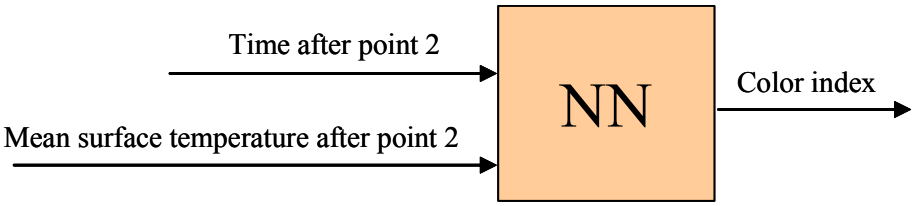

Figure 10. NN model for color predictor

2.3 Model performance evaluation

The modeling method for each sub model in Figure 4 is different, so the model performance evaluation method for each model is also different. The following sections explain the model performance evaluation methods in details.

2.3.1 Model performance evaluation for temperature profile model

As mentioned in 2.1, the temperature profile model is calculated using experimental data with regression models. The performance evaluation of the regression models can usually be assessed from several aspects: residuals, goodness of fit, and significance of terms in the model.

- Residuals

The difference between the actual data point y_i and the predicted data point $\hat{y}_i$ for each point in a data set is called the residual ε_i, as shown in Figure 11:

$$\varepsilon_i = y_i - \hat{y}_i \tag{2-10}$$

Residuals are a measure of the prediction error of the model, so we want them to be as small as possible.

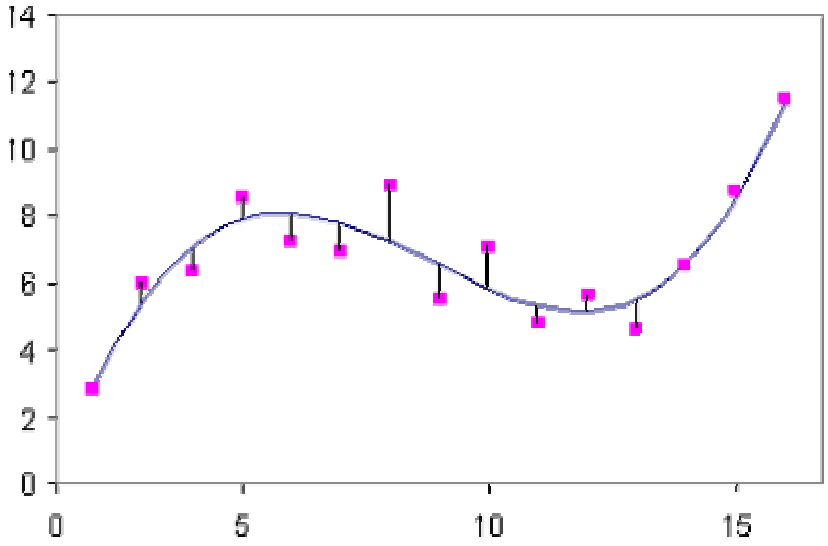

Figure 11. Residuals (errors) between the model (solid line) and data points (pink rectangles)

- Goodness of fit

Two statistics are often used in regression to measure the goodness of fit: *R-squared* and *Adjusted R-squared*.

R-squared is a measurement of how well the behavior of y is captured by the design parameters used in the model. Mathematically, R-squared is computed as the ratio of the regression sum of squares (SSR) to the total sum of squares (SST) where $\bar{y}$ is the average of the data points y and n is the total number of data points.

$$R^2 = \frac{\text{SSR}}{\text{SST}} = \frac{\sum_{i=1}^{n}(\hat{y}_i - \bar{y})^2}{\sum_{i=1}^{n}(y_i - \bar{y})^2} \tag{2-11}$$

R-squared is a number between 0 and 1, where the higher the number, the better the model captures the behavior of y. Adding more design parameters (x's) to a model

will always increase R-squared. However, the added design parameters may be statistically insignificant and cause poor predictions at regions in between the data points used to fit the model.

Adjusted R-squared uses the number of design parameters plus constant used in the model p and number of data points n to correct the R-squared statistic for cases where unnecessary parameters are introduced in the model.

$$\text{Adjusted } R^2 = 1 - \left(\frac{n-1}{n-p} \right) \cdot (1 - R^2) \tag{2-12}$$

In most cases, the adjusted R-squared will not increase when additional design parameters are added to the regression model. Overall, the Adjusted R-squared statistic penalizes the inclusion of insignificant model terms. It is a better indicator of how well the model explains the behavior of y.

- Significance of terms in the model

We want to have confidence that all the design parameters (x's) in the predictive model actually belong in the model. We can achieve this by individually testing the regression coefficients (b) in the model to see if they are statistically insignificant, or unimportant. If a regression coefficient is close to zero, there is a chance it might really be zero or insignificant, and we can remove it from the model. If all the insignificant terms are removed from a model, then we are left with a model that contains design parameters that contribute significantly to the prediction of the behavior of y.

We can calculate the risk of being wrong if we assume that a regression coefficient is not zero. This risk is called the *p-value* in most regression software. The

maximum amount of acceptable risk is often 0.05 in the regression literature, so we can now say the following:

- *p-value* > 0.05: regression coefficient is statistically insignificant.
- *p-value* <= 0.05: regression coefficient is statistically significant

If the regression coefficient is statistically insignificant, the corresponding design parameter can be removed from the model. P-values less than 0.05 indicate that the regression coefficient is significant and that we have 95% confidence (1-0.05) that we can leave the corresponding parameter in the model.

2.3.2 Model performance evaluation for profile-quality mapping model

The profile-quality mapping model is trained using feed-forward neural networks after the features are selected for each quality metric. The performance evaluation of the NN models is assessed from two aspects: root mean squared error (RMSE), and the model sensitivities.

- Mean root mean squared error (RMSE)

$$\text{RMSE} = \frac{1}{M}\sum_{i=1}^{M}\sqrt{\frac{\sum_{j=1}^{N}(y_{ij}-\hat{y}_{ij})^2}{N}} \tag{2-13}$$

Where y_{ij} is the jth measurement belonging to the ith experiment and $\hat{y}_{ij}$ is the corresponding model prediction. M is the total number of experiments used for each calculation and N is the number of measurements in each experiment.

- Examination of model sensitivities

The model sensitivities reflect the trend of the model output change to each input change. It uses “+” sign and “-” sign to examine the sensitivity. A “+” sign indicates that the output is increased, if the respective input is increased, whereas a “-” sign indicates the opposite trend. After the sensitivities are calculated, the result is compared to process behaviour as verified by the experts to evaluate the performance of the model.

CHAPTER 3

APPLICATION EXAMPLE – PRODUCT QUALITY MODELING

3.1 Problem Description

The project of automated vision-based inspection and control of high-volume baking processes serves as a test bed for the proposed methodology in this research. The objective of the project is to produce a consistent product through shift changes, daily and seasonal temperature and humidity changes, and variations in oven's working conditions using advanced quality monitoring and control systems for commercial bakeries.

In order to model the process, we acquired data from the hamburger bun baking process in Flowers Bakeries, Inc. located in Villa Rica, Georgia. The production rate of that oven is up to 1000 buns / minute. The average baking time for buns is 8.4 minutes. The baking oven at that facility is a spiral convection gas oven made by Bake Tech, Inc., as shown in Figure 12. Buns are placed in pans, 24 buns per pan, and the pans are placed on the conveyor as shown in Figure 12 (a). The unbaked buns are shown in bottom portion of the figure entering the oven, and the baked buns are shown midway in the figure exiting the oven. There is a mechanism on the line to space out the buns evenly. This even spacing helps the bun pans to maneuver the turns in the oven and helps to even the oven load on the burners.

As shown in Figure 12 (b), the conveyor enters and exits the oven on the same side. Inside the oven, the conveyor spirals up 3.5 cycles on the right side of the oven and

then spirals down 3.5 cycles on the left side of the oven. The oven is partitioned into 7 baking zones, with zone 1 being the first zone that the product enters and zone 7 being the last. The conveyor enters and exits the other zones in succession. Figure 13 shows cross cuts of the oven from a top view. This sequence of pictures shows the topology of each zone in succession. Imagine a baking pan entering the oven and moving on the conveyor belt. The red star in Figure 13 shows the starting point of the baking pan in each zone, and the red triangle shows the end point.

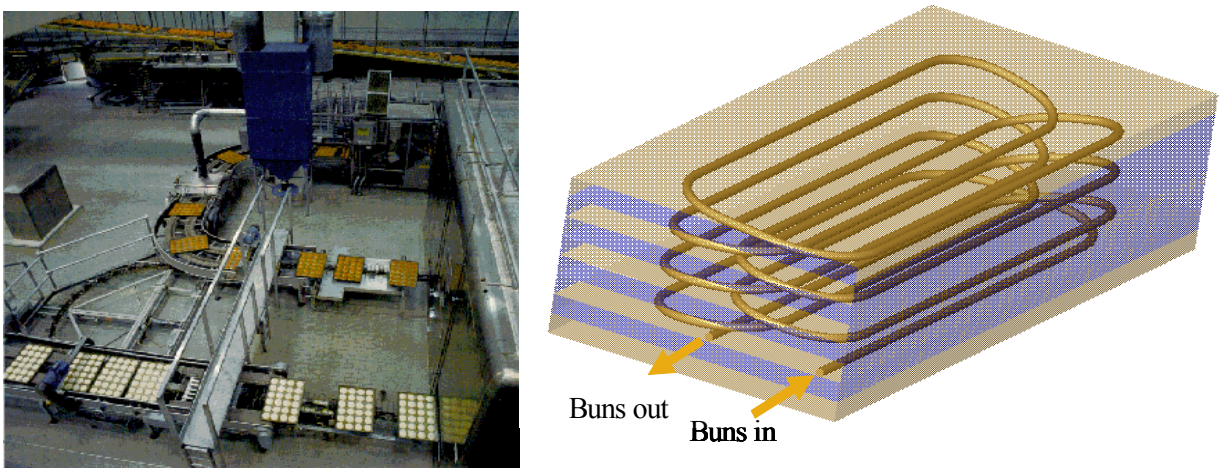

(a) Baking oven in Flowers Bakeries (b) Oven topology

Figure 12. Baking oven and oven topology

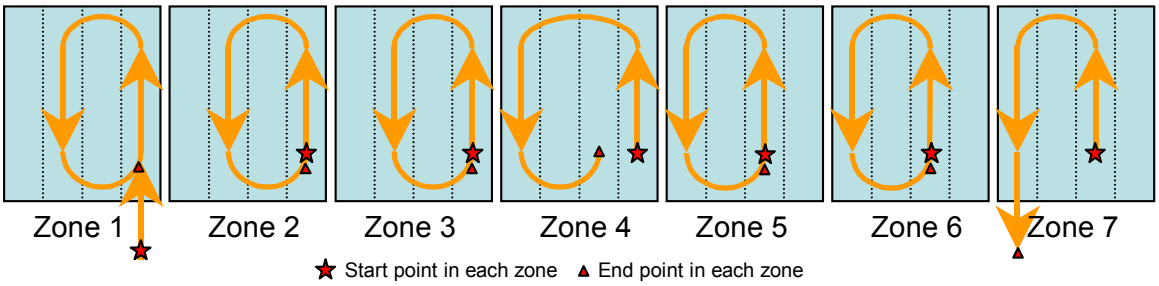

Figure 13. Cross cuts of the oven from a top view

To simplify the controls, zones are grouped as zones 1 and 2, zones 3 and 4, zones 5 and 6, and zone 7 resulting in a total of 4 control loops. In each control loop, there is a low level temperature controller using one thermocouple per zone group. The control action for the zone temperatures is the flow rate of the gas in the burners, there are 4 burners per zone. The low-level temperature controllers are implemented by Rockwell Automation PLCs. A touch screen operator interface is available for the operators to input the set points of the low-level controllers for zone temperatures and baking time and also to monitor the process data. All the data is available on the local network Data Highway plus. The oven is currently configured for the operator to enter one oven temperature set point. The control logic then converts this into 4 separate zone temperature set points, where the average of the zone set points being the oven temperature set point. This logic is determined experimentally during the tuning process of the oven during its installation. The operator can also adjust the baking time, which is done by adjusting the conveyor speed. There is a separate control loop for conveyor speed that is implemented by VFD Variable Speed Controls of the conveyor belt drive motor.

Recall from Chapter 2 that the zones in a multi-zone oven are coupled in that the burners from one zone affect the temperatures in other zones. In a linear oven, where the conveyor follows a linear line, the zones are physically adjacent to one another so that each zone is coupled primarily with only with its preceding zone and subsequent zone. In a spiral oven, however, the zones are on top of one another, so the heat transfer in one zone affects the preceding zone, the subsequent zone, and the zones that are on top or below or along side. This leads to a more complicated zone coupling model than needed for a linear oven.

3.2 Product Quality Modeling

A generic product quality model was developed as described in Chapter 2 for baking processes. This section further develops that model for application to this particular bun baking process. The developed model is used in the mid-level control module as described in Chapter 5.

3.2.1 Temperature profile model

The generic temperature profile model is described in Section 2.1 and shown in Figure 5. For this application, the details of each block are defined as in the following sections.

3.2.1.1 Heat transfer physical model

There are two primary modes of heat transfer inside the bun baking oven: forced convection from the hot air to the bun surface and conduction from the bun surface to the bun core. The radiation and conduction from the baking pan to the bun core are negligible compared to the convection heat transfer mode.

In modeling the heat transfer inside the oven, the following assumptions have been made:

- The heat transfer coefficients and thermal conductivity of the bun both depend on temperature and humidity. However, we can consider them to be constant near specific operating points.
- The heat flux from the center of the hot air to the center of the bun is continuous, therefore, the heat flux near the bun surface due to convection from the hot air is equal to the heat flux at the surface due to conduction of heat to the bun center.

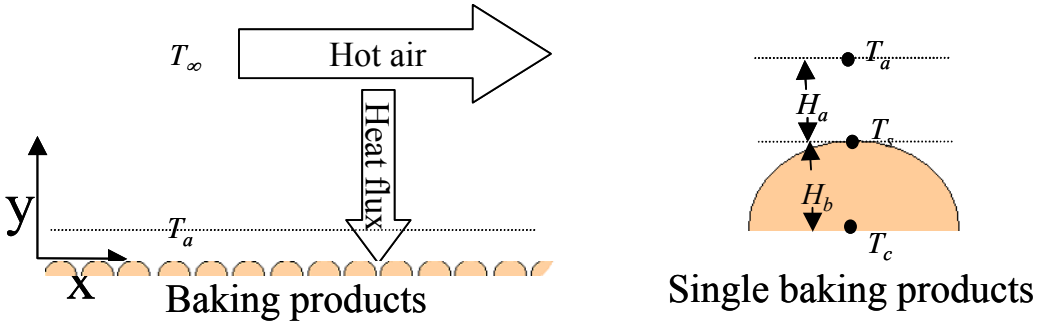

Figure 14. Physical heat transfer model.

Figure 14 shows the heat flux, both from the hot air to the product surface and from the product surface to the bun core. The general equations describing the convection and conduction heat transfer are given in Section 2.1.1 as equations (2-1) and (2-2). Table 4 gives the definition of the terms in Figure 14 along with the corresponding terms used in equations (2-1) and (2-2).

Table 4. Definition of terms in Figure 14.

Terms in Figure 14	Definition	Corresponding terms in equations (2-1) and (2-2)
T_∞	temperature from thermocouple in each oven zone	N/A
k_b	Average thermal conductivity of the baking product	K
h	Heat transfer coefficient for convection	h_f
T_c	Core temperature of bun	T_i
T_a	Temperature of the air 2 cm above the bun surface	T_a
T_s	Surface temperature of bun	T_s , T_h
H_b	Thickness between bun hot surface and bun core	X

Heat flux q'' is the heat flow through a unit of area. Using (2-1) and (2-2) with the substitutions in Table 4, the following equations for heat flux are obtained:

For conduction: $q'' = q_c / A_c = k_b(T_s - T_c)/H_b$ (3-1)

For convection: $q'' = q_f / A_r = h(T_a - T_s)$ (3-2)

With the assumption that the heat flux is equal at the bun surface,

$$q'' = h(T_a - T_s) = k_b \cdot (T_s - T_c)/H_b \quad (3\text{-}3)$$

Solving for T_s yields

$$T_s = \frac{h}{h + \frac{k_b}{H_b}} T_a + \frac{k_b / H_b}{h + \frac{k_b}{H_b}} T_c = a_1 \cdot T_a + a_2 \cdot T_c \quad (3\text{-}4)$$

where a_1 and a_2 are constants to be determined.

From Newton's law, we also have a first order model for T_c:

$$\frac{dT_c}{dt} = r(T_s - T_c) \tag{3-5}$$

where r is a positive variable and a function of T_c.

To determine the form of the function $r = f(T_c)$, r is derived from experimental data of T_c, T_s and from equation (3-5). Figure 15 shows an example of r versus T_c. From this example, r can be approximated as a second order polynomial of T_c:

$$r = f(T_c) = c_0 + c_1 T_c + c_2 T_c^2 \tag{3-6}$$

where c_0, c_1 and c_2 are constants to be determined.

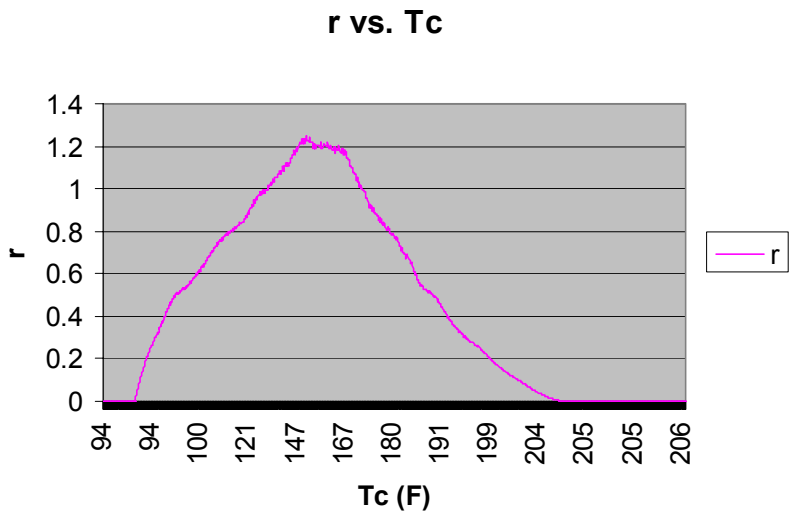

Figure 15. Example of r versus core temperature Tc

Equations (3-4) and (3-5) depend on the value of T_a. As the bun travels through the oven, the value of T_a varies depending on the different zone temperatures. A sample air temperature profile is shown in Figure 16. Since each zone has a very large space, and temperatures might be affected by neighboring zones or room temperature, the air temperature within the oven is not uniformly distributed. In industrial ovens, there is generally only one temperature measurement per zone, and this is at the location of the thermocouple in that zone. An example of that zone temperature measurement is also shown in Figure 16.

From the oven topology, we construct an effectiveness function for each zone temperature. This effectiveness function calculates how much effect each zone temperature has on the hot air temperature profile T_a along the baking process. For example, the effectiveness function for zone 1 has the largest value during the initial part of the baking process. Recall that the industrial oven has 7 zones, but combined some of these zones for control purposes yielding effectively four zones: zones 1 and 2, zones 3 and 4, zones 5 and 6, and zone 7. Therefore, we need to define four effectiveness functions, one for each of these combined zones. Since the effectiveness functions are the functions of the location in the oven, they can be also converted to functions of baking time when the conveyor speed is known. Figure 17 shows the effectiveness functions for the four zones versus time, where x_i corresponds to the effectiveness function of the *i*th zone. Each zone temperature has the maximum effect on T_a at the center of that zone. It can also affect neighboring zones, but the effectiveness will decrease with increasing distance from the zone center.

These effectiveness functions can be used as basis functions for determining an expression for T_a :

$$\begin{aligned} T_a &= f(T_1, T_2, \cdots T_n, x_1, x_2, \cdots x_n) \\ &= b_0 + b_1 T_1 + b_2 T_1 x_1 + b_3 T_2 + b_4 T_2 x_2 + \cdots + b_{2n-1} T_n + b_{2n} T_n x_n \end{aligned} \tag{3-7}$$

where $T_1, \cdots T_n$ are the thermocouple measurements of the *n* zone temperatures, which correspond to the T_∞ in Figure 14, $x_1, \cdots x_n$ are the effectiveness functions of each corresponding zone temperature. A more general expression makes use of second-order terms in x_i.

$$\begin{aligned} T_a &= f(T_1, T_2, \cdots T_n, x_1, x_2, \cdots x_n) \\ &= b_0 + b_1 T_1 + b_2 T_1 x_1 + b_3 T_1 x_1^2 + b_4 T_2 + b_5 T_2 x_2 + b_6 T_2 x_2^2 + \cdots \\ &\quad + b_{3n-2} T_n + b_{3n-1} T_n x_n + b_{3n} T_n x_n^2 \end{aligned} \tag{3-8}$$

This gives a relationship between the zone temperatures and the air temperature profile.

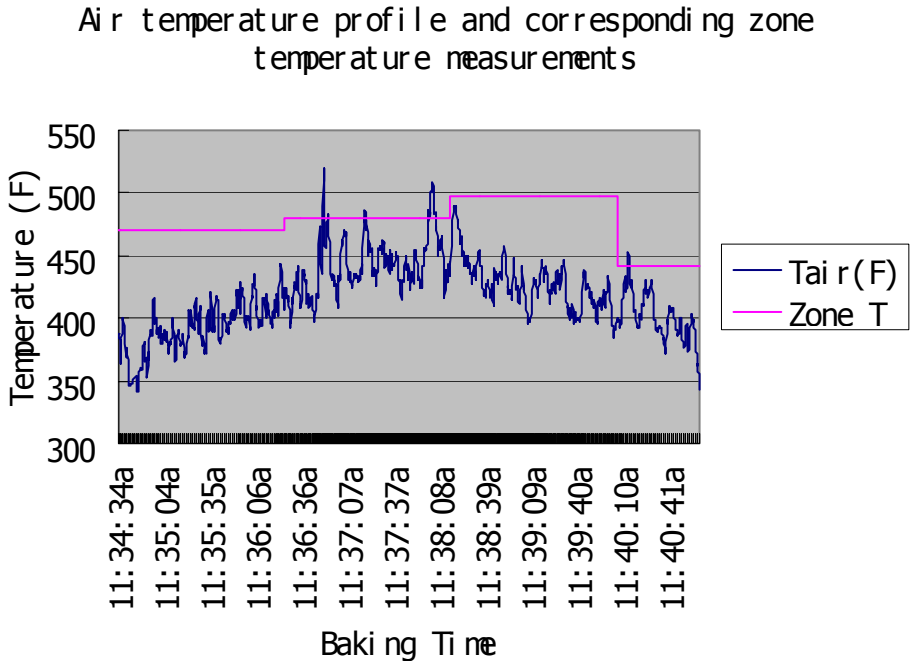

Figure 16. A typical hot air temperature profile (Ta)

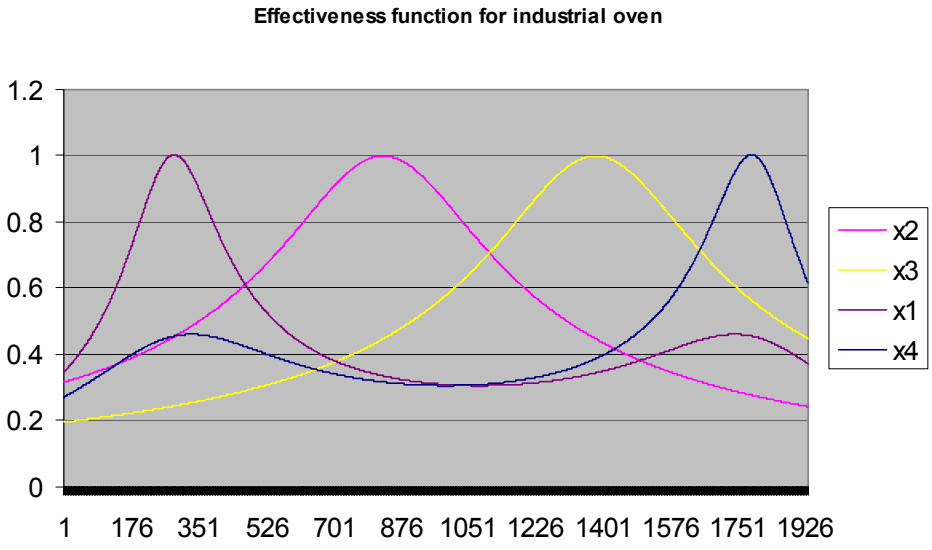

Figure 17. Effectiveness function for the 4 controlled zones of the oven in Figure 12

3.2.1.2 Data measurements and calculation of coefficients

Expressions for calculating T_a, T_s, and T_c are given by equations (3-4) through (3-8). To determine the coefficients in these equations, experiments are designed and implemented.

In order to measure the air temperature profile above the bun surface (T_a), the bun surface temperature profile (T_s) and core temperature profile (T_c) inside the oven a special high temperature measuring device called a M.O.L.E.® is used. This device has thermocouples and data logging capability that are used to record bun and ambient temperatures as the M.O.L.E. rides through the oven mounted on a bun pan. The M.O.L.E. used in this experiment is shown in Figure 18. There is an insulated box, shown open in the figure, that protects the instrument from extreme temperatures inside of the oven. Figure 19 shows sample temperature profiles for $T_a, T_s,$ and T_c taken with the M.O.L.E.

Figure 18. M.O.L.E. device for measurement of temperature profile

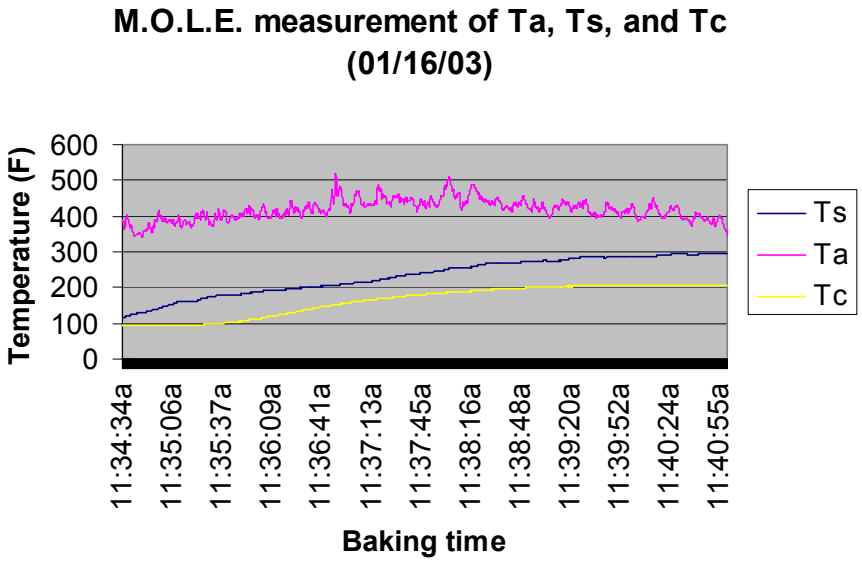

Figure 19. M.O.L.E. measurements. (Ta is the air temperature profile right above the bun surface, Ts is the bun surface temperature profile, and Tc is the bun core temperature profile)

In Section 2.1.2, a regression methodology was introduced to estimate coefficients of functions given a set of data. According to the physical model established by (3-4), (3-5), (3-6), and (3-8), we need to do the following three regressions:

1) Using the measured $T_a, T_1, \cdots T_n$, and constructed $x_1, \cdots x_n$, calculate the values of $b_0, b_1, \cdots, b_{3n}$ in (3-8) by multiple regression;
2) Using the measured T_s, T_a and T_c, calculate the values of a_1 and a_2 in (3-4) by regression;
3) Using the measured T_s and T_c, calculate r using (3-5). Then we can then use regression to calculate the coefficients c_0, c_1 and c_2 in (3-6).

We have nine groups of experimental data (bun temperature profiles $T_a, T_s,$ and T_c with corresponding zone temperatures $T_1, T_2, T_3,$ and T_4) from the industrial oven. The regression was performed twice. In one case, all nine sets of data are used to determine the model. In the other case, five are used for the regression and then the resulting model is validated using the remaining four data sets. The results from using all nine data points are shown first.

Case I: All nine sets of data are used to determine the model.

1) The values of $b_0, b_1, \cdots, b_{3n}$ in equation (3-8) found from using regression on the nine groups of data is shown in Table 5.

Table 5. Regression result for coefficients in (3-8) using data from industrial oven in Case I

	Coefficients	***P-value***
b_0	**-57.3415**	**0.16636**
b_1	**1.913734**	**1.1E-181**
b_2	**-0.10744**	**0.000456**
b_3	**0.128958**	**2.2E-11**
b_4	**-1.69725**	**0**
b_5	**0.901399**	**0**
b_6	**-0.46124**	**1E-184**
b_7	**-1.02096**	**3.6E-104**
b_8	**0.165184**	**7.05E-08**
b_9	**-0.0202**	**0.31994**
b_{10}	**1.540737**	**1.2E-219**
b_{11}	**-0.00361**	**2.82E-10**
b_{12}	**0.189065**	**0**
	Regression Statistics	
R Square		**0.697462**
Adjusted R Square		**0.697254**

Substituting these values into equation (3-8) along with the effectiveness functions and the zone temperatures results in the nine air temperature profiles shown in Figure 20, where the profiles are plotted sequentially for comparison and for ease of viewing. Also shown in Figure 20 is the corresponding experimental data showing good agreement between the model and the data. Figure 21 shows the partial derivative of the hot air temperature to each zone temperature.

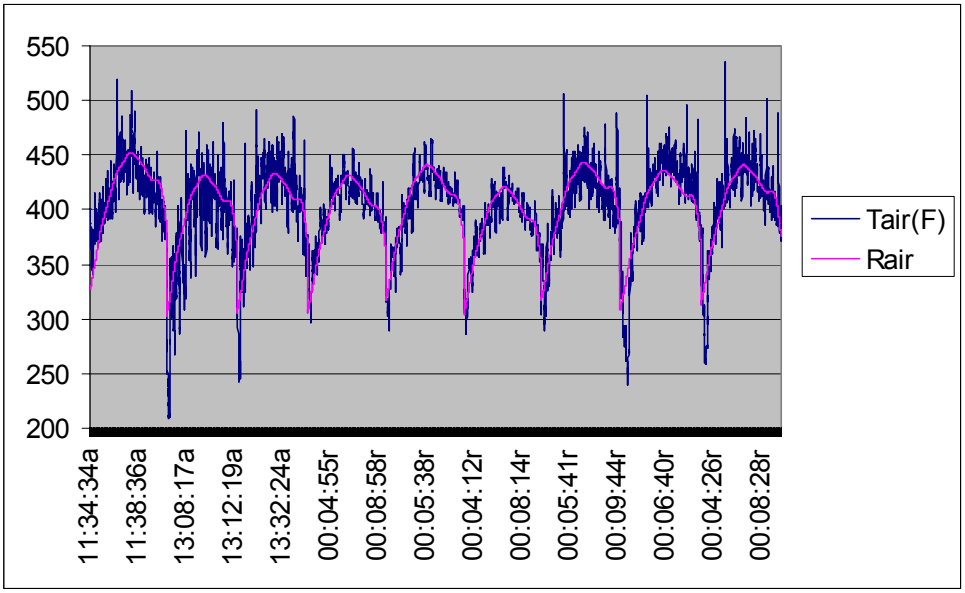

Figure 20. Experimental Tair compared with regression result (industrial oven, case I)

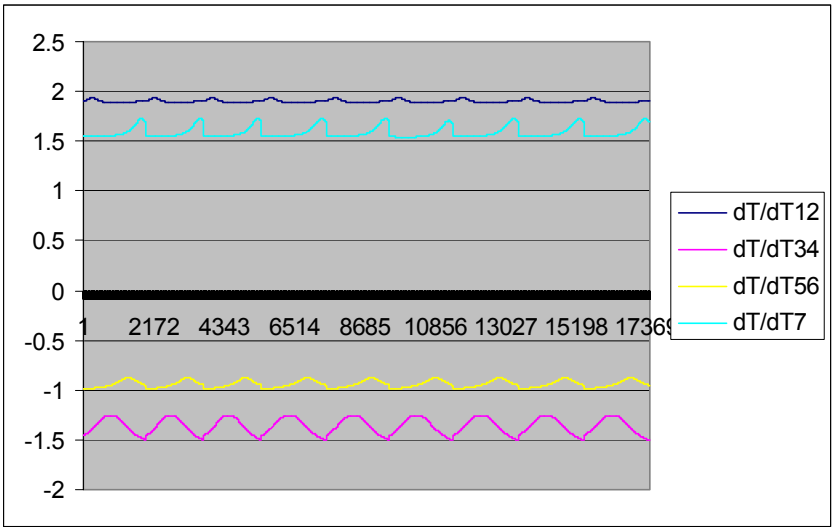

Figure 21. Partial derivatives of Tair to each zone temperature (industrial oven, case I)

This regression has good performance in terms of the *R-square, Adjusted R-square*, and *p-values* as shown in Table 5. The plots shown in Figure 20 also show good agreement with the experimental data. However, in Figure 21, we can see that the partial derivatives of T_a to the temperature of zones 3&4, and T_a to temperature of zones 5&6 are negative. This means that if we raise the temperature of zones 3&4, or the temperature of zones 5&6, the air temperature profile T_a will decrease. This is not realistic.

The reason for the discrepancy is that the nine groups of data were acquired under very similar zone temperature set point settings. The differences between the zone temperature set point settings are too small to produce sufficient air temperature profile differences. We did not have enough access to the industrial oven when we acquire data. Because the normal production cannot be interrupted and the zone temperature set point

cannot be changed as planned during the normal production. Thus, to get a better access to the oven for the experimental data, we constructed a lab-scale test environment.

2) The regression results for determining the coefficients a_1 and a_2 for the surface temperature in equation (3-4) are shown in Table 6. A P-value of 0 shows that both coefficients are necessary in the equation. The goodness of fit metrics, R Square and the adjusted R Square, show good results compared to the ideal values of 1. Figure 22 compares the bun surface temperature profile of experimental data to the regression result, obtained by using equation (3-4) with these coefficients.

Table 6. Regression result for coefficients in (3-4) using data from industrial oven in Case I

	Coefficients	***P-value***
a_1	**0.131085**	**0**
a_2	**1.118482**	**0**
Regression Statistics		
R Square	**0.763389**	
Adjusted R Square	**0.763318**	

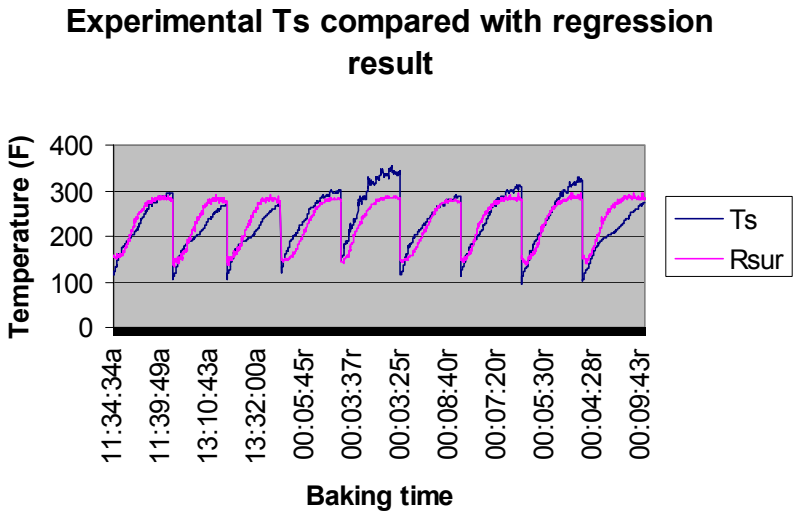

Figure 22. Experimental Ts compared with regression result (industrial oven, case I)

This regression has good performance with respect to the *R-square, Adjusted R-square*, and *p-values*. From Figure 22, we can see that some groups of data have a better match between the experimental data and the regression result than other groups. One of the reasons for this problem is measurement error. It is very difficult to keep a thermocouple exactly on the bun surface when placing the pan in the oven and while the bun is expanding during baking. Moreover, the bun surface is not well-defined in that it is a 2-D surface, yet the thermocouple and the bun itself are 3-D, so there is some ambiguity in placement of the thermocouple. Another reason for the errors is that a_1 and a_2 in (3-4) are functions of temperature and humidity inside the oven as mentioned in Section 3.2.1.1. The assumption that these coefficients are constant within the temperature and humidity ranges in the oven may cause errors, especially at the beginning and the end stages of the profile.

Nevertheless, this estimation of bun surface profile can still be used for feature extraction and prediction of the bun quality. It gives the correct trend of profile change when baking condition changes. Small errors in the model can be tolerated since the model will be used in a feedforward control loop, as discussed in Chapter 5, in conjunction with a feedback control loop that will correct for these errors.

3) The regression results for determining the coefficients c_0, c_1 and c_2 in equation (3-6) are shown in Table 7. These coefficients are used in equation (3-5) to determine the core temperature of the bun. Figure 23 compares the derived r from experimental data to the regression result. These results correlate well with the surface temperature results. These results are not as accurate as the air temperature results. As in the case of the surface temperature errors, these errors are due to measurement accuracy. It is difficult to place a thermocouple into the center of the dough since the dough is very elastic and the size changes during baking. Also, there are slight variations in the size and shape of buns from different experimental runs.

Table 7. Regression result for coefficients in (3-6) using data from industrial oven in Case I

	Coefficients	*P-value*
c_0	-5.98703	0
c_1	0.097049	0
c_2	-0.00033	0
Regression Statistics		
R Square	0.601275	
Adjusted R Square	0.601229	

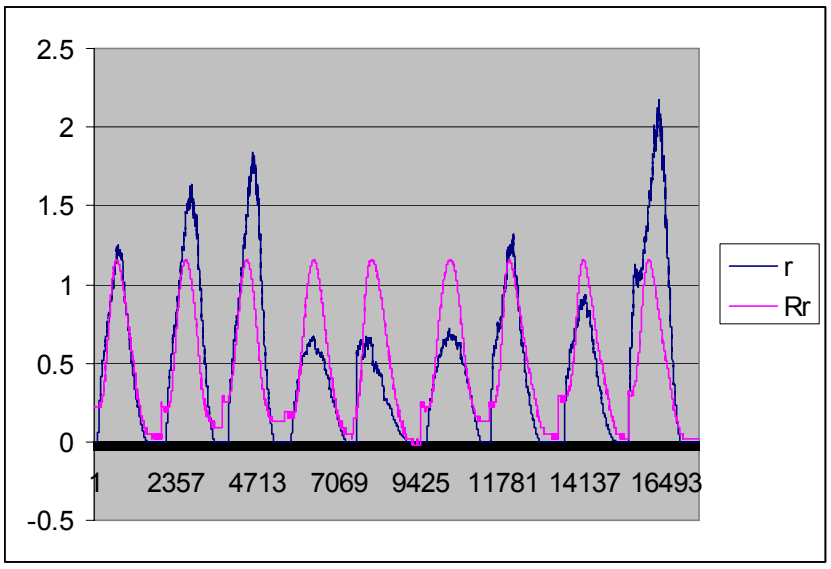

Figure 23. Derived r compared with regression result (industrial oven, case I)

Case II: Five groups of data are used for the regression, and then the resulting model is validated using the remaining four data sets. As in Case I, regression is used to find coefficients for the air temperature equation (3-8), the bun surface temperature equation (3-4), and the bun core temperature equations (3-5) and (3-6).

1) The values of $b_0, b_1, \cdots, b_{3n}$ in equation (3-8) found from using regression on the five groups of data are shown in Table 8. The five groups of data were selected from the nine groups of data so that the zone temperature settings of the five groups cover the maximum dynamic range. Substituting these values into equation (3-8) along with the effectiveness functions and the zone temperatures results in the five air temperature profiles shown in Figure 24, where the profiles are plotted sequentially for comparison and for ease of viewing. Also shown in Figure 24 is the corresponding experimental data showing good agreement

between the model and the data. Figure 25 shows the partial derivative of the hot air temperature to each zone temperature. It also has some nonphysical negative partial derivatives which are consistent with the nine data set results shown in Figure 21. Note that there is some difference in these values for b_i when compared to the results in Table 5 for the nine data set case. This is due to the selection of the five groups of data. Some of the remaining four groups of data had discrepancies in that small variations in zone temperatures produced large variations in the air temperature profile. This introduced some noise in the regression model.

Table 8. Regression result for coefficients in (3-8) using data from industrial oven in Case II

	Coefficients	***P-value***
b_0	**-182.589**	**0.000121**
b_1	**3.068196**	**1.7E-260**
b_2	**-0.04284**	**0.250462**
b_3	**0.102394**	**1.19E-05**
b_4	**-1.65796**	**0**
b_5	**0.698602**	**1.5E-132**
b_6	**-0.33294**	**4.37E-67**
b_7	**-3.03867**	**5.8E-167**
b_8	**0.258634**	**4.83E-12**
b_9	**-0.08711**	**0.000433**
b_{10}	**2.847132**	**7.4E-229**
b_{11}	**0.00099**	**0.139987**
b_{12}	**0.151757**	**3.7E-146**

Regression Statistics	
R Square	**0.712361**
Adjusted R Square	**0.712002**

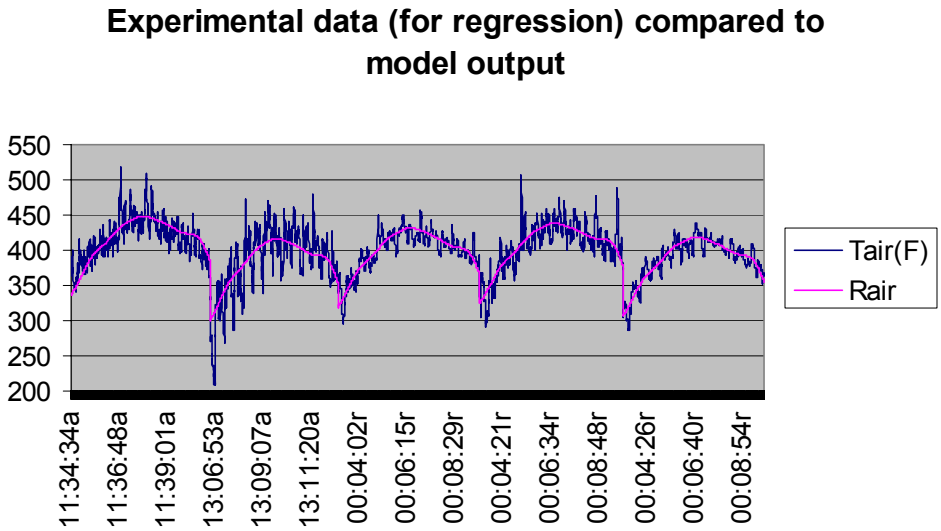

Figure 24. Experimental Tair compared with regression result (industrial oven, case II, data for regression)

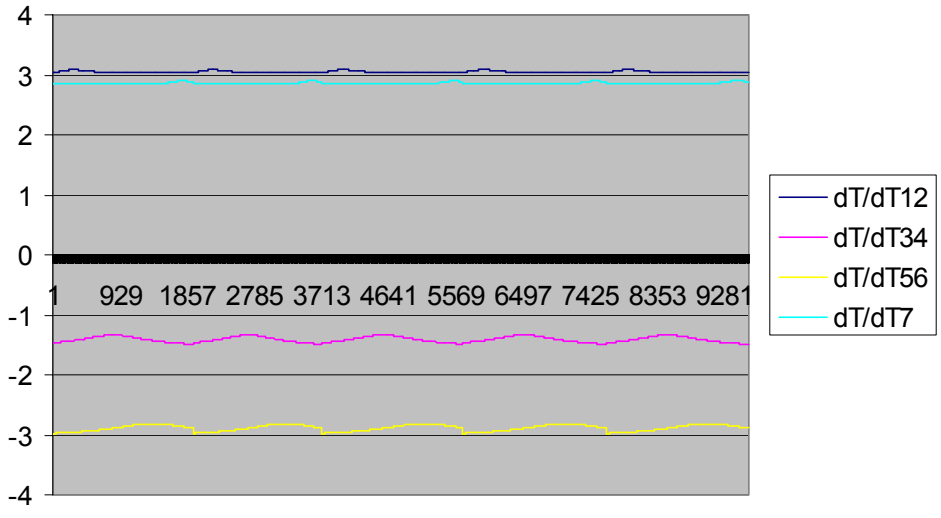

Figure 25. Partial derivatives of Tair to each zone temperature (industrial oven, case II)

This model is then validated using the remaining four groups of data sets. Substituting the zone temperatures of the four validation data sets into the model results in the four air temperature profiles shown in Figure 26. Also shown in Figure 26 is the corresponding experimental data showing good agreement between the model and the data. The *R square* and *Adjusted R square* values are also calculated for the validation data. As shown in Table 9, they also show the good agreement with those values for regression data.

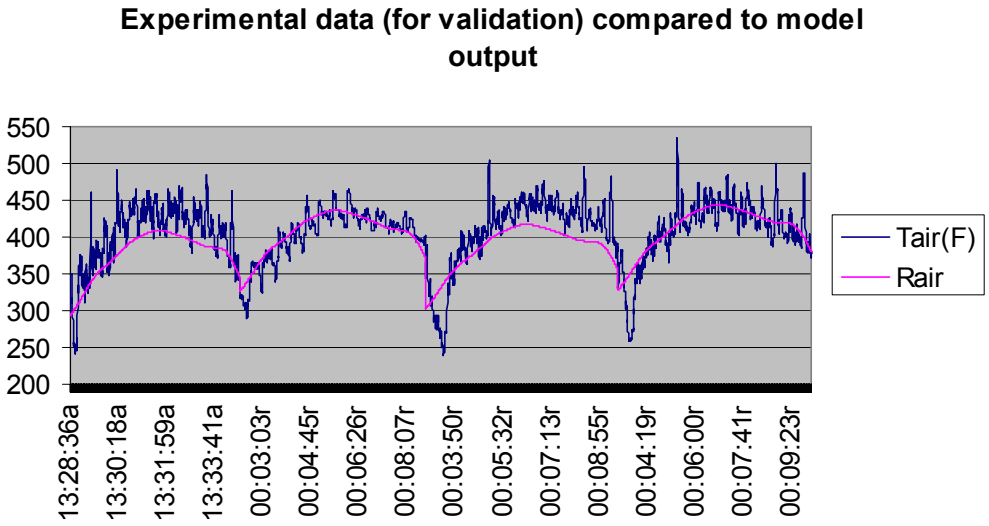

Figure 26. Experimental Tair compared with regression result (industrial oven, case II, data for validation)

Table 9. Goodness of fit (regression data compared to validation data for Ta, industrial oven)

	Regression data	Validation data
R Square	0.712361	0.599406
Adjusted R Square	0.712002	0.598789

2) The same five groups of data are also used for calculating the coefficients a_1 and a_2 in equation (3-4). The result is shown in Table 10.

Table 10. Regression result for coefficients in (3-4) using data from industrial oven in Case II

	Coefficients	*P-value*
a_1	0.157761	0
a_2	1.055864	0
Regression Statistics		
R Square	0.865274	
Adjusted R Square	0.865157	

This model is also validated using the remaining four groups of data. Figure 27 shows the plot of surface temperatures calculated by the model output and the experimental data for validation. Table 11 also compares the *R square* and *Adjusted R square* values from both regression data and validation data. They have good agreement.

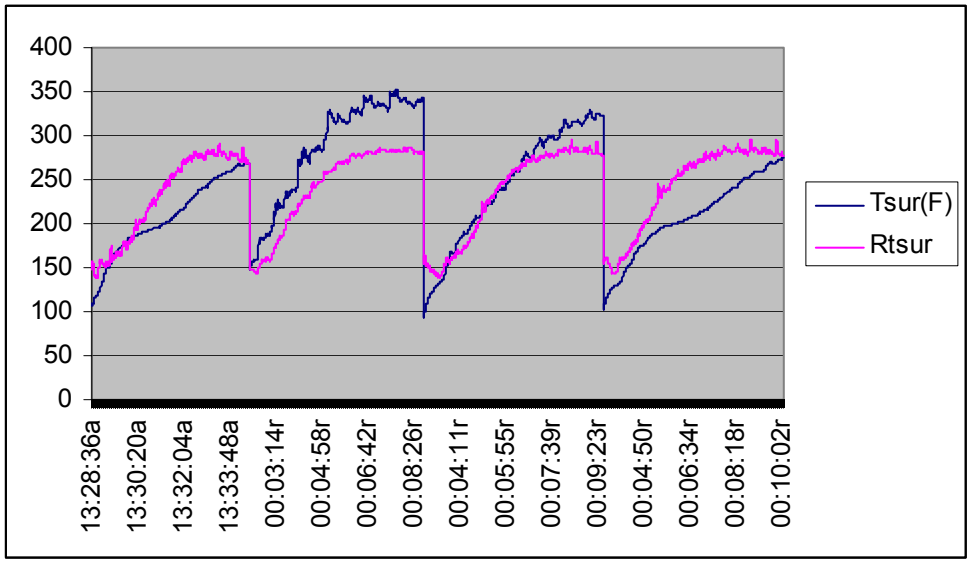

Figure 27. Experimental Ts compared with regression result (industrial oven, case II, data for validation)

Table 11. Goodness of fit (regression data compared to validation data for Ts, industrial oven)

	Regression data	Validation data
R Square	**0.865274**	**0.599693**
Adjusted R Square	**0.865157**	**0.599641**

3) The same five groups of data are also used for calculating the coefficients c_0, c_1 and c_2 in equation (3-6). The result is shown in Table 12.

Table 12. Regression result for coefficients in (3-6) using data from industrial oven in Case II

	Coefficients	*P-value*
c_0	-5.53574	0
c_1	0.089891	0
c_2	-0.00031	0

Regression Statistics	
R Square	0.73077
Adjusted R Square	0.730714

This model is also validated using the remaining four groups of data. Figure 28 shows the plot of *r* calculated by equation (3-6) and *r* calculated using experimental data for validation. Table 13 also compares the *R square* and *Adjusted R square* values from both regression data and validation data. They show qualitative agreement, but the errors are larger here than for the air temperature regression results. Again, this is due to measurement inaccuracies.

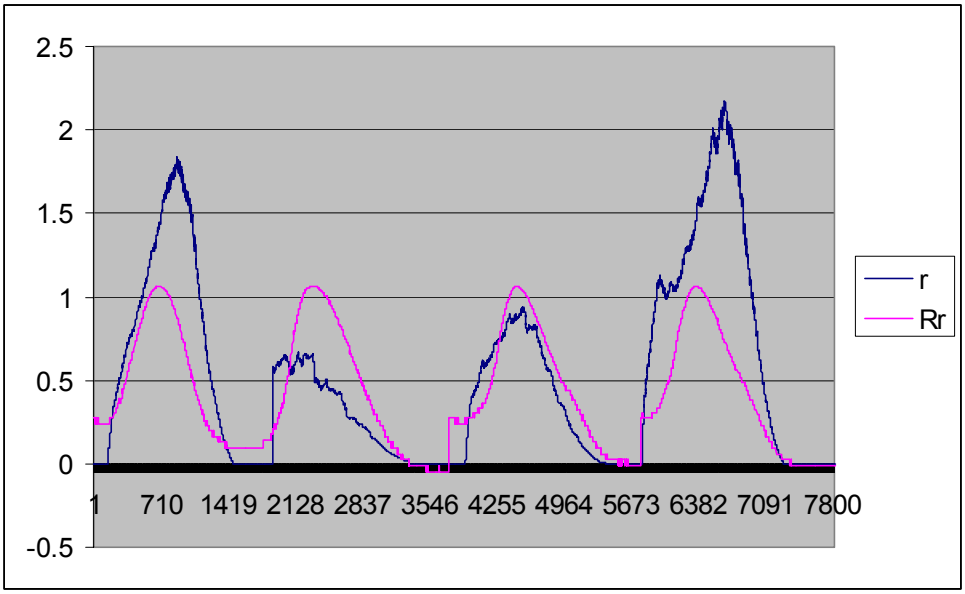

Figure 28. Derived *r* compared with regression result (industrial oven, case II, data for validation)

Table 13. Goodness of fit (regression data compared to validation data for *r*, industrial oven)

	Regression data	Validation data
R Square	0.73077	0.43669
Adjusted R Square	0.730714	0.436546

3.2.1.3 Adaptive zone coupling model

As mentioned in Section 2.1.3, we assume linearity to establish the model for the coupling effect between oven zones. Under this assumption, an adaptive zone coupling model was built for simulation purposes in Matlab. A PID controller is designed for each zone to control the burner's energy as shown in Figure 29. The "bstate" is a continuous value within the range [0,1] and reflects the burner's working condition where "0" means

totally failed, and "1" mean working properly. The energy generated by the burner is then multiplied by the coupling coefficients "gain1", "gain2", and "gain3". "Qout1" and "Qout2" are the output energies to the neighboring zones. "Qin1" and "Qin2" are the input energies from the neighboring zones. The first dashed block calculates the overall gained energy of the particular zone after the coupling effects. The second block calculates the energy lost in the zone, including two parts. The first part is the energy that absorbed by the baking products. This value is proportional to the baking product load, and the temperature difference between the oven temperature and the baking product surface temperature. The second part is the energy lost from disturbances such as cold ambient temperature. We use a sine wave to simulate this part.

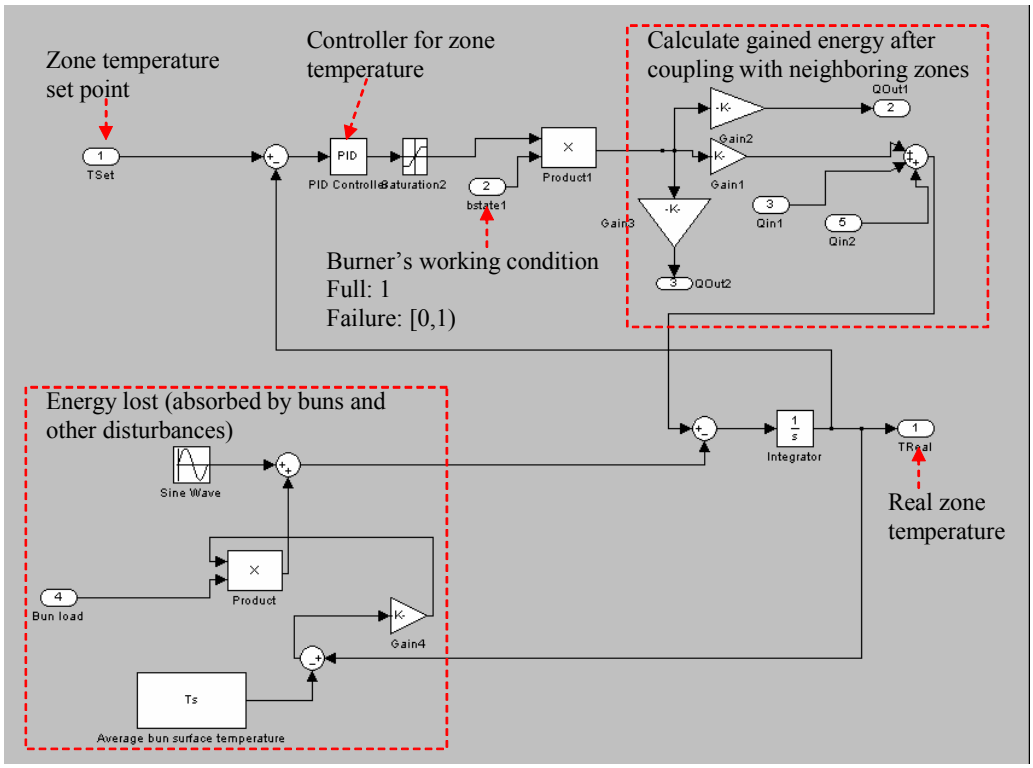

Figure 29. Simulation block diagram for each zone

Figure 30 shows the simulation block diagram of the entire oven with four temperature control loops. The links from "Qout"s to "Qin"s are determined by the oven topology. For the particular oven topology, we make the assumption that zone 1&2 doesn't have influence on zone 5&6, zone 3&4 doesn't have influence on zone 7, and vice versa.

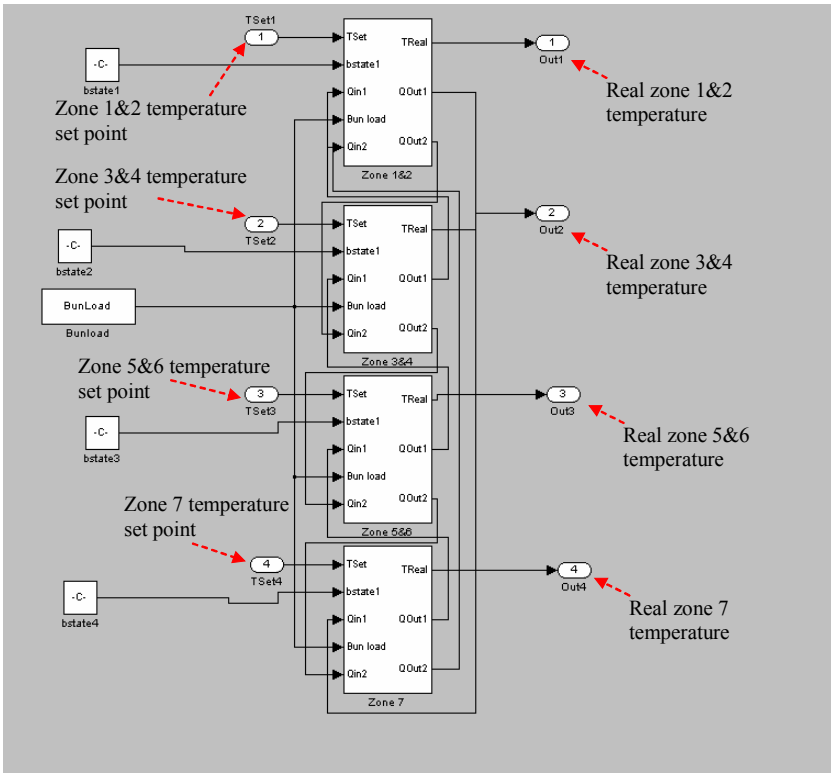

Figure 30. Simulation blocks for whole oven

The simulation result is shown in Figure 31:

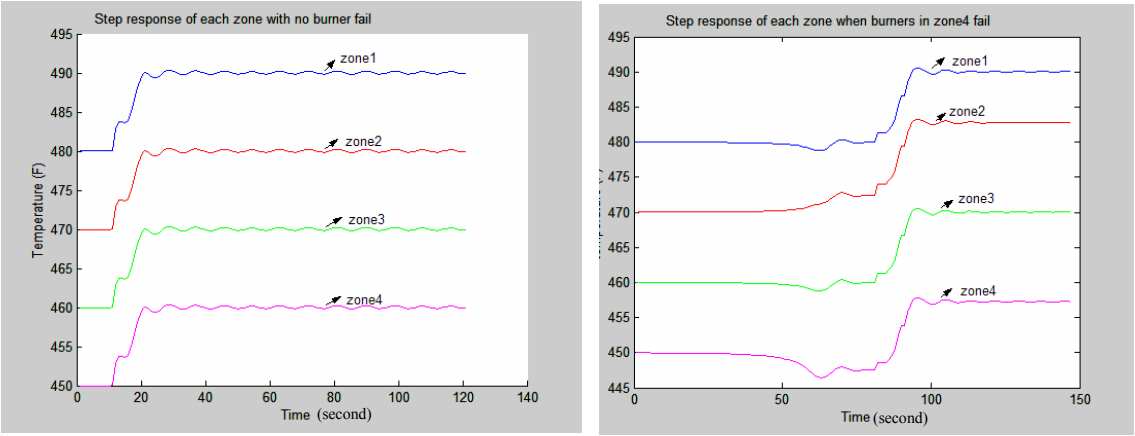

Figure 31. Simulation result of oven zone coupling model

As shown in Figure 31, when all the burners are working fine (left side in Figure 31), the zone temperatures follow the set points very accurately and with a fast time response. In this case the temperature set points are changed at 10 second to 460 F for zone 4, 470 F for zone 3, 480 F for zone 2, and 490 F for zone 1. When one of the burners has a failure condition (one of the burners in zone 4 failed at some time before 50 second in right side of Figure 31), zone 4's temperature can't track the set point exactly when it changed from 450 F to 460 F. While the burner's failure condition can lead to a steady state error in zone temperature, the error is quite small (3 F in this simulation case). This illustrates the coupling effect, which allows for heat compensation from other zones.

3.2.2 Profile-quality mapping model

Bun color is selected as the feedback quality metric for mid-level control module in this research. A color index is generated from the inspection system. The range of the index is

from 1 to 100, corresponding from lightest to darkest. To establish the profile-color mapping model, two features of the profile are selected as inputs to the NN model developed in Section 2.2:

- Average bun surface temperature after core temperature enters steady state
- Time that core temperature stays in the steady state

A sugeno type NN fuzzy model is established in Matlab using ANFIS to map the profile features to the color metric. All the features extracted and the color output are normalized to the range of [0,1] for modeling purpose. Nine rules are generated. Totally 22 groups of data are used for the establishment of the NN profile-quality mapping model. Half of them are used for training and half for validation. Figure 32 compares the model prediction to the validation data.

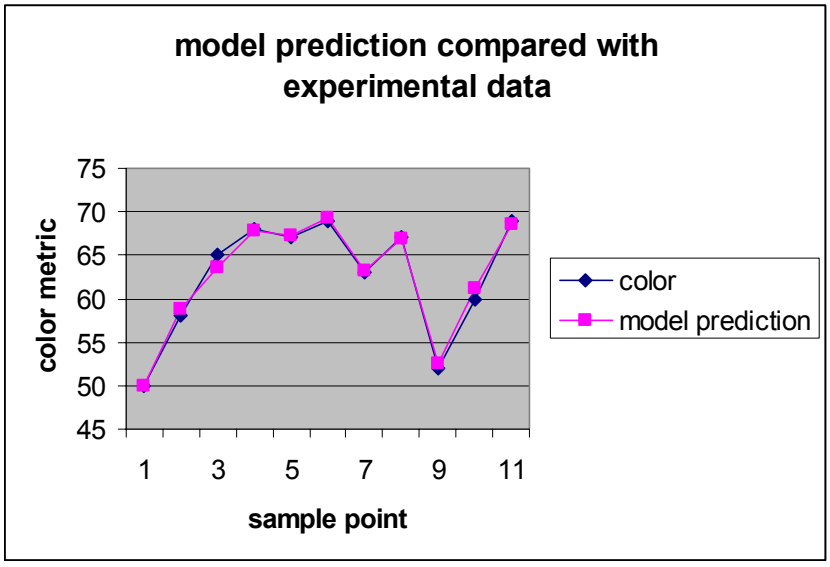

Figure 32. NN model prediction compared to validation data

The root mean squared error (RMSE) is:

$$\text{RMSE} = \frac{1}{M}\sum_{i=1}^{M}\sqrt{\frac{\sum_{j=1}^{N}(y_{ij}-\hat{y}_{ij})^2}{N}} = 0.624638$$

The examination result of model sensitivities is shown in Table 14.

Table 14. Examination of model sensitivity

	Time spans during steady state (feature1)	Mean surface temperature during steady state (feature 2)
Color metric	+	+
Expert experience	+	+

As discussed in Section 2.3.2, a "+" sign indicates that the color metric is increased, if the respective input (Time span or mean surface temperature) is increased, whereas a "-" sign indicates the opposite trend. Since the model sensitivity is consistent with the experience from expert knowledge, we can conclude that the model validated.

3.3 Modeling using lab-scale test bed

In order to gain better access to an oven process than could be obtained from the production oven located at Flowers Villa Rica bakery, we developed a smaller scale oven experiment located at the Georgia Tech Research Institute facility. The oven that we purchased is typically used in small scale commercial bakeries. We outfitted it with

sensors and measurement equipment to model the process. We designed a proofer that could proof the dough at 110 degrees for 1 hour (proofing is the process to let the dough rise under controlled environmental conditions). As shown in Figure 33(c), we purchased SCXI signal conditioning module from National Instrument to acquire the thermocouple data from both the oven and the proofer. A relay control is also designed to automatically control the proofer temperature to 110 degree. A pan of water with saturated salt is also put into the proofer to get the desired humidity. With a recipe supplied by Flowers, we were able to bake buns with the same color attributes as the commercial products.

(a) Oven (b) Proofer (c) Signal conditioning

Figure 33. Experiment set up in GTRI

3.3.1 Design of the experiments

The objective of the test plan is to utilize the minimum test numbers for enough experimental data to build the baking product quality model framework. The convection oven in GTRI is used to emulate industrial ovens with several zones by setting different temperature set points during different baking periods. We used 4 zones, with 2 minutes baking time in each zone. The hot air temperature profile T_a, bun surface temperature profile T_s and bun core temperature profile T_c of each run are recorded. The zone temperature settings are also recorded correspondingly. Coefficients in (3-4), (3-5), (3-6), and (3-7) are then calculated using regression.

We use Taguchi $L_9(3^4)$ design introduced in Section 2.1.2 to design the test. The control variables are listed as in Table 15:

Table 15. Control variables

Controllable variables	Level 1	Level 2	Level 3
Zone1 temperature (A)	390 F	410 F	430 F
Zone2 temperature (B)	410 F	430 F	450 F
Zone3 temperature (C)	420 F	440 F	460 F
Zone4 temperature (D)	400 F	420 F	440 F

The experiment design and the test results are shown in Table 16:

Table 16. L_9 Orthogonal Array for the control variables and results

	Control variables				Temperature profile file name	Color measurement (L value)
Run	A	B	C	D		
1	1	1	1	1	Test1.mpc	65.58, 62.98
2	1	2	2	2	Test2.mpc	61.02, 60.69
3	1	3	3	3	Test3.mpc	64.66, 63.02
4	2	1	2	3	Test4.mpc	57.81, 59.28
5	2	2	3	1	Test5.mpc	64.12, 58.91
6	2	3	1	2	Test6.mpc	63.31, 64.27
7	3	1	3	2	Test7.mpc	65.3, 63.97
8	3	2	1	3	Test8.mpc	64.12, 64.50
9	3	3	2	1	Test9.mpc	57.48, 58.37

For each run, two buns were taken for color measurement. The mean value is used for modeling.

3.3.2 Test result

We also have nine groups of experimental data (bun temperature profiles $T_a, T_s,$ and T_c with corresponding zone temperatures $T_1, T_2, T_3,$ and T_4) from the lab-scale oven. Regression is used to find coefficients for the air temperature equation (3-8), the bun surface temperature equation (3-4), and the bun core temperature equations (3-5) and (3-6). A different effectiveness function is constructed based on the different oven topology. As stated before, the convection oven in GTRI is used to emulate industrial ovens with several zones by setting different temperature set points during different baking periods. In this way, only the former zones will have effect on the later zones, while the later

zones will have no effect on former zones. An effectiveness function based on this topology is constructed as shown in Figure 34. As in Case II in Section 3.2.1.2, five groups of data are used for the regression, and then the resulting model is validated using the remaining four data sets.

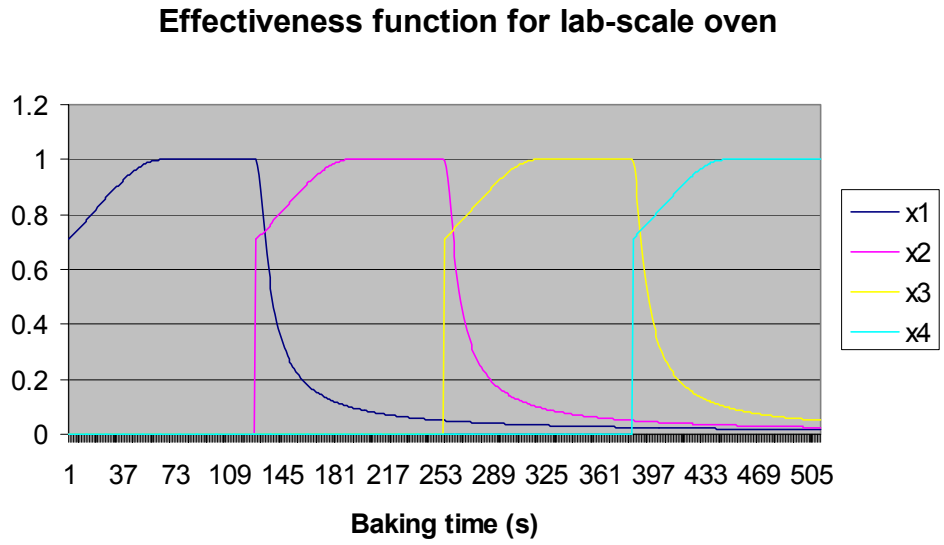

Figure 34. Effectiveness function for lab-scale oven

1) The values of $b_0, b_1, \cdots, b_{3n}$ in equation (3-8) found from using regression on the five groups of data are shown in Table 17. Substituting these values into equation (3-8) along with the effectiveness functions and the zone temperatures results in the five air temperature profiles shown in Figure 35, where the profiles are plotted sequentially for comparison and for ease of viewing. Also shown in Figure 35 is the corresponding experimental data showing good agreement between the model

and the data. Figure 36 shows the partial derivative of the hot air temperature to each zone temperature. Note that there are still nonphysical negative partial derivatives, though they look a little bit better than that of the industrial oven. We attribute this to the construction of the heuristic effectiveness function. Continuing work is being conducted to analyze the effectiveness of each zone temperature set point to the temperature profile using statistical method.

Table 17. Regression result for coefficients in (3-8) using data from lab-scale oven

	Coefficients	***P-value***
b_0	**88.37524**	**7.41E-11**
b_1	**0.579372**	**8.1E-153**
b_2	**0.062371**	**0.081991**
b_3	**0.092418**	**0.000107**
b_4	**-0.14135**	**1.41E-07**
b_5	**-0.07562**	**2.6E-05**
b_6	**0.235192**	**1.97E-30**
b_7	**0.442931**	**7.72E-97**
b_8	**0.078935**	**3.11E-07**
b_9	**0.130623**	**7.12E-17**
b_{10}	**-0.28202**	**3.56E-15**
b_{11}	**0.03945**	**0.010692**
b_{12}	**0.139904**	**1.2E-16**
Regression Statistics		
R Square	**0.790648**	
Adjusted R Square	**0.789628**	

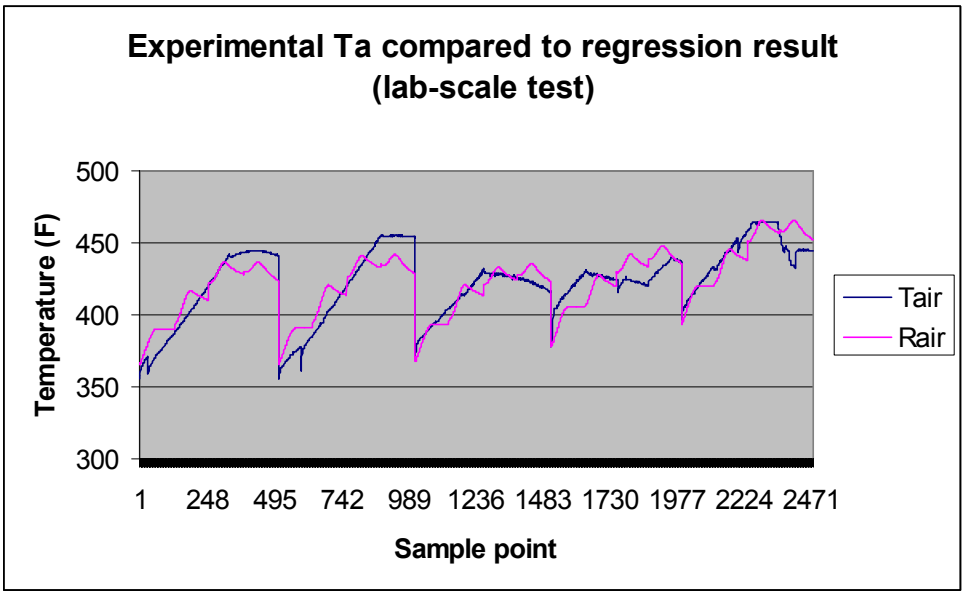

Figure 35. Experimental Tair compared with regression result (lab-scale oven, data for regression)

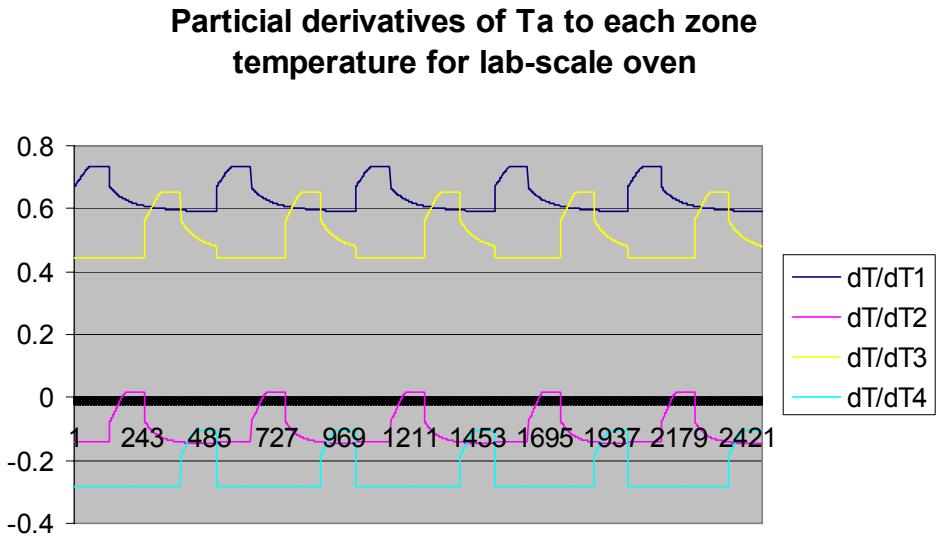

Figure 36. Partial derivatives of Tair to each zone temperature (lab-scale oven)

This model is then validated using the remaining four groups of data sets. Substituting the zone temperatures of the four validation data sets into the model results in the four air temperature profiles shown in Figure 37. Also shown in Figure 37 is the corresponding experimental data showing good agreement between the model and the data. The *R square* and *Adjusted R square* values are also calculated for the validation data. As shown in Table 18, they also show the good agreement with those values for regression data.

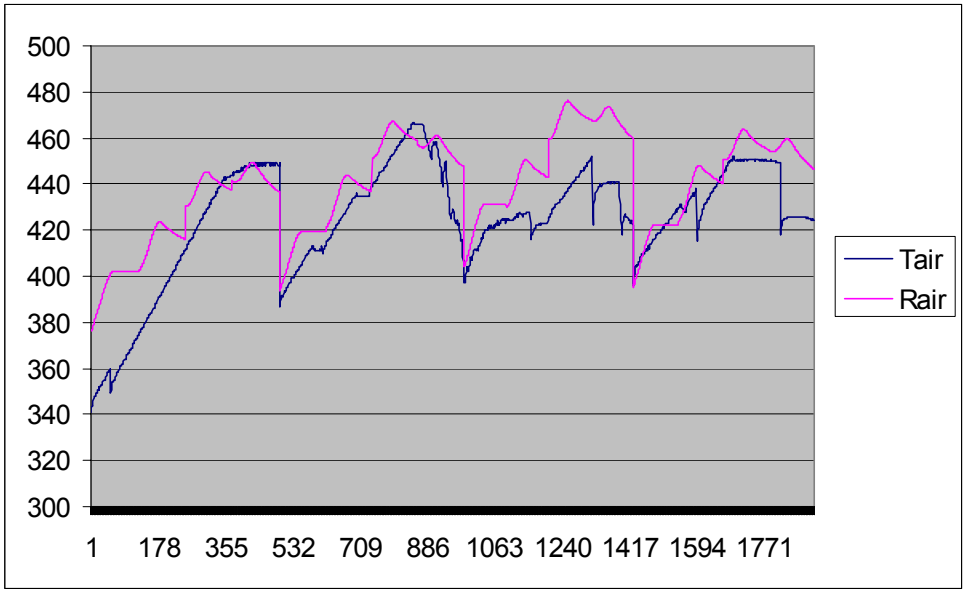

Figure 37. Experimental Tair compared with regression result (lab-scale oven, data for validation)

Table 18. Goodness of fit (regression data compared to validation data, lab-scale oven)

	Regression data	Validation data
R Square	**0.790648**	**1.039642**
Adjusted R Square	**0.789628**	**1.039894**

2) The same five groups of data are also used for calculating the coefficients a_1 and a_2 in equation (3-4). The result is shown in Table 19.

Table 19. Regression result for coefficients in (3-4) using data from lab-scale oven

	Coefficients	*P-value*
a_1	0.072471	8.01E-18
a_2	1.193233	0
Regression Statistics		
R Square	0.755986	
Adjusted R Square	0.755483	

This model is also validated using the remaining four groups of data. Figure 38 shows the plot of surface temperatures calculated by the model output and the experimental data for validation. Table 20 also compares the *R square* and *Adjusted R square* values from both regression data and validation data. They have good agreement.

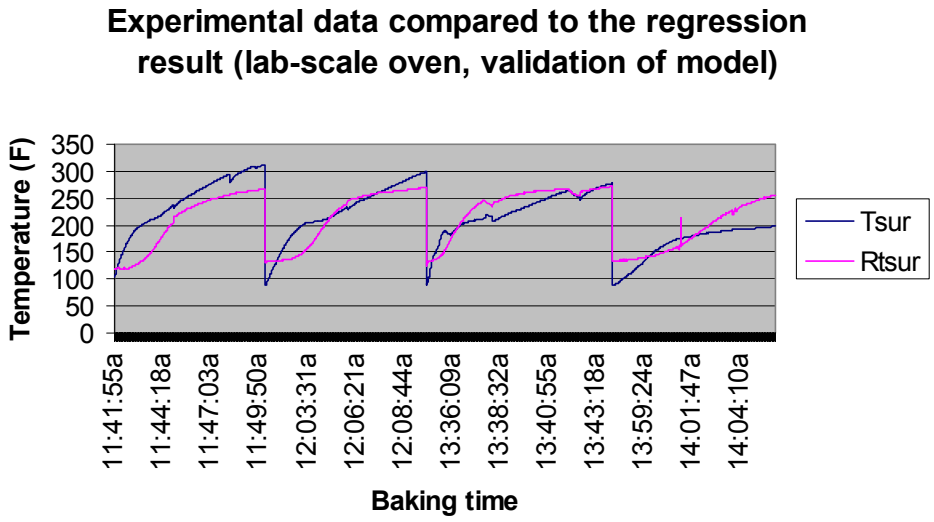

Figure 38. Experimental Ts compared with regression result (lab-scale oven, data for validation)

Table 20. Goodness of fit (regression data compared to validation data for Ts, lab-scale oven)

	Regression data	Validation data
R Square	0.755986	0.964375
Adjusted R Square	0.755483	0.964357

3) The same five groups of data are also used for calculating the coefficients c_0, c_1 and c_2 in equation (3-6). The result is shown in Table 21.

Table 21. Regression result for coefficients in (3-6) using data from lab-scale oven

	Coefficients	*P-value*
c_0	-3.17969	9.3E-118
c_1	0.060431	3E-177
c_2	-0.00022	1.3E-197
Regression Statistics		
R Square	0.55222	
Adjusted R Square	0.551616	

This model is also validated using the remaining four groups of data. Figure 39 shows the plot of *r* calculated by equation (3-6) and *r* calculated using experimental data for validation. Table 22 also compares the *R square* and *Adjusted R square* values from both regression data and validation data. They show qualitative agreement, but the errors are larger here than for the air temperature regression results. Again, this is due to measurement inaccuracies.

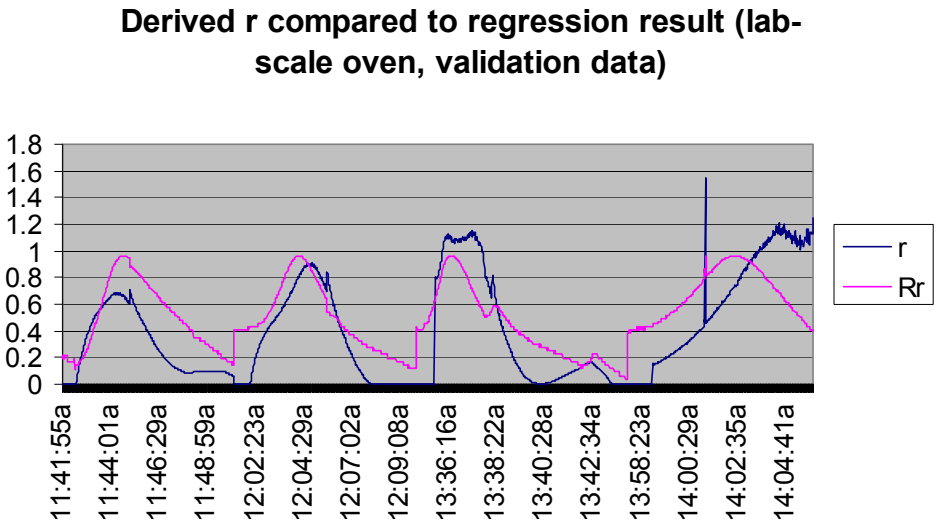

Figure 39. Derived r compared to regression result (lab-scale oven, data for validation)

Table 22. Goodness of fit (regression data compared to validation data for *r*, lab-scale oven)

	Regression data	Validation data
R Square	0.55222	0.562112
Adjusted R Square	0.551616	0.561665

CHAPTER 4

CONTROL STRATEGY

The objective of the proposed research is to create a hierarchical and integrated system approach for product monitoring and process control of complex food processes. In contrast with previous work, the proposed method consists of not only an automated vision-based inspection system that is monitoring the quality of products, but also a hierarchical intelligent control system which uses the quality information as one source of the feed-back information. Within this context, the following will be addressed:

1) An hierarchical control architecture will be presented and the advantages of the architecture will be highlighted;
2) A sensor module that includes both process monitoring data and product quality data derived from a quality inspection system will be generated;
3) A mid-level control strategy will be addressed.

4.1 The hierarchical control architecture

Currently, most existing control methods for food processes are limited to low-level controls, which only use process monitoring data as the feed-back information to the automated control system. As shown in Figure 40, the food process generally involves several operations, with a separate control loop for each one. The coupling effect between some operations may also be present. For example, in a baking oven that has several baking zones, the baking temperature in zone n affects its neighboring baking zones.

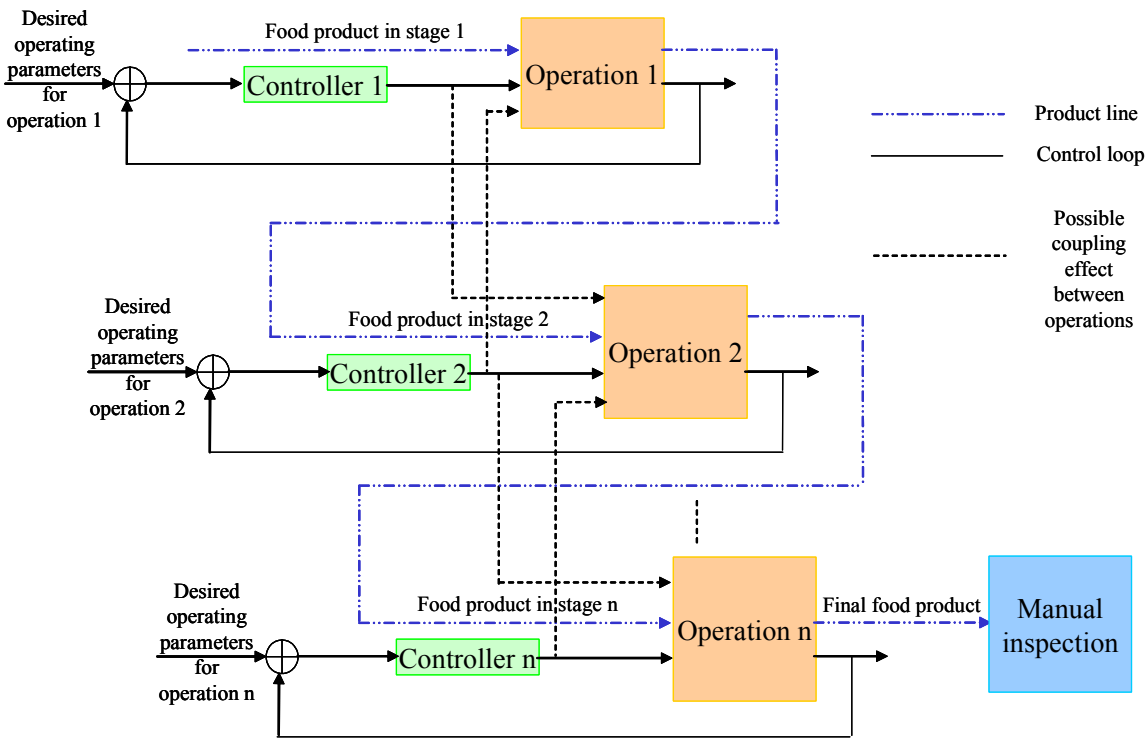

Figure 40. General food process

Although these controls are usually relatively simple (such as PID) and effective, they are not enough to maintain the food product's quality under several circumstances. Many operations in the food process require an operator to readjust the set points under some circumstances. For example, environmental parameters like ambient temperatures and/or humidity levels change from day to day or from season to season; food ingredients have variability from different suppliers or simply from different batches (for example, winter wheat differs from summer wheat); batch loads vary; and failures occur on instruments in the process. Readjusting the set points of low-level controllers in an unintelligent manner can easily cause the whole process to become unstable (producing unacceptable product). Since this is a common problem with operators on the production

line, a hierarchical control strategy is proposed in this work to consistently improve the product quality and monitoring the whole process.

For a typical food process, the proposed hierarchical control strategy is shown in Figure 41. The control architecture consists of a high-level module, a mid-level module and a low-level module.

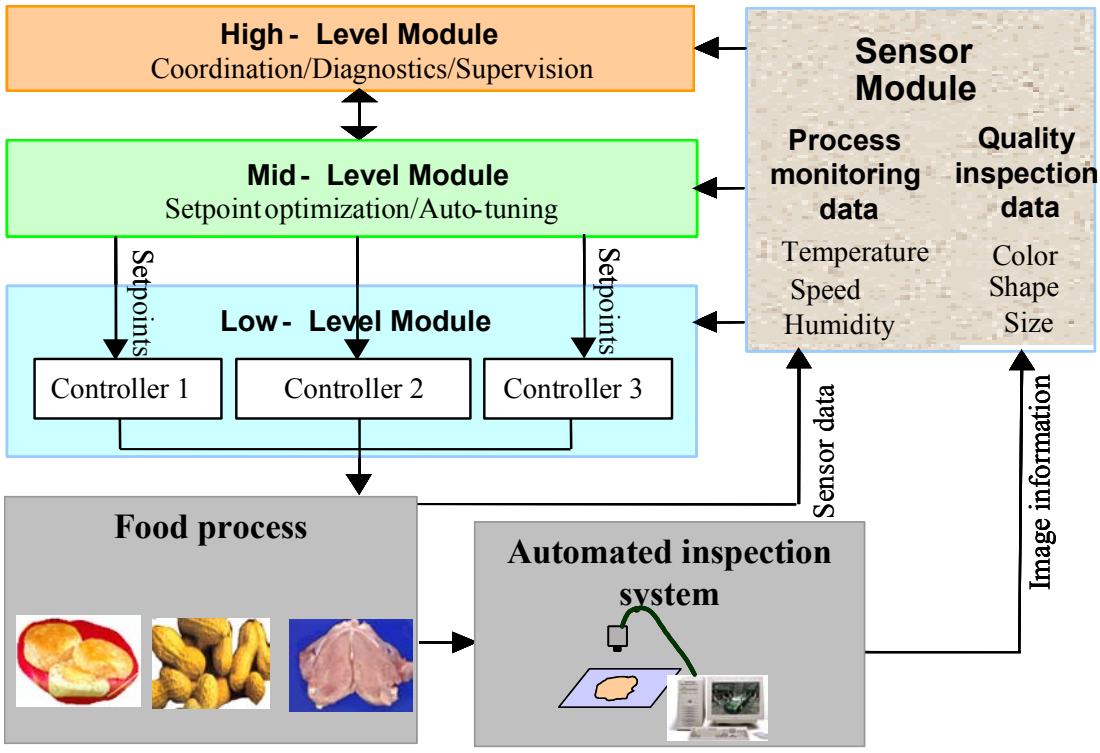

Figure 41. Overall control strategy for product quality improvement

The low-level control module shown in the figure generally is available in the food process industry: they are used to control the operation parameters in the food

process so that the food product can be processed to meet certain quality criteria. For example, a temperature controller is used in the baking process to control the oven temperature.

The purpose of the mid-level control module is to generate the optimum set points for the low-level module to improve the quality of the product by accounting for process variations. The controllers extract the product quality information and the process monitoring information from the sensor module and then use that information to determine the appropriate set points for the low level controllers and to auto-tune their parameters.

The high-level control module in the figure involves coordination of multiple plant processes, diagnostics of the failure condition in the process, and the supervision of the whole process.

The work is mainly focused on the mid-level control part. The following sections will explain the sensor module, the mid-level control strategy, and the validation of the control algorithms in detail.

4.2 Sensor module

The sensor module in the architecture is responsible for providing the product quality information and the process monitoring data [41]. Depending on the requirements of these data, the detailed composition of this module is introduced.

4.2.1 Machine vision-based quality inspection

The advantage of the vision-based quality inspection system lies in the following aspects:

- Removes the subjectivity of manual inspection by workers.

- Assures 100% inspection levels.
- Automatically feeds back the quality information to the control module.

For the food product, the quality inspection data generally refers to color, shape, size, and color/shape distribution, etc. Depending on the quality metrics of the food product, the hardware composition of the vision-based inspection system may be different. For example, a visual-based inspection system can generate information on color and color distribution, while a laser-based inspection can provide the information about the product thickness. Multiple sensors and sensor data fusion techniques might be necessary depending on the quality metrics. A generalized vision-based quality inspection scheme will be addressed in this context.

- Image acquisition

The hardware composition for an image acquisition system includes a camera, a data acquisition board, and an illuminator. When they are used for the quality inspection purpose on a baking process, the following issues should be carefully considered

  - Image resolution: the resolution should be high enough to recognize the quality differences;
  - Speed: the frame grabber should be fast enough to grab each individual product image on the conveyor belt to ensure 100% inspection;
  - Lighting: The illuminator should be designed to enable the picture to be taken under uniformly distributed lights without any reflections, and with maximum contrast;

- Location: The choice of the whole system location should also consider the product temperature since the products of baking processes are generally at a very high temperature when they are removed from the oven.

- Image processing

On-line image processing is carried out to extract useful information from the images acquired, and thus obtain the quality features of the product. Segmentation is a critical step in this image understanding process to extract the useful information.

The time window for the image processing algorithm is usually short for real-time inspection depending on the process speed. Thus techniques that take full advantage of *a priori* knowledge of the object/background characteristics should be utilized. For example, a simple threshold may be enough for segmentation of the baking product on a uniform color background.

- Decision making

Candidate quality features for baking products include: color and color distribution, shape, size, seed coverage and seed distribution, and other features that include a priori information about the object and its background, such as moisture and thickness.

To select appropriate features for the feedback control module, a cause-effect relationship should be carefully studied. Quality features should only be fed back to the control module if the process stage controlled by this module can affect the specific features. Table 23 lists main defects and potential stages that can cause these defects.

Table 23. Main defects and potential stages

Defects	Potential stages
1. Color is too dark/light	Mixing stage Oven baking stage
2. Poor shape and size	Dividing and Rounding stage Proofing stage Baking stage
3. Seed coverage/distribution	Seeding stage
4. Symmetry	Dividing and Rounding stage Moulding stage

4.2.2 Process monitoring data

Besides the quality feedback information from the vision-based inspection system, the process monitoring data is also critical feedback for the control module. For a baking process, this generally includes baking temperature, burner energy, oven load, oven humidity and baking time.

To select appropriate sensors for these data, the following issues should be addressed:

- Working temperature range
- Accuracy
- Sampling rate
- Number of sensors

Generally data from these sensors should first be pre-processed before they are fed back to the control module. The purpose of data processing is to eliminate unreasonable/abnormal data caused by noise occurring during data acquisition. Generally a low pass filter is applied to the data to remove the noise.

Data are also processed for modeling and control purposes. For example, because the baking process is generally a high-volume production line, it is not possible to control the quality of every single product. A reasonable control objective is to control the quality distribution of the products over a period of time, i.e., the mean of the product quality factor and the standard deviation of the product quality factor over a period of time. Thus a sliding window will be defined and the quality distribution within this window will be calculated to acquire the trend of error.

4.3 Mid-level control

The baking process has the following characteristics:

- High production rate
- Long processing time (long time delay of feedback information)

Considering the above two characteristics, the overall mid-level control strategy is proposed as shown in Figure 42.

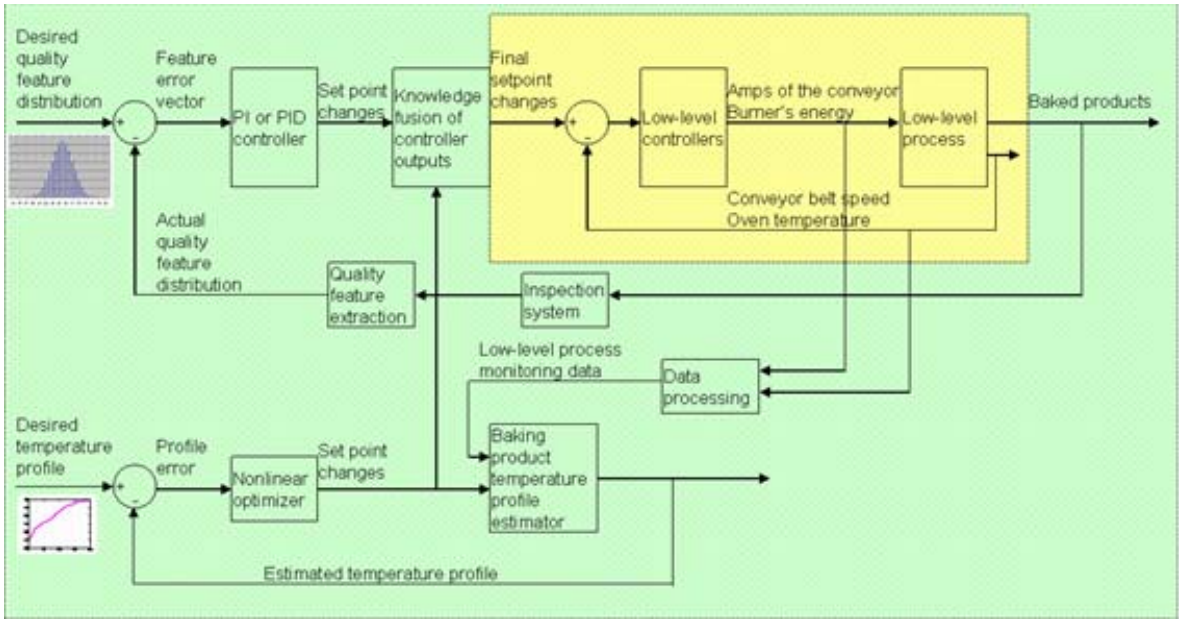

Figure 42. Mid-level control schematic

Due to the high production rate, it is impossible to control the quality of each single baking product. Thus, the control objective is to control the distribution of the baking product's quality over a period of time to be as close as possible to the desired distribution. A sliding window will be defined to calculate the quality distribution inside this window and will be used to calculate the error vector. A possible desired distribution and real distribution is shown in Figure 43:

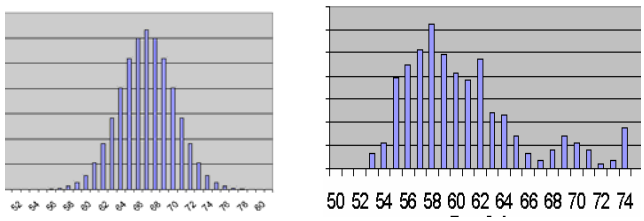

Figure 43. Desired vs. actual distribution of quality index

4.3.1 Feed-forward controller design

To compensate the long delay of the feedback information, the quality model is used to predict the baking product quality metrics, so that the quality error caused by changes in any variable that can be measured will be compensated a priori by the changes in the set points of low-level process. This feed-forward controller design forms the optimization problem:

$$\begin{aligned} &\min\ e = abs(\hat{Q} - Q) \\ &\text{subject to}: Tset \in [\min\_ Tset, \max\_ Tset] \\ &\qquad\qquad bakingtime \in [\min\_ bakingtime, \max\_ bakingtime] \end{aligned}$$

Where $\hat{Q}$ represents the desired quality metrics, and $Q = f(Tset, bakingtime)$ represents the predicted model output of the quality metrics. f is the nonlinear function that represents the quality model, $Tset$ is the vector of the oven zone temperature set points, and $bakingtime$ is the baking time of the baking product.

We want to minimize the error between the desired quality metrics and the predicted model output by setting $Tset$ and $bakingtime$. There is more than one solution to solve this nonlinear optimization problem. In this research, a *Particle Swarm*

Optimization algorithm is selected to search for the set points of the low-level process. *Particle swarm optimization* (PSO) [45,46] is a population based stochastic optimization technique developed by Dr. Eberhart and Dr. Kennedy in 1995, inspired by social behavior of bird flocking or fish schooling. Consider the following scenario: a group of birds are randomly searching for food in an area. There is only one piece of food in the area being searched. All the birds do not know where the food is. But they know how far the food is in each iteration. So the effective strategy is to follow the bird which is nearest to the food.

In PSO, each single solution is a "bird" in the search space. We call it a "particle". All of the particles have fitness values which are evaluated by the fitness function to be optimized, and have velocities which direct the flying of the particles. The particles fly through the problem space by following the current optimum particles.

PSO is initialized with a group of random particles (solutions) and then searches for optima by updating generations. In every iteration, each particle is updated by following two "best" values. The first one is the best solution (fitness) that it has achieved so far, called *pbest. Pbest* is a vector with elements equal to the optimization parameters. (The fitness value is also stored.) Another vector-valued "best" solution is tracked by the particle swarm optimizer and is the best value obtained so far by any particle in the population. This best value is a global best and called *gbest*. After finding the two best values, each particle updates its velocity and positions with the following equation (4-1) and (4-2).

$$v_n = v_{n-1} + c1 * r * (pbest - present) + c2 * r * (gbest - present) \quad (4\text{-}1)$$

$$present_{n+1} = present_n + v_n \tag{4-2}$$

where v is the particle velocity, *present* is the current particle (solution). *pbest* and *gbest* are defined as stated before. r is a random number between (0,1). $c1, c2$ are learning factors. This calculation is repeated for each particle, where v, *present* and *pbest* pertain to that particle.

Figure 44 illustrates the evolution process of PSO. The circle particles are the "present" particles, and the triangle particles are the updated result after one generation. The values for *pbest* and *gbest* are updated in each generation after all the particles are updated.

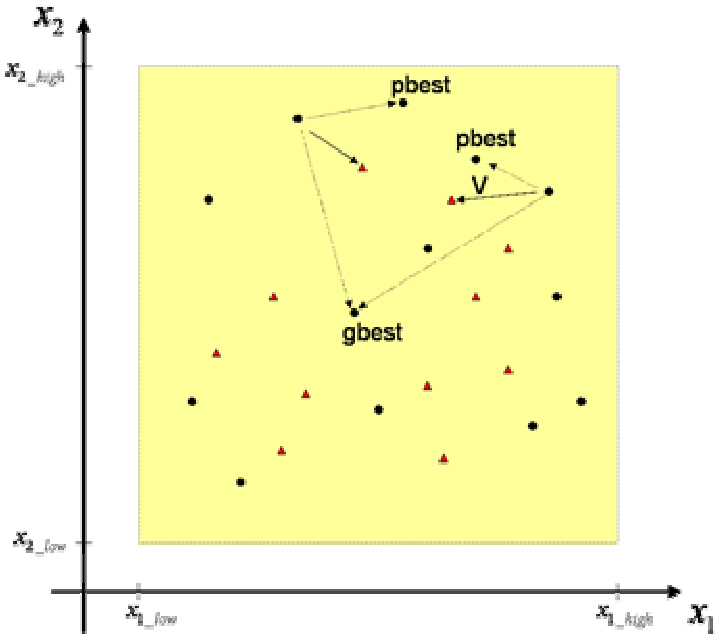

Figure 44. Particle swarm optimization

There are not many parameters that need to be tuned in PSO. Here is a list of the parameters and their typical values.

- The number of particles: the typical range is 20 - 40. Actually for most of the problems 10 particles is large enough to get good results. For some difficult or special problems, one can try 100 or 200 particles as well.
- Dimension of particles: It is determined by the problem to be optimized.
- Range of particles: This is the range within which the particles (solutions) should be. It is also determined by the problem to be optimized. Different ranges can be specified for different dimension of particles. For example, for a two dimension optimization problem shown in Figure 30, the range for dimension x_1 is $[x_{1\_low}, x_{1\_high}]$, while the range for dimension x_2 is $[x_{2\_low}, x_{2\_high}]$.
- Learning factors: $c1$ and $c2$ are usually equal to 2. However, other settings were also used in different papers. But usually $c1$ equals to $c2$ and ranges from [0, 4].
- The stop condition: the maximum number of iterations the PSO executes and the minimum error requirement.

PSO shares many similarities with evolutionary computation techniques such as Genetic Algorithms (GA). The system is initialized with a population of random solutions and searches for optima by updating generations. The potential solutions, called particles, fly through the problem space by following the current optimum particles.

The advantages of using PSO for this optimization problem are:

- PSO takes real numbers as particles. It is not like GA, which uses binary encoding.
- PSO does not have genetic operators like crossover and mutation. Particles update themselves with the internal velocity. They also have memory, which is important to the algorithm.
- PSO has a significantly different information sharing mechanism compared with GA. In GAs, chromosomes share information with each other. So the whole population moves like one group towards an optimal area. In PSO, only the global best particle (or the local best particle) gives out the information to others. It is a one -way information sharing mechanism. The evolution only looks for the best solution.

There are a few examples that utilize PSO in controller design. Gaing [53] presented a design method for determining optimal PID controller parameters of an AVR system using PSO algorithm. Okada [54] used PSO for parameter tuning of a fixed structure controller for power system stability enhancement. Elwer [55] presented a modern approach of speed control for a Permanent Magnet Synchronous Motor (PMSM) using the PSO algorithm to optimize scaling factors of a Fuzzy Logic Controller (FLC). Fukuyama [56] utilized PSO for reactive power and voltage control (RPVC) in electric power systems. All of these utilizations of PSO presented superior features, including easy implementation, stable convergence characteristic, and good computational efficiency compared to other evolution algorithms such as GA.

In this research, the model based feed-forward controller in Figure 42 utilizes PSO to search for the optimum set points of the low-level controllers. The model serves as the function to calculate the fitness value of the solution. The searching procedures of the feed-forward controller are shown as below:

Step1. Specify the lower and upper bounds of the feed-forward controller outputs. Initialize randomly the individuals of the population including searching points, velocities, *pbests*, and *gbest*.

Step2. Calculate the fitness value of each individual in the population using the model developed. For example, the quality model developed in Figure 4 is used to calculate the predicted color (fitness value) for each particle (solution of feed-forward controller output).

Step3. Compare each individual's fitness value with its *pbest*. The best fitness value among the *pbest* is denoted as *gbest*.

Step4. Modify the member velocity v of each individual according to (4-1). If v reaches the lower or upper bounds, substitute v with the lower or upper bounds of the velocity.

Step5. Modify the member position of each individual according to (4-2). If the current position reaches the lower or upper bounds of the individual member, substitute the position with the lower or upper bounds.

Step6. If the number of iterations reaches the maximum, then go to Step 7. Otherwise, go to Step 2.

Step7. The individual that generates the latest *gbest* is an optimal solution for the feed-forward controller.

4.3.2 Feedback controller design

The feed-forward controller is designed to be active when there are changes in the process operating environment, such as the burner's failure. In this case, the feed-forward controller will be responsible for the nonlinear property of the whole system and generate new set points for the low-level process. Since there also exist modeling errors and disturbances, online feedback control is still needed.

As mentioned before, the typical industrial baking oven generally has several zones, either linear or spiral, with a conveyor belt moving inside the oven. In most of the ovens, separate control loops exist for burners in each oven zone. Changing the temperature set point of any one of these zones will affect the final baking product quality. So, different feedback controllers are designed for controlling each separate zone set point to achieve the best control effect.

Based on the data analysis, the system can be treated as a linear system within a certain range of operating parameters. So a PI (proportional/integral) controller is designed for each zone to tune the low-level set points according to feedback of the quality information. While color is the quality metric used in this research, the procedure is not limited to color. Assuming that there are N zones, each zone has a separate mid-level feedback controller to calculate the new set point for the low-level temperature controller in the corresponding zone, and that only one mid-level feedback controller is active at a time, the closed loop system is shown in Figure 45.

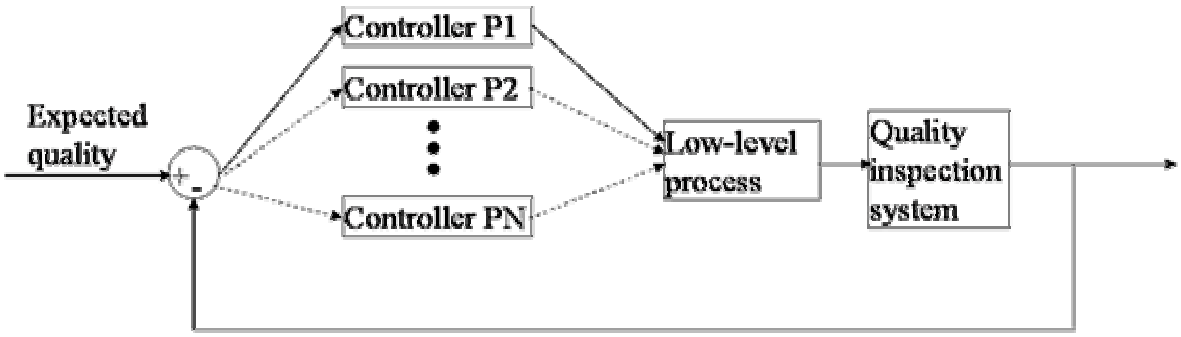

Figure 45. Close loop system with Mid-level feed back controllers

Controller P1 is defined as the controller with the highest priority, and controller PN is defined as the controller with the lowest priority. When there is a failure condition occurring in the zone that corresponds to the current controller, or when the set point generated by the current controller reaches the upper/lower limit, the active controller will be switched to the one with the next lower priority. The controllers are prioritized to take function based on the particular quality metric to be controlled. For example, P1 might have the highest priority for color while PN might have the highest priority for size of the product.

There is a problem that arises when the current PI controller reaches saturation status, and no other controllers can be switched on. In this case, an anti-windup configuration will take effect to prevent the integrator state in the active PI controller from growing large and causing overshoot and limit cycles.

Whenever a linear controller has been designed under the assumption that its output will affect the plant input directly and unaltered, then, any input nonlinearity, such

as rate- and/or amplitude saturation, causing deviation between the controller output and the plant input, almost always degrades the performance, and stability of the closed loop system may be put at risk. Anti-windup compensation is the simplest and most commonly used modification of a linear controller, aiming at retaining stability and most of the performance in such a system.

An anti-windup compensator consists of a nominal (most often linear) controller appended with anti-windup compensation. An important property of anti-windup compensation is that it leaves the loop unaffected as long as saturation does not occur. Consequently, the control action provided by the anti-windup compensator is identical to that of the nominal controller, as long as the control signals operate within the saturation limits. The design can be split into two parts where the first part concerns the linear controller and the second the anti-windup modification. Hence, when designing anti-windup compensators in this way, input saturations are taken into account *a priori*.

There are several ways to design the anti-windup compensator (AWC). We will use the one proposed by Franklin in [51] as shown in Figure 46.

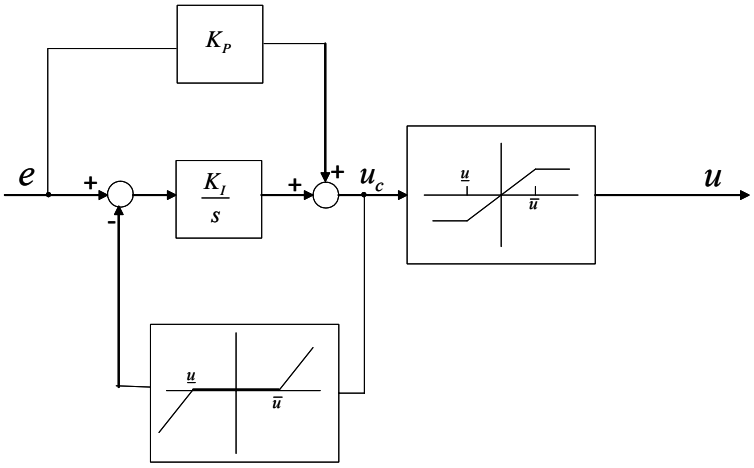

Figure 46. Anti-windup compensation

4.4 Stability analysis for feedback controller

The switching between the mid-level feedback controllers makes the system a switched system. We use hybrid system methodologies to analyze the stability. Davrazos [50] reviewed the stability result for switched and hybrid systems as shown in Figure 47.

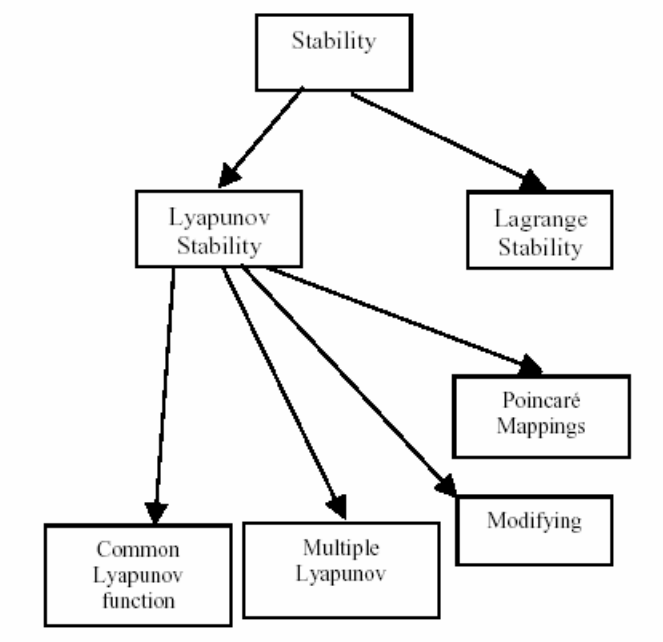

Figure 47. Different ways of proving stability

Among all these methods, the multiple Lyapunov functions technique is the most common one for switched systems. The idea behind the technique is that even if we have Lyapunov functions for each system f_i individually, we need to impose restrictions on switching to guarantee stability.

Consider the following description of the system:

$$\begin{aligned} \dot{x} &= Ax + B_i u_i \\ y &= Cx \\ \dot{f} &= y \\ u_i &= -\beta_i f - \alpha_i y \end{aligned} \qquad i \in \{1, \cdots K\} \qquad (4\text{-}3)$$

Where K is the number of the mid-level feedback PI controllers. We associate with system (4-3) the following switching sequence, indexed by an initial state x_0:

$$S = x_0; \qquad (i_0, t_0), (i_1, t_1), \cdots, (i_n, t_n), \cdots \qquad i_k \in \{1,2,\cdots, K\}, k \in N \qquad (4\text{-}4)$$

Here we adopt some of the results in [47, 48].

For any i such that $1 \le i \le K$, we denote by $S \mid i$ the endpoints of the times that system $\dot{x} = f_i(x)$ is active. The interval completion $I(T)$ of a strictly increasing sequence of times $T = \{t_0, t_1, \cdots, t_n, \cdots\}$ is the set

$$\bigcup_{j \in Z_+} [t_{2j}, t_{2j+1}]$$

Hence, $I(S \mid i)$ is the set of times that the ith system is active. Let $\varepsilon(T)$ denote the even sequence of $T : t_0, t_2, t_4, \cdots$

We say that V is a candidate *Lyapunov function* if V is a continuous positive definite function (about the origin, 0) with continuous partial derivatives. Note this assumes $V(0) = 0$. The following concept of Lyapunov-like function is used in [47].

Definition 4.1: Given a strictly increasing sequence of times T in R, we say that V is *Lyapunov-like* for function f and trajectory $x(\cdot)$ over T if:

- $\dot{V}(x(t)) \le 0$ for all $t \in I(T)$;
- V is monotonically nonincreasing on $\varepsilon(T)$.

Using this definition of Lyapunov-like function, a stability criterion was established in [47] as stated below.

Theorem 4.1: Suppose we have candidate Lyapunov functions $V_i, i = 1, \cdots, K$ and vector fields $\dot{x} = f_i(x)$ with $f_i(0) = 0$ for all i. Let ζ be the set of all switching

sequences associated with the system. If for each $S \in \zeta$ we have that for all i, V_i is Lyapunov-like for f_i and $x_S(\cdot)$ over $S \mid i$, then the system is stable in the sense of Lyapunov.

Figure 48 shows the general case of Lyapunov function values versus time for multiple Lyapunov stability in case $K = 2$. Solid/dotted denotes corresponding system active/inactive.

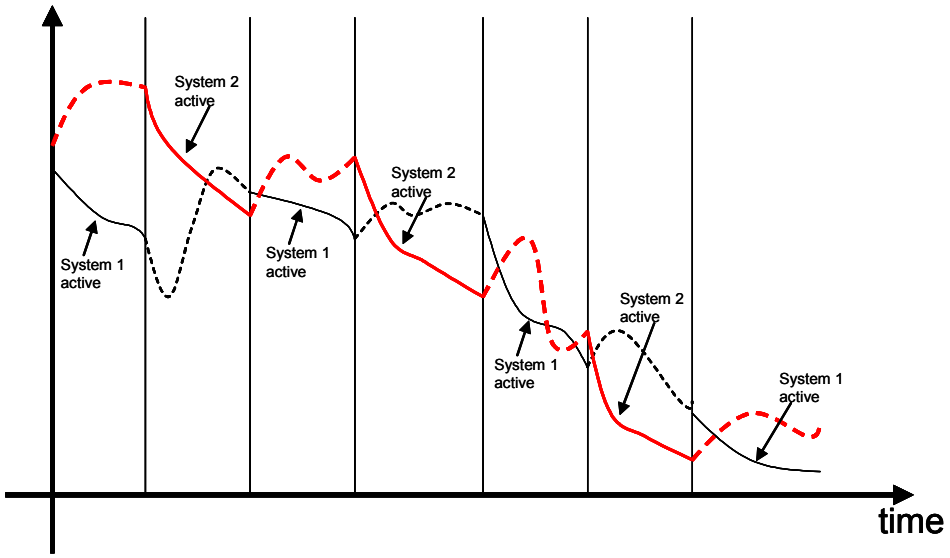

Figure 48. Multiple Lyapunov fuction values vs. time, K=2.

To illustrate theorem 4.1, we constructed the following example. Consider $f_i(x) = A_i x$ where:

$$A_1 = \begin{bmatrix} 1 & 1000 \\ -4 & -10 \end{bmatrix} \qquad A_2 = \begin{bmatrix} 1 & -100 \\ 40 & -10 \end{bmatrix}$$

Then $\dot{x} = f_i(x)$ is globally exponentially stable for $i = 1,2$. Figure 49 shows the trajectories for f_1 and f_2 starting from (5,5).

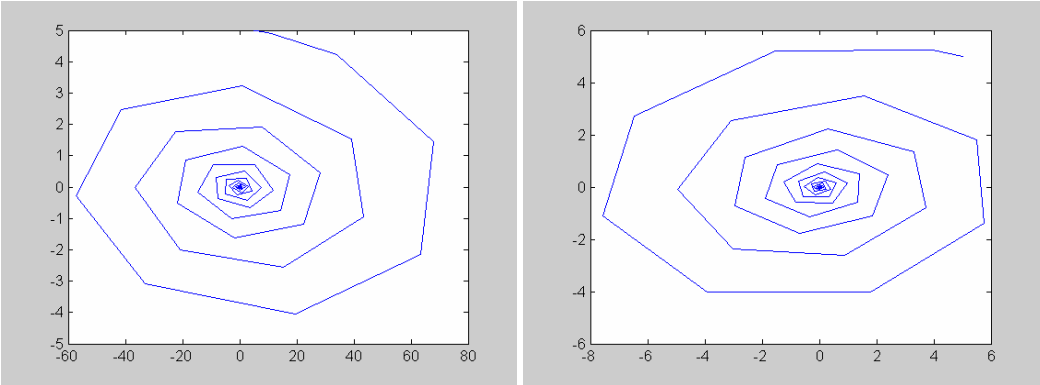

Figure 49. Trajectory of f_1 and f_2

Now consider two cases that the two systems switch to each other.

Case I. System starts using f_1 from (5,5). Then for every second, it switches to the other system. It is easy to see that the system is unstable, and the multiple lyapunov function values are not monotonically nonincreasing on $\varepsilon(S \mid 1)$ and $\varepsilon(S \mid 2)$, as shown in Figure 50 and Figure 51.

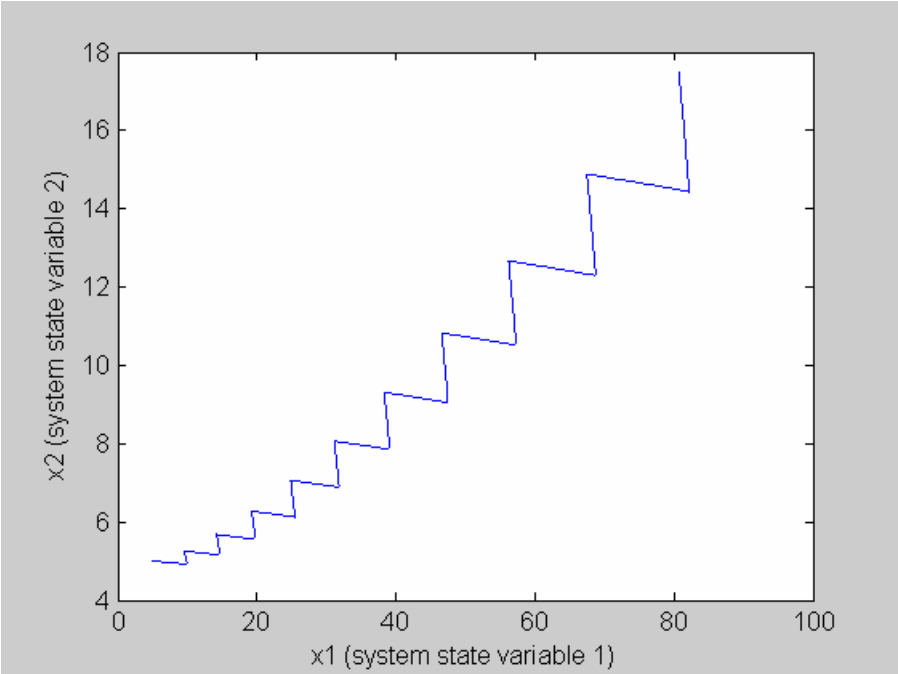

Figure 50. System trajectory with time-based switching

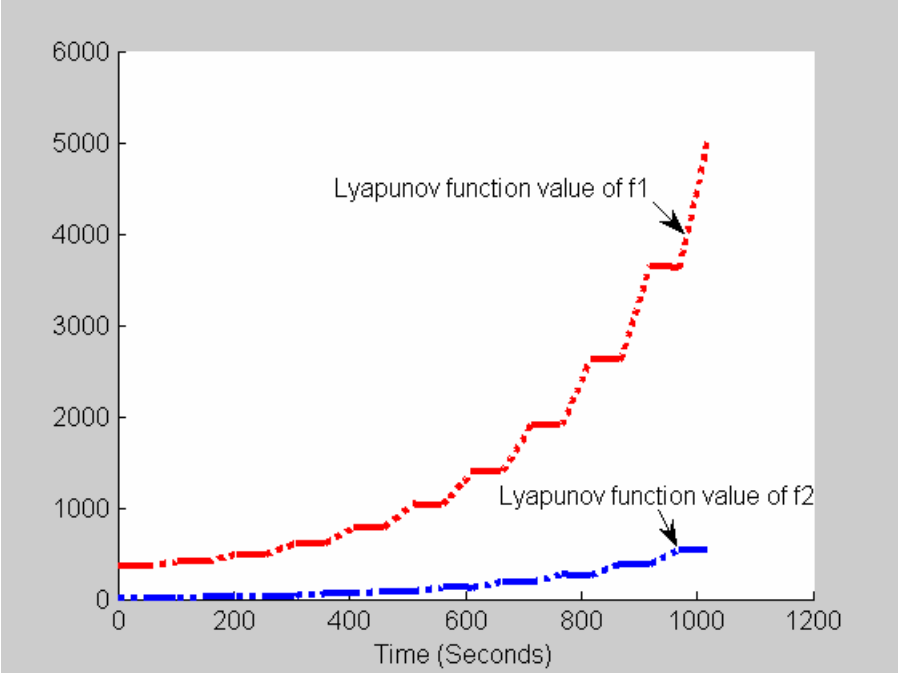

Figure 51. Multiple Lyapunov function values for time-based switching. Solid/dotted denotes corresponding system active/inactive

Case II. System starts using f_1 from (5,5). Then after it switches to f_2 for one time, it checks if the V_i satisfies the *Lyapunov-like* function every second before it switches to system i. If V_i is *Lyapunov-like* function under the switching, then it switches; otherwise, there would be no switching. It is easy to see that the system is stable, and the multiple lyapunov function values are monotonically nonincreasing on $\varepsilon(S \mid 1)$ and $\varepsilon(S \mid 2)$, as shown in figure 52 and figure 53.

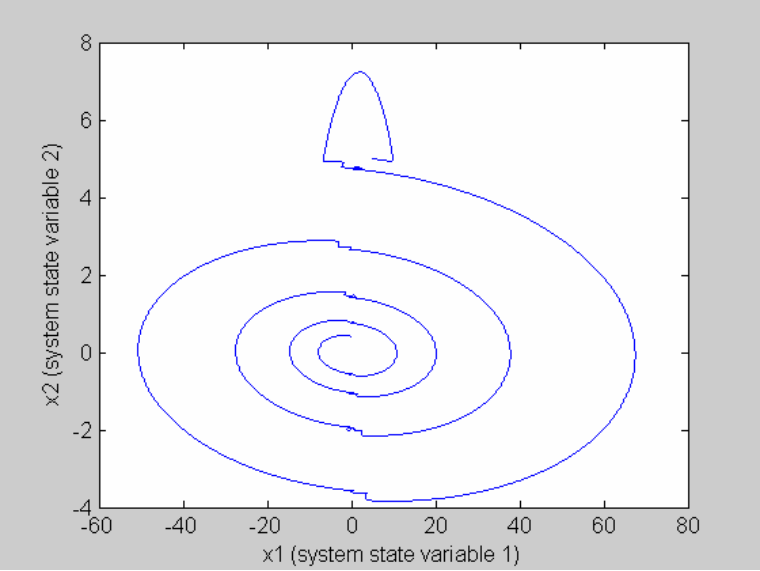

Figure 52. System trajectory with stability guaranteed switching

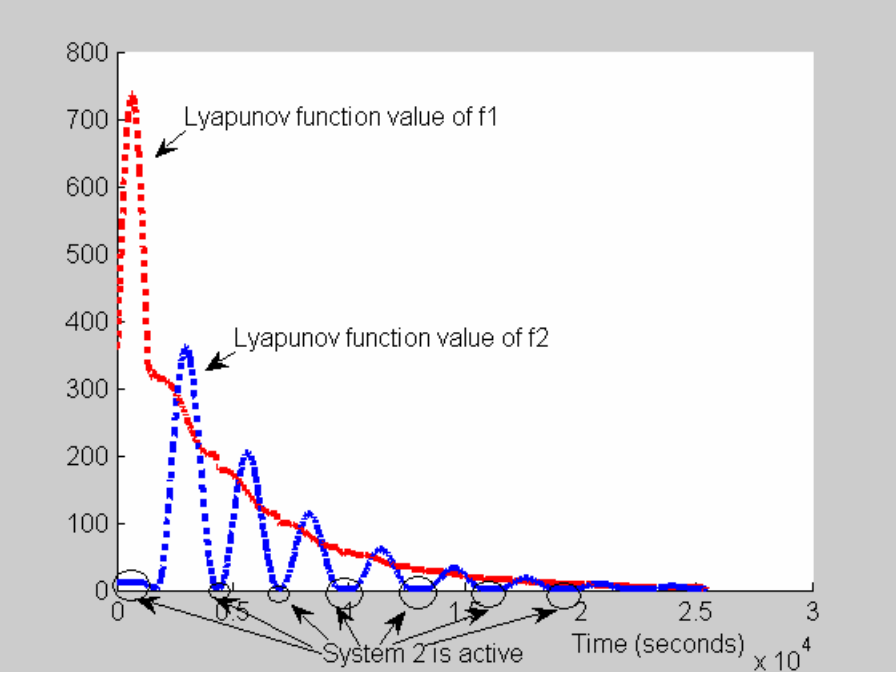

Figure 53. Multiple Lyapunov function values for stability guaranteed switching . Solid/dotted denotes corresponding system active/inactive

Using this result, considering our system (4-3) and switching sequence (4-4), we can generate a controller switching scheme that guarantees stability when we need to switch the controller under the condition that one mid-level PI controller reaches its saturation status. Assume for each PI controller design, we can find a Lyapunov function $V_i(x(t)) = x^T P_i x$ that satisfies $\dot{V}_i(x(t)) < 0$ by adjusting the parameters β_i and α_i. This will guarantee the stability of the system with each individual controller. When switching is needed, we still need to do the stability check to guarantee the stability during the switch.

Figure 54 shows the switching scheme of the controllers on how to determine the value of i_{k+1} by the priority of the controllers and stability check, when switching is

needed at time t_{k+1}. Assume controller P1 is the controller with the highest priority, and controller PK is the controller with the lowest priority:

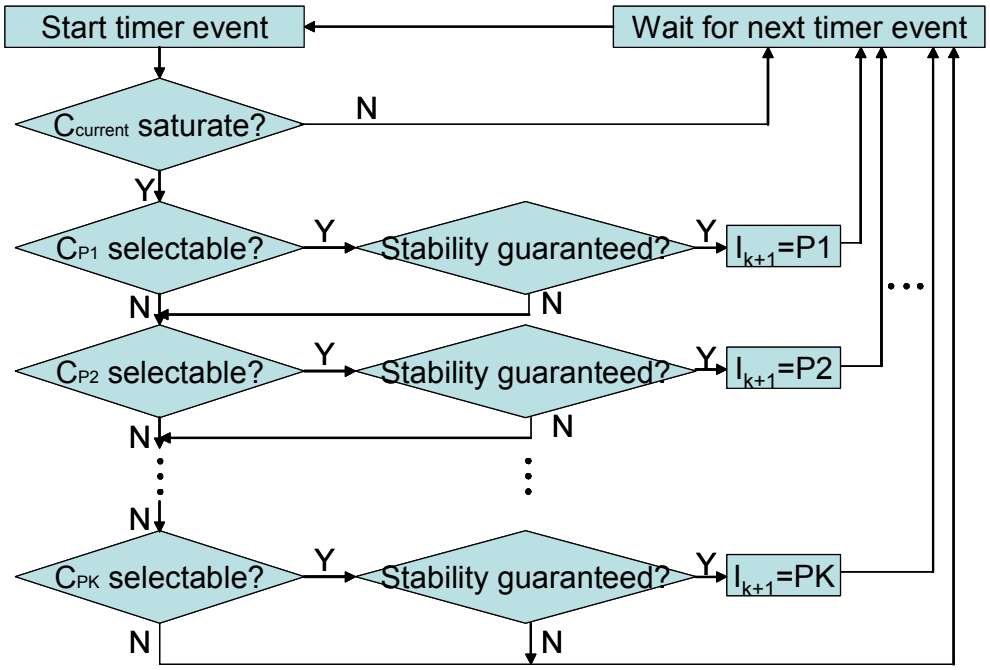

Figure 54. Switching scheme of the mid-level feedback controllers

Whenever a timer event happens, we'll first check if the current controller is in the saturation condition. If so, the process will be initiated to find the next controller to switch on. This includes several steps:

1. Check if the controller of next priority is in saturation or the corresponding low-level controller fails. If so, continue to find other controllers;

2. If a controller (C_{PN}) is pre-selected, we'll check if the switching will cause unstable conditions. From the result of *Theorem 4.1*, if $V_{PN}(t) \le V_{PN}(t_0)$, where t_0 is the start time that controller C_{PN} was active last time, then the stability will be guaranteed if we choose $i_{k+1} = PN$;

3. If no controller can be selected to switch from the stability check result, the current controller will remain on duty. The anti-windup configuration will be effective after the controller enters saturation status.

With this switching scheme, the stability of the whole system with mid-level feedback controller will be guaranteed under regularity conditions. However, this scheme does not cover the stability under the abnormal conditions such as all the controllers fail or saturate.

CHAPTER 5

APPLICATION EXAMPLE – CONTROL STRATEGY

The project of automated vision-based inspection and control of high-volume baking processes introduced in Section 3.1 also serves as the test bed for the control methodology. As a reminder, the process is briefly introduced again as following.

The production rate of the bun is 1000 buns / minute. The average baking time for the bun is 8.4 minutes. There are four control loops to control the zone temperatures and a control loop to control the conveyor belt speed (baking time). The control action for the zone temperature is the flow rate of the gas in the burners. The zones are grouped for control purposes as zones 1 and 2, zones 3 and 4, zones 5 and 6, and zone 7. The low-level temperature controllers are implemented by Rockwell Automation PLCs and the conveyer belt motor controller is implemented by VFD Variable Speed Controls. A touch screen operator interface is available for the operators to input the set points of the low-level controllers and also to monitor the process data. All the data is available on the local network Data Highway plus. Currently the inspection of the bun quality is done manually by operators with a sampling rate of one bun / half hour.

5.1 Data Acquisition

Data was acquired from both the quality inspection system and the process monitoring sensors, and saved in the sensor module as shown in Figure 27 in Chapter 4. Details are presented below.

- Quality inspection data

High-quality images of buns are acquired using an on-line imaging system as shown in Figure 55 designed by researchers at Georgia Tech Research Institute (GTRI) [57,58]. Image processing algorithms are utilized to inspect the bun defects such as bake level (color), garnish coverage, 2D shape and size, crowsfeet, blisters, punctures, and crescents. Figure 56 shows some quality inspection data for the hamburger buns. In this research, color is selected as a quality feature to feed back to the mid-level control module for the baking oven control.

Figure 55. Online imaging system

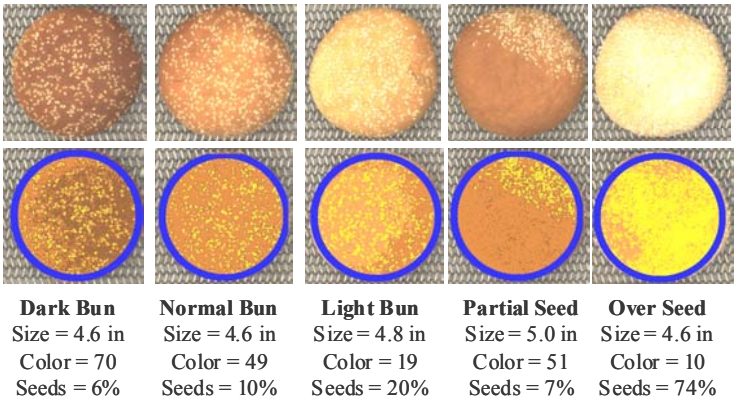

Figure 56. Quality inspection data

- Process monitoring data

Process monitoring data such as oven zone temperatures, conveyor speed and each burner's energy are obtained through the local network. Oven load is measured using photo detectors. An example of zone 1&2's temperature profile is presented in Figure 57.

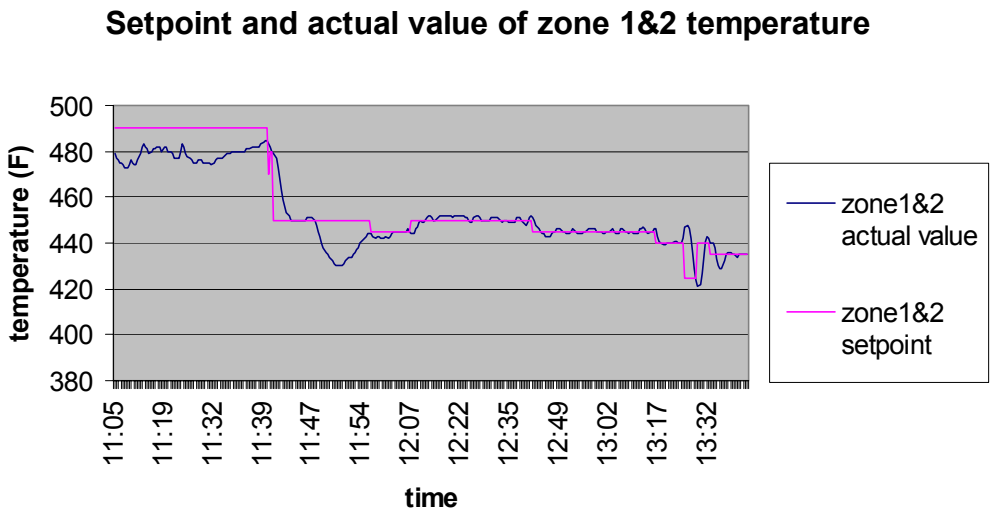

Figure 57. Process monitoring data

Both the bun color measurement and the process monitoring data are collected at a sampling rate of 6 samples / minute and saved in the sensor module.

5.2 Mid-level Control

5.2.1 Feed-forward controller

The model developed in Section 3.2 was used for model prediction of color. Particle Swarm Optimization (PSO) introduced in Section 4.3.1 was used for nonlinear optimization. The simulation of the feed-forward controller was done in Matlab to find the optimal set points of the zone controllers.

We simulated the following condition: the burners in zone 3 failed at time 10 minutes so that it can only generate 60% output of expected output (bstate=0.6). Figure 58 compared the color output of the system with and without the mid-level feed-forward

controller. Figure 59 shows the feed-forward controller output. Figure 60 shows the real oven zone temperatures without & with feed-forward controller.

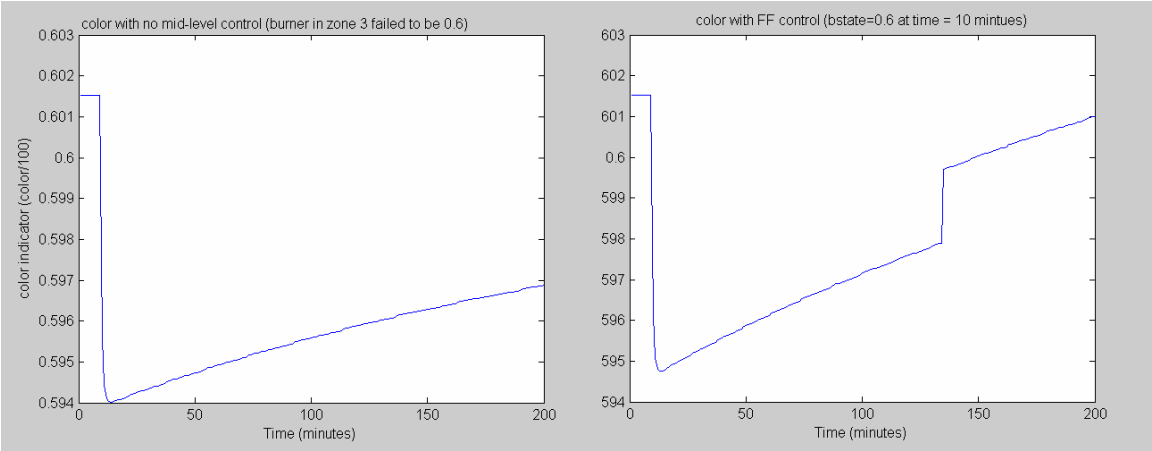

Figure 58. Color output: no mid-level controller compared with feed-forward controller

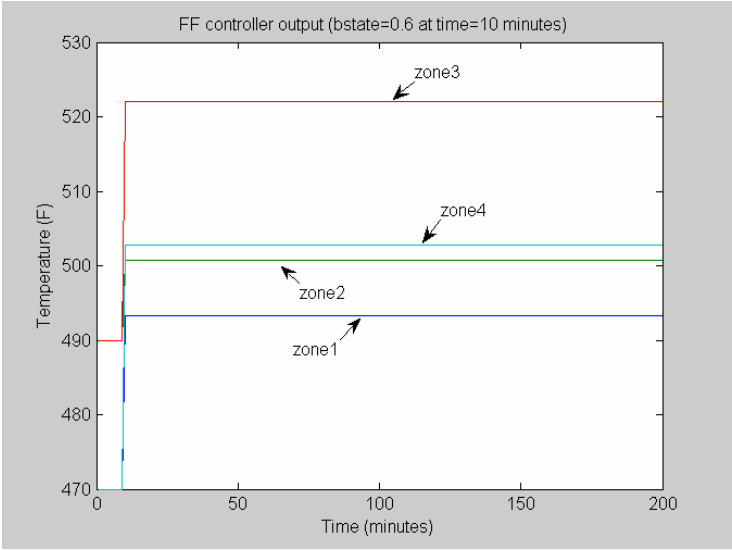

Figure 59. Feed-forward controller output (i.e., set points for low-level zone temperature control)

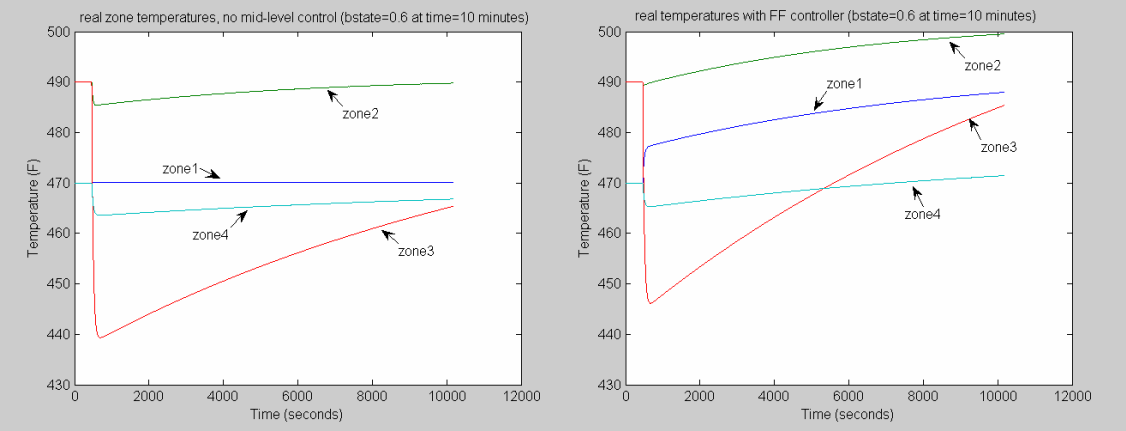

(a) (b)

Figure 60. Real oven zone temperature (without & with feed-forward controller)

We can see from the result in part (a) of Figure 60 that when a burner fail condition happens, the corresponding zone temperature (temperature in zone 3) drops. Even though it can be compensated by neighboring zone temperatures, it still will have a steady state error. As a result, the color output will also deviate from the set point. With the feed-forward controller, the new set points of the low-level controller will set the oven temperature to a higher level (from 490F to more than 520F for zone 3 as shown in Figure 59) so that the color will be brought back to its desired value. The real oven zone temperature with feed-forward controller is shown in part (b) of Figure 60.

5.2.2 Feedback controller

Figure 61 compares the color output without mid-level feedback controller, with PI controller but no anti-windup configuration, and with PI controller & anti-windup controller. There is only one feedback PI controller active and no switching occurs in this example. The switching example will be given in section 5.2.4. The set point of the color

is 60.45. The color started to deviate from the set point at time 10 minutes because of the disturbances. In the case without controller, it dropped all the way down to 59.5, and then went back to the set point after the disturbances disappeared. For the case with the mid-level controller, the color is controlled within a belt range with 60.45 in the center. Given the target range of the color [59.9, 61], the bun color quality after the controller was applied all fell into the target range. The result shows that the PI controller greatly improved the bun color quality. Also, with the anti-windup configuration, even after the controller entered saturation, the overshoot was not as high as without AWC.

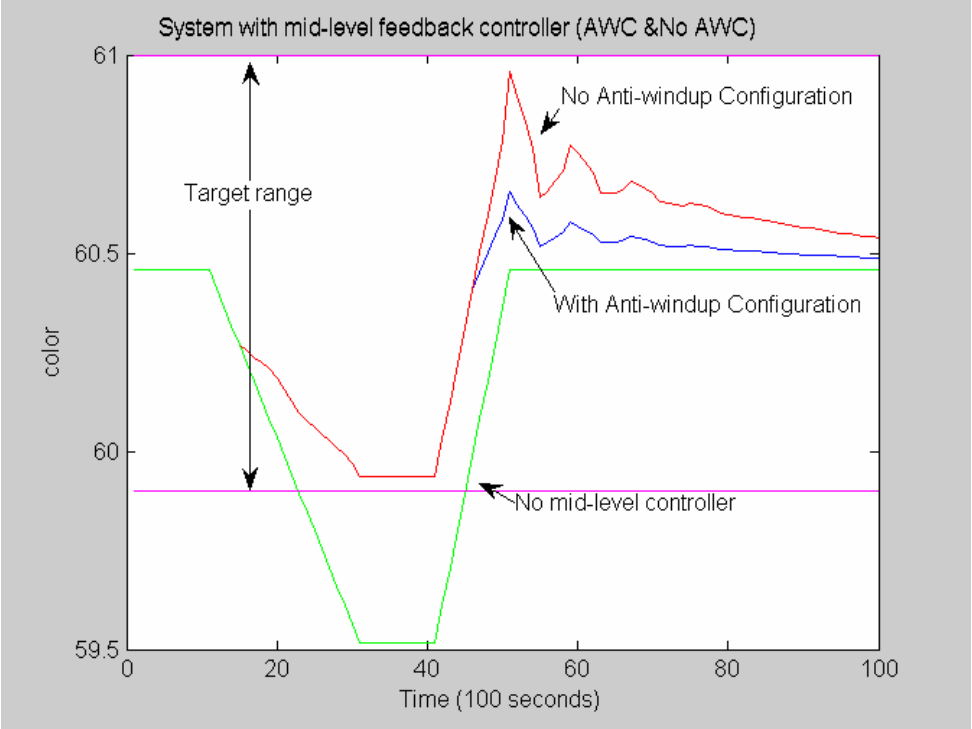

Figure 61. Feedback controller result

Figure 62 shows the controller output (a) and the simulated oven temperature (b) for both AWC and no AWC cases. This example only uses PI controller for set point change of zone 3. The example that switches among all PI controllers will be given later.

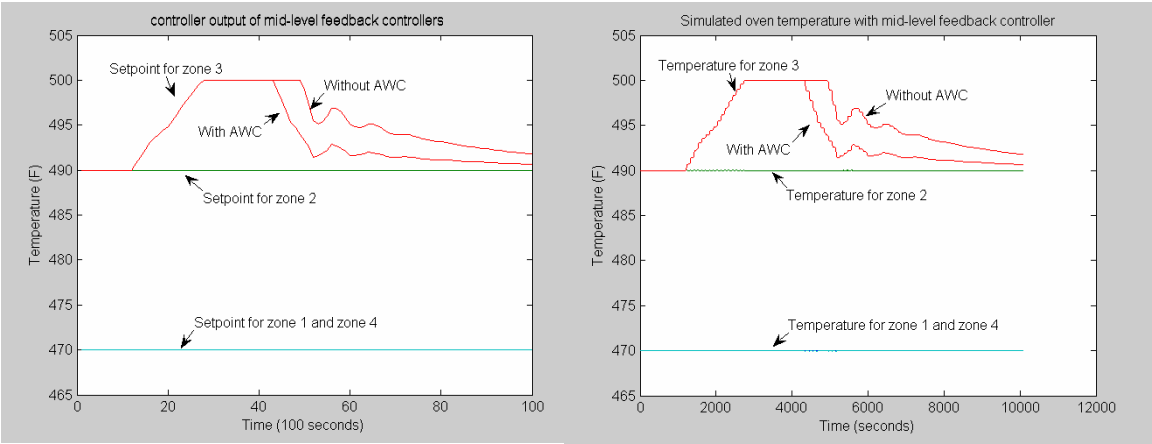

(a) (b)

Figure 62. Feedback controller output (i.e., set point for low-level zone temperature control) and real oven temperature

5.2.3 Feed-forward combined with feedback controller

Figure 63 compares the color output of the system under the following cases: no controller, only feed-forward controller, and feed-forward combined with feedback controller. The simulation simulated the condition that burner 3 failed at time 10 minutes. The result shows that even though the feed-forward controller is very effective in setting the oven to a new equilibrium point to optimize the color output, there still is a steady state error due to the model prediction error. The feedback controller is very effective in eliminating the steady state error under this case.

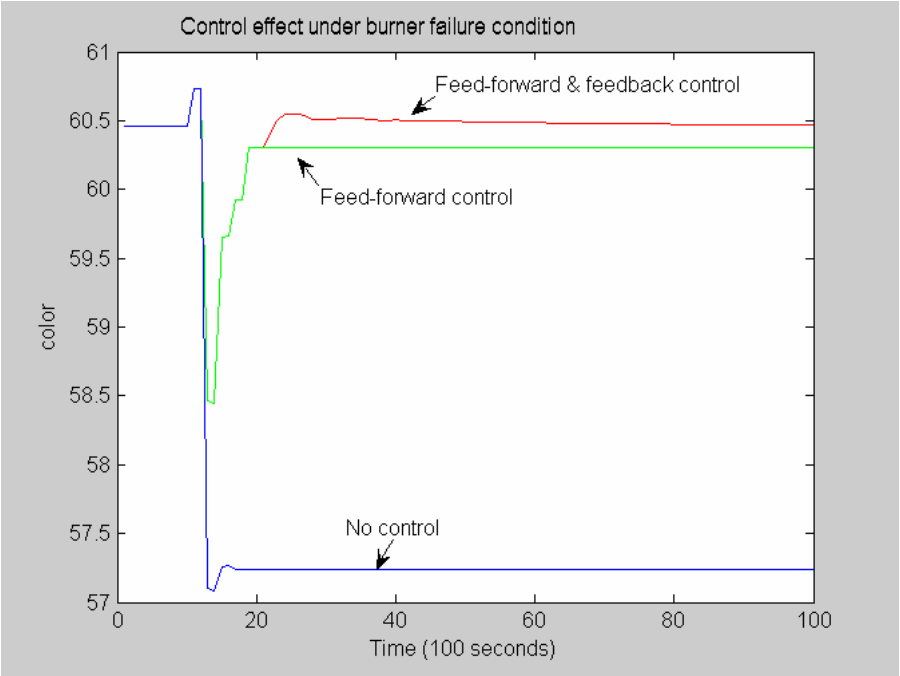

Figure 63. Control effect of feed-forward combined feedback controller

Figure 64 shows the controller output (a) and the simulated oven temperatures (b) under both cases: feed-forward (ff) controller only, and feed-forward controller combined with feedback controller (ff&fd).

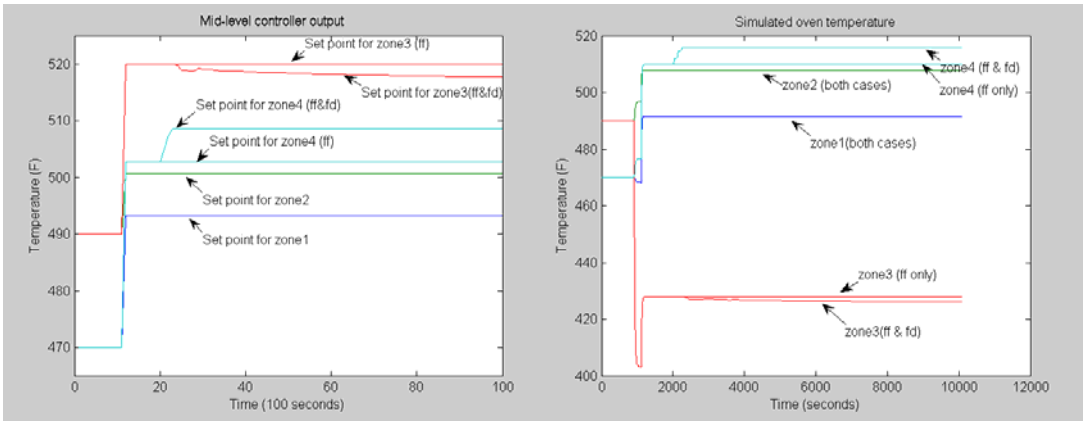

(a) (b)

Figure 64. Mid-level controller output and real oven temperature

5.2.4 Stability guaranteed switch of feedback controllers

As stated before, there are four PI feedback controllers in the mid-level controller configuration. At one time only one controller is effective. When the controller switches, we need to verify stability.

The procedure to check stability is shown in Section 4.4. Here we present some results. We also simulate the condition that the color starts to deviate from the set point at time 10 because of the disturbances. Figure 65 shows the color output of the system when all the PI controllers switch based on time sequence without a stability check. For example, the switching sequence is:

$$S = x_0; \qquad (1,1),(2,2),(3,3),(4,4),(1,5),(2,6),(3,7),(4,8),(1,9),\cdots,(i_n,t_n),\cdots \quad .$$

We can see that even though the system was stable using each single controller, the switch caused unstable output.

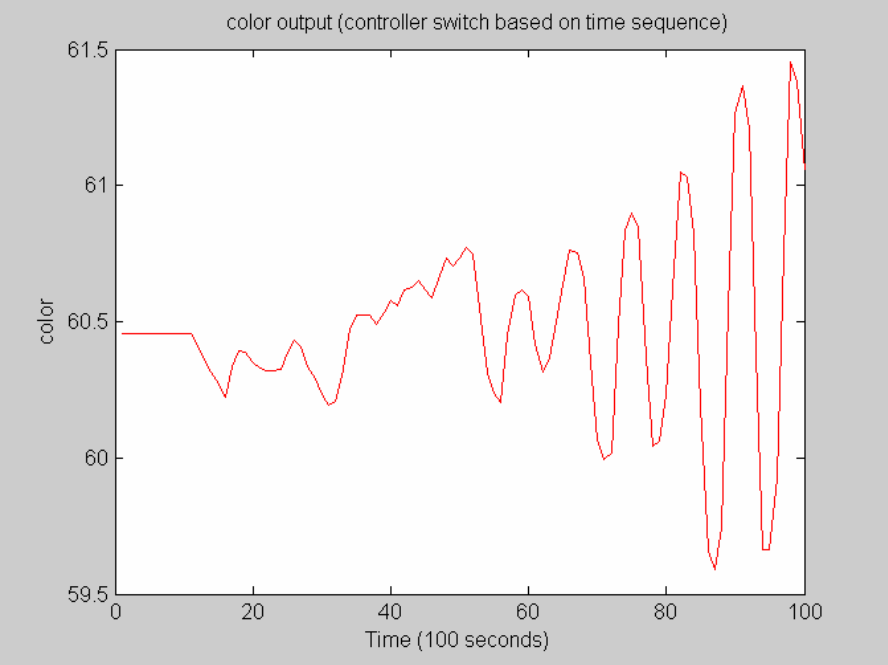

Figure 65. Color output with PI controller switch based on time sequence

Figure 66 shows the corresponding controller output (a) and the simulated oven temperature (b).

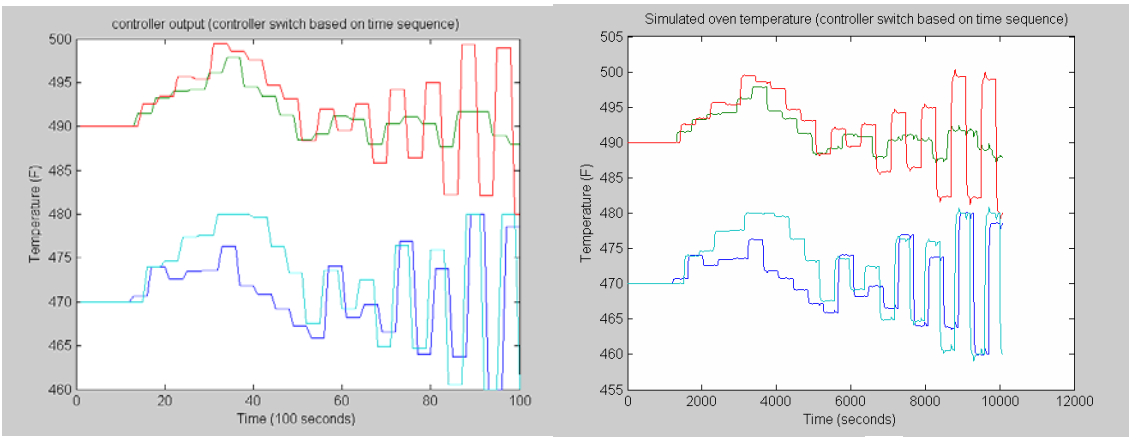

(a) (b)

Figure 66. Controller output and oven temperature with no stability check

Figure 67 shows the color output of the system when the switching scheme presented in Section 4.4 is implemented. We can see that with the stability check, the system is stabilized.

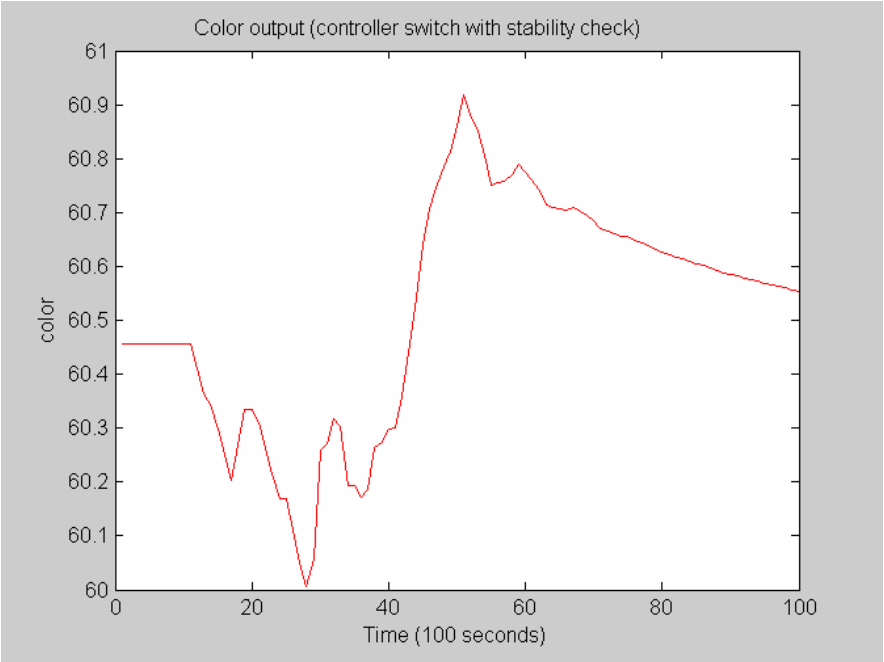

Figure 67. Color output (PI controller switch with stability check)

Figure 68 shows the corresponding controller output (a) and the simulated oven temperature (b).

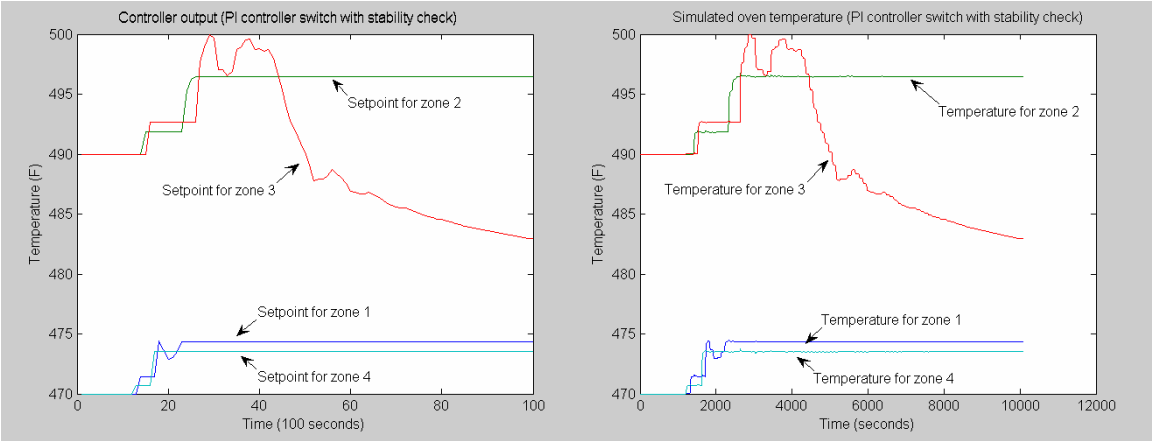

(a) (b)

Figure 68. Controller output and oven temperature with stability check

Figure 69 shows the corresponding active controller ID vs. time. We can see that the system starts with the controller for zone 3 active. Then it switched to controllers for zone 4, zone 1, zone 2, zone3, zone 4 in sequence, and then stayed with controller for zone 1 for a period time. It then switched to controller for zone 2 for a short time before it switched back to controller for zone 3.

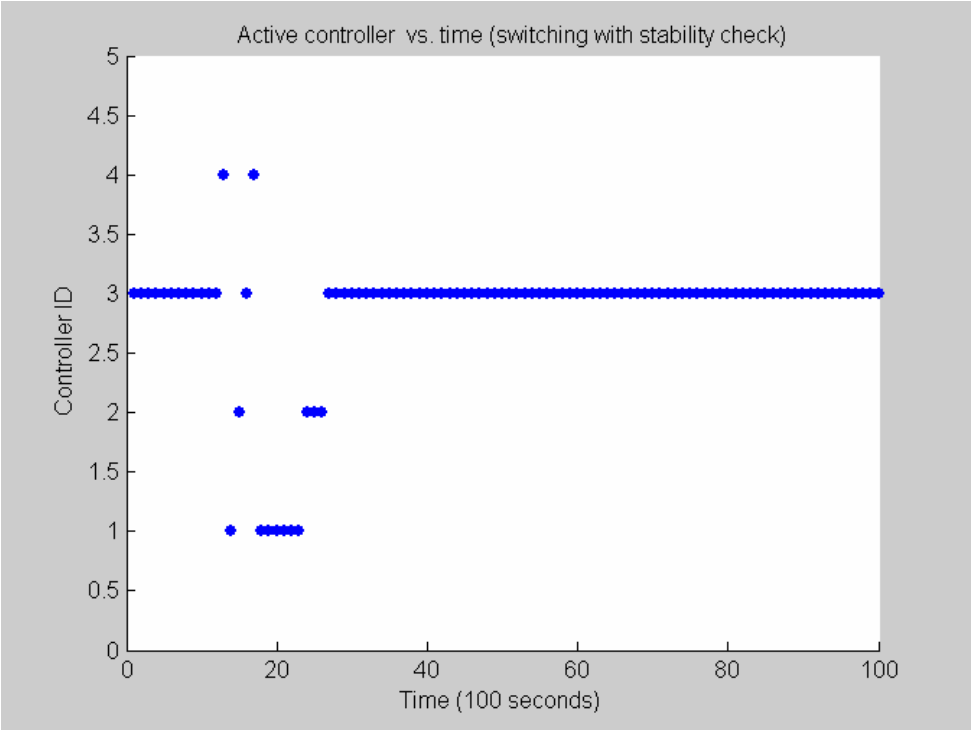

Figure 69. Active controller ID vs. time

5.2.5 On-line test of feedback controller performance

Both the PI feedback controller and the PID feedback controller were tested online in the Flowers Bakery, Villa Rica, Georgia. Figure 70 shows the bun color index (L-value) measured from the online inspection system and the temperature versus time. In this case, the controller was not yet activated. The actual temperature (in pink) tracks the set point temperature (in yellow) reasonably well. These are the lower two plots and should be read using the scale on the left. The L-value is an indication of the color value and computed by the online vision inspection system. Flowers Bakery has a specification for the color index from their customers. For the buns being baked at the time of testing, the target L-value was 60.5 with a target range 59-62. The acceptable range was 57-64.

Notice that the measured L-value (using the scale on the right) spent the majority of the time outside of the target value, and even strayed outside of the acceptable value. There was some oscillation that we attribute to the variation that occurs as a batch of dough ages.

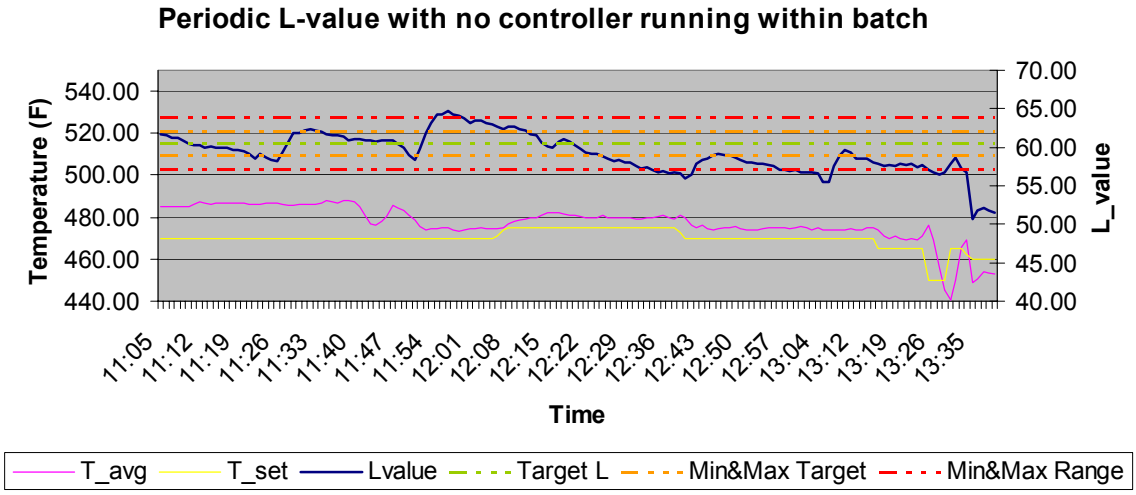

Figure 70. Online test of color without controller

Figure 71 shows the result of one test after turning on the PI controller. The controller calculated a new temperature setpoint for the oven every 30 seconds based on the color measurements. With the controller on, the color index stayed within the acceptable region at all times and was regulated very closely to the desired value of 60.5. To test the control, the temperature was taken out of control by adjusting the temperature manually in order to bring the color off target. In Figure 71, this point in time is marked as 1. At time 2, the controller is turned on. There is a slight delay in the response, but the control is clearly bringing the color back to the target value at time point 3.

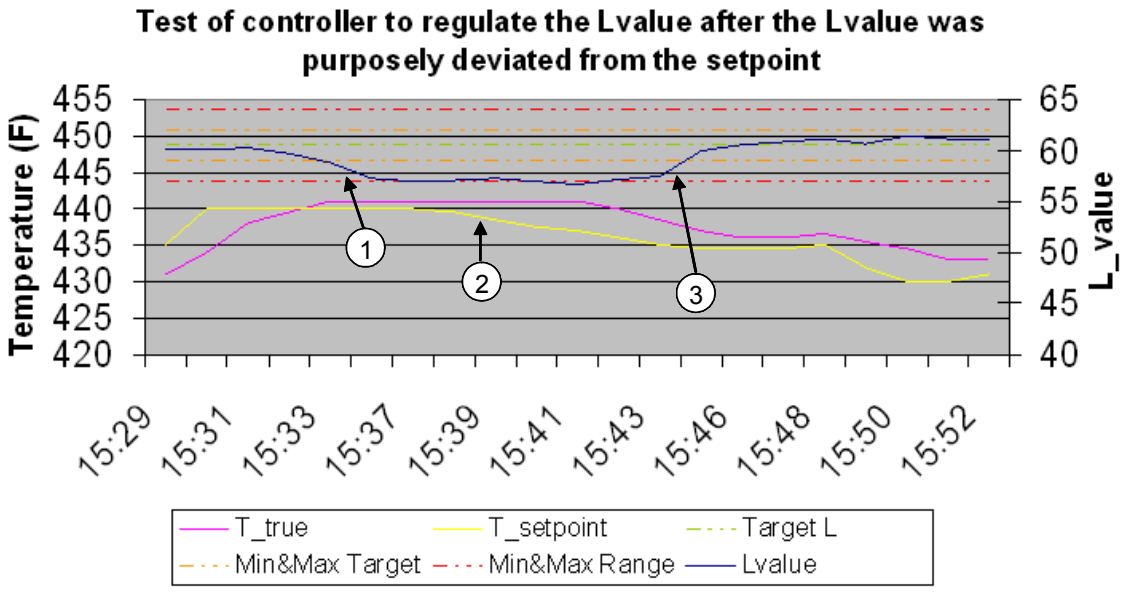

Figure 71. Online test of color with mid-level PI controller

Figure 72 shows the result of another test after turning on the PI controller with a different coefficient setting. The controller calculated a new temperature setpoint for the oven every 10 seconds based on the color measurements. The desired value of the Lvalue is 59 in this test. Figure 72 showed the situation that the controller made changes to temperature setpoint continuously to maintain the Lvalue very close to the desired value during the normal operation, so that the variations appeared in the open loop situation were eliminated.

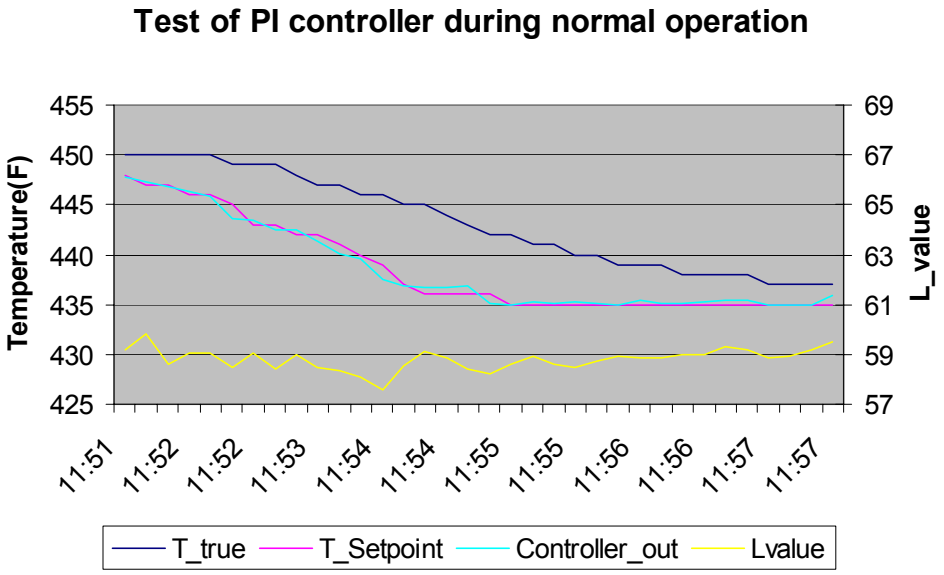

Figure 72. Example of PI controller for normal operation

CHAPTER 6

SUMMARY AND FUTURE WORK

6.1 Summary

Although vision-based inspection and process control are not new, their application to real-time, on-line, 100 percent inspection of high-volume product is new. Thanks to the emerging advanced technologies in sensing, computing, signal and image processing, and pattern recognition, the online control of product quality based on vision inspection is possible. The objective of this research is to create a vision-based systems approach to product monitoring and process control for a complex industrial process such as baking.

The first part of this dissertation described a general methodology for product quality modeling, especially for baking products. High fidelity models are essential to control and optimize the process. They establish the relationship between the process operating variables and the final product quality. This modeling methodology illustrates how to combine physical based and data-driven models to simplify the modeling process and increase the model flexibility. The physical-based modeling is used to model the product temperature profile, and the data-driven modeling is used to train the mapping from the product temperature profile to each quality metric. The partitioning into sub models increased the flexibility of model development and reduced the effort to change the model when the quality metrics change. The model generated is used by model-based control algorithms to do model prediction.

In the second part of the dissertation, a feed-forward combined with feedback controller strategy is presented for the purpose of quality improvement based on vision-inspection. In this strategy, the feed-forward controller takes responsibility to generate the low-level oven temperature set points considering the nonlinear nature of the model. It also generates set points when there are failure conditions. Meanwhile, the feedback controllers are effective in fine tuning the low-level temperature set points to improve the product quality in the operating range in which the system can be treated as a linear system. The nonlinear optimization of the feed-forward controller is done using a Particle Swarm Optimization algorithm. The feedback controller design utilizes the traditional PI controller design with anti-windup configuration. The system stability is studied using hybrid system analysis method to guarantee the stability when the individual feedback controllers switch between one another. The controller performance is tested by Matlab simulation. The result shows that the feed-forward combined with feedback controller strategy can greatly improve the product quality. The PI feedback controller is also tested in a real baking plant, and the result shows that it is very effective in quality improvement.

6.2 Significant contributions

This work leads to the following contributions:

- We generate a novel quality modeling method, which combines both physics-based and data-driven models. Since the quality model is broken down into several sub-models, its flexibility is greatly increased. The effort required to change the model when quality metrics change is greatly reduced.

- We apply a hierarchical control architecture to baking processes, which provides a systematic way to incorporate advanced process control techniques based on feedback provided by machine vision-based quality inspection systems.
- We verify the proposed modeling method and control architecture using advanced Design of Experiment (DOE) methods.
- We implement hybrid system analysis methods to validate the performance of the vision-based feedback controller.

6.3 Future work

Potential for extending the material in this thesis exists in the following.

1. Consistent measurements in experiments

   Currently, during the experiments to acquire temperature profile data, the thermocouples were inserted into the baking products at a depth that was estimated by people who conducted the experiments. Because the thermocouples are very thin and soft, it was very hard to fix the end of the thermocouple in place. The measurements of the surface and the core temperature profiles were done at the locations that approximate the "surface" and "core" as much as possible each time, and this will cause some inconsistency of the thermocouple locations in measurements from experiment to experiment. More consistent measurements in experiments would require a better way to fix the thermocouples accurately in the baking products.

2. Temperature profile model

Currently, the coefficients in equation (3-4) are treated as constants. A more accurate model would treat those coefficients as functions of air temperatures, surface temperatures, and locations inside the oven. This would require more thorough study of the topology and heat transfer modes inside the oven, and then formulate the function for these coefficients.

3. Multiple objective optimization with multiple quality metrics

   Currently, only color was used to measure the baking product quality, and only a color quality model was developed. When all other quality factors like shape, size, and thickness are taken into consideration, the optimization will turn into a multiple objective optimizaiton problem. The control strategy may also need to be modified to balance the quality improvement of all quality factors.

4. Application to other baking process --- biscuits, cookies, pies

   The methodology presented in this research is currently being applied to a hamburger bun baking process. Eventually the generic aspect of this methodology can be utilized in all kinds of baking processes. Some details in modeling and control algorithms may need to be modified according to the particular process/product characteristics.

5. Application to proofing

   The same methodology/technique can also be utilized in the proofing process. Rather than color, the product size (height and diameter) can be used to control the proofing parameters. These qualities can also be measured by the imaging system.

REFERENCES

1. Industrial process control [Guest Editorial]**,** *Piovoso, M.J.* IEEE Control Systems Magazine , Volume: 20 Issue: 3 , June 2000, Page(s): 22 –24

2. Advanced control methods for French fry quality improvement, Montague, G.A.; Glassey, J.; Willis, M.J.; Smith, R.; Wiggins, G.; Key, A. Computing & Control Engineering Journal , Volume: 13 Issue: 1 , Feb. 2002, Page(s): 26 –32

3. Classifier design for computer grading systems for food processing, Hu, B.-G.; Gosine, R.G.; de Silva, C.W. Systems, Man and Cybernetics, 1995. Intelligent Systems for the 21st Century, IEEE International Conference on, Volume: 1 , 1995 Page(s): 730 -735 vol.1

4. Evaluation of colour spaces in computer vision application of wood defects detection, Adel, M.; Wolf, D.; Vogrig, R.; Husson, R. Systems, Man and Cybernetics, 1993. 'Systems Engineering in the Service of Humans', Conference Proceedings, International Conference on, 1993 Page(s): 499 -504 vol.2

5. A computer vision system for automated grading of rough hardwood lumber using a knowledge-based approach, Cho, T.-H.; Conners, R.W.; Araman, P.A. Systems, Man and Cybernetics, 1990. Conference Proceedings, IEEE International Conference on, 1990 Page(s): 345 –350

6. Sensor Fusion for Real Time Quality Evaluation of Biscuit during Baking. Comparison between Bayesian and Fuzzy Approaches, N. Perrot, G. Trystram, D. Le Guennec and F. Guely Journal of Food Engineering, Volume 29, Issues 3-4, August-September 1996, Pages 301-315

7. Non-standard application of SPC in sugar quality monitoring, Ooi, G.K.; McFarlane, D.C. Control '98. UKACC International Conference on (Conf. Publ. No. 455) , Volume: 1 , 1998 Page(s): 485 -490 vol.1

8. Statistical process control in UK food production: an overview, Grigg, Nigel P, British Food Journal; Volume 100 No. 8; 1998

9. Statistical process control-the British Sugar experience, Sanigar, K.M.A. Applied Statistical Process Control, IEE Colloquium on , 1990 Page(s): 5/1 -5/5

10. Experiences of introducing SPC in a confectionery factory, Bidder, P.L. Applied Statistical Process Control, IEE Colloquium on , 1990 Page(s): 2/1 -2/2

11. Advanced process control techniques for the food industry, Timothy A. Haley and Stevan J. Mulvaney. Trends in Food Science & Technology, April 1995 Page(s):103-110

12. Sensory evaluation in quality control: an overview, new developments and future opportunities, Alejandra M. Munoz. Food Quality and Preference, 2002 Page(s): 329-339

13. Inspection and Quality Control – An Overview, Danial Irvine, Mysore Narayanan, IEEE

14. Systems Engineering and Information Technology: Catalysts for Total Quality in Industry and Education, Andrew P. Sage, IEEE Transactions on Systems, Man, and Cybernetics, Vol. 22, No. 5, September/October 1992

15. Closed Loop Quality Control in Printed Circuit Assembly, Klaus Feldmann and Jurgen Sturm, IEEE Transactions on Components, Hybrids, and Manufacturing Technology --- Part A, Vol. 17, No. 2, June 1994

16. Machine vision based control of the ball and beam, Petrovic, I.; Brezak, M.; Cupec, R.; Advanced Motion Control, 2002. 7th International Workshop on , 3-5 July 2002 Pages:573 – 577

17. Autonomous landing of airplanes by dynamic machine vision, Dickmanns, E.D.; Schell, F.-R.; Applications of Computer Vision, Proceedings, 1992., IEEE Workshop on , 30 Nov.-2 Dec. 1992 Pages:172 – 179

18. Machine vision in the tire industry, Blackwell, G.F.; Electrical Engineering Problems in the Rubber and Plastics Industries, 1989., IEEE Conference Record of 1989 Forty-First Annual Conference of , 10-11 April 1989 Pages:67 – 79

19. Mobile vision-based vehicle tracking and traffic control, Rabie, T.; Shalaby, A.; Abdulhai, B.; El-Rabbany, A.; Intelligent Transportation Systems, 2002. Proceedings. The IEEE 5th International Conference on , 2002 Pages:13 – 18

20. Uncalibrated vision-based mobile robot obstacle avoidance, Piepmeier, J.A.; Southeastern Symposium on System Theory, 2001. Proceedings of the 33rd , 18-20 March 2001 Pages:251 – 255

21. Vision-based implementation of feedback control of unicycle robots, Kwolek, B.; Kapuscinski, T.; Wysocki, M.; Robot Motion and Control, 1999. RoMoCo '99. Proceedings of the First Workshop on , 28-29 June 1999 Pages:101 – 106

22. Vision-based finger tracking of breast palpation for improving breast self-examination, Jianchao Zeng; Yue Wang; Turner, R.; Freedman, M.; Mun, S.K.; Engineering in Medicine and Biology Society, 1996. Bridging Disciplines for Biomedicine. Proceedings of the 18th Annual International Conference of the IEEE, Volume: 1 , 31 Oct.-3 Nov. 1996 Pages:148 - 149 vol.1

23. Vision-based lateral control of vehicles, Kosecka, J.; Blasi, R.; Taylor, C.J.; Malik, J.; Intelligent Transportation System, 1997. ITSC 97. IEEE Conference on , 9-12 Nov. 1997 Pages:900 – 905

24. Identification of secondary flow pattern in a heated curved rectangular channel using image processing technique, Chun Che Fung; Kien-Ping Chung; Chandratilleke, T.; Eren, H.; Instrumentation and Measurement Technology Conference, 2001. IMTC 2001. Proceedings of the 18th IEEE , Volume: 3 , 21-23 May 2001 Pages:2093 - 2098 vol.3

25. Wavelet analysis to fabric defects detection in weaving processes, Sungshin Kim; Man Hung Lee; Kwang-Bang Woo; Industrial Electronics, 1999. ISIE '99. Proceedings of the IEEE International Symposium on , Volume: 3 , 12-16 July 1999 Pages:1406 - 1409 vol.3

26. Machine vision reaches top gear, Graves, C.; IEE Review , Volume: 44 , Issue: 6 , 19 Nov. 1998 Pages:265 – 267

27. An Integrated Approach to Real-Time multisensory Inspection with an Application to Food Processing, Ding, Yuhua, Ph.D. thesis, Georgia Institute of Technology, December, 2003

28. Robust Engineering, Genichi Taguchi, Subir Chowdhury, Shin Taguchi, New York : McGraw-Hill, c2000

29. The quality trilogy: A universal approach to managing for quality, Juran Joseph, Quality Progress, pp. 19-24, Aug. 1988.

30. Modeling of Simultaneous Heat and Water Transport in the Baking Process, S. S. Sablani, M. Marcotte, O. D. Baik and F. Castaigne, Lebensmittel-Wissenschaft und-Technologie, Volume 31, Issue 3, April 1998, Pages 201-209

31. Optimisation of the temperature profile in bread baking, Nantawan Therdthai, Weibiao Zhou and Thomas Adamczak, Journal of Food Engineering, Volume 55, Issue 1, November 2002, Pages 41-48

32. Product quality control and its application to the flash smelting process, Weihan Wan; Haizhou Wang; Li Yongjun; Baiwu Wan; Intelligent Control and Automation, 2002. Proceedings of the 4th World Congress on , Volume: 2 , 10-14 June 2002. Pages:1369 - 1375 vol.2

33. French fry quality improvement using advanced control techniques, G. A. Montague, J. Glassey and M. J. Willis Journal of Food Engineering, Volume 57, Issue 4, May 2003, Pages 357-365

34. Feed-back quality control in the baking industry using fuzzy sets, Perrot N., Trystram G., Guely F., Chevrie F., Schoesetters N. et Dugre E. J. Food Proc. Eng. 2000 (23): 249-279.

35. Neural network modeling and fuzzy control simulation for bread-baking process, Kim, S., Cho, S.I., Transactions of the ASAE, v 40 n 3 May-Jun 1997, p 671-676.

36. Nonlinear model based predictive control using multiple local models, Shane Townsend and George W. Irwin, Nonlinear predictive control theory and practice, IEE control engineering series 61, 2001.

37. Multivariable control design in the frequency domain for an industrial electrical tubular oven, Galvez, J.M.; de Araujo, L.P.; Circuits and Systems, 1995., Proceedings., Proceedings of the 38th Midwest Symposium on , Volume: 1 , 13-16 Aug. 1995 Pages:421 - 424 vol.1

38. Adaptive decoupling predictive temperature control for an extrusion barrel in a plastic injection molding process, Chi-Huang Lu; Ching-Chih Tsai; Industrial Electronics, IEEE Transactions on , Volume: 48 , Issue: 5 , Oct. 2001 Pages:968 – 975

39. Simultaneous adaptive decoupling and model matching control of a fluidized bed combustor for sewage sludge, Yingmin Jia; Kokame, H.; Lunze, J.; Control Systems Technology, IEEE Transactions on , Volume: 11 , Issue: 4 , July 2003 Pages:571 – 577

40. A Shape-Based Approach to Curve Evolution for Segmentation of Medical Imagery, A. Tsai, A. Yezzi, W. Wells, C. Tempany, D. Tucker, A. Fan, W. Grimson, and A. Willsky, IEEE Trans. Medical Imaging, submitted.

41. An Integrated Systems Approach to Monitoring and Control of Complex Industrial Processes, Yingchuan Zhang, D. Britton, Yong Zhang, B. Heck and G. Vachtsevanos, 7th WSEAS International Multiconference on Circuits, Systems, Communications and Computers (CSCC 2003), Corfu, Greece, July 7-10, 2003.

42. Design and Analysis of Experiments, Douglas C. Montgomery, 4h Edition, Wily &Sons. Inc.

43. ASTEQ, Artificial Sensing Techniques for the Evaluation of Quality, Douglas Neil Rutledge, Institute National Agronomique, Paris-Gignon.

44. Food Quality Sensors, Finn Holm, Flair-Flow 4 synthesis report, FoodGroup Denmark, Denmark, January, 2003.

45. A new optimizer using particle swarm theory, Eberhart, R. C. and Kennedy, J. Proceedings of the sixth international symposium on micro machine and human science pp. 39-43. IEEE service center, Piscataway, NJ, Nagoya, Japan, 1995.

46. Particle swarm optimization: developments, applications and resources. Eberhart, R. C. and Shi, Y. Proc. congress on evolutionary computation 2001 IEEE service center, Piscataway, NJ., Seoul, Korea., 2001.

47. Multiple Lyapunov functions and other analysis tools for switched and hybrid systems, Branicky, M.S.; Automatic Control, IEEE Transactions on , Volume: 43, Issue: 4 , April 1998, Pages:475 - 482

48. Supervisory hybrid systems, Lemmon, M.D.; He, K.X.; Markovsky, I.; Control Systems Magazine, IEEE , Volume: 19 , Issue: 4 , Aug. 1999, Pages:42 – 55

49. The stability analysis of switched systems, Zhou Da-tian; Xiao Yang; Mu Jian-Cheng; Info-tech and Info-net, 2001. Proceedings. ICII 2001 - Beijing. 2001

50. A Review of Stability Results for Switched and Hybrid Systems, G. N. Davrazos, N. T. Koussoulas, 9th Mediterranean Conference on Control and Automation June 27-29, Dubrovnik, Croatia 2001

51. Feedback Control of Dynamic Systems, Franklin, G. F., Powell, J. D. and Emani-Naeini, A, Addison-Wesley, 1987, pp 100-101

52. Object-Oriented Testing, Copeland, Lee, Software Quality Engineering. STAR East 2001. The Rosen Centre Hotel, Orlando, Florida. 14 May 2001.

53. A particle swarm optimization approach for optimum design of PID controller in AVR system, Zwe-Lee Gaing; Energy Conversion, IEEE Transactions on , Volume: 19 , Issue: 2 , June 2004, Pages:384 - 391

54. Parameter tuning of fixed structure controller for power system stability enhancement, Okada, T.; Watanabe, T.; Yasuda, K.; Transmission and Distribution Conference and Exhibition 2002: Asia Pacific. IEEE/PES , Volume: 1 , 6-10 Oct. 2002, Pages:162 - 167 vol.1

55. Intelligent fuzzy controller using particle swarm optimization for control of permanent magnet synchronous motor for electric vehicle, Elwer, A.S.; Wahsh, S.A.; Khalil, M.O.; Nur-Eldeen, A.M.; Industrial Electronics Society, 2003. IECON '03. The 29th Annual Conference of the IEEE , Volume: 2 , 2-6 Nov. 2003 Pages:1762 - 1766 Vol.2

56. A particle swarm optimization for reactive power and voltage control in electric power systems, Fukuyama, Y.; Yoshida, H.; Evolutionary Computation, 2001. Proceedings of the 2001 Congress on , Volume: 1 , 27-30 May 2001, Pages:87 - 93 vol. 1

57. Software design for bread grading system, Doug Britton, GTRI internal report for bread grading system, 2003

58. Automated vision-based inspection and control of high-volume baking processes, Georgia's traditional industries program for food processing fiscal year 2003-2004 report to industry

59. Baking technology, Online course of American Institute of Baking, American Institute of Baking, 2001.

VITA

Yingchuan Zhang was born in P. R. China in November 1975. She received a B.S. and a M.S. in Automation from Shanghai Jiao Tong University, Shanghai, China in July 1996, and January 1999 respectively. She joined the Intelligent Control Systems Lab in School of Electrical and Computer Engineering, Georgia Institute of Technology, Atlanta, Georgia in 2000, where she started to work as a research assistant under the supervision of Dr. Bonnie Heck Ferri and Dr. George Vachtsevanos. She received her second M.S. in Electrical and Computer Engineering from Georgia Institute of Technology in December 2001. Her research interest includes vision-based inspection, quality modeling, process improvement & control, and artificial intelligence techniques.